Washington University in St. Louis
Washington University Open Scholarship

Arts & Sciences Electronic Theses and Dissertations

Arts & Sciences

Spring 5-15-2020

Pathophysiology and Treatment of Murine Globoid Cell Leukodystrophy

Yedda Li
Washington University in St. Louis

Follow this and additional works at: https://openscholarship.wustl.edu/art_sci_etds

Part of the Biology Commons, Genetics Commons, and the Medicine and Health Sciences Commons

Recommended Citation

Li, Yedda, "Pathophysiology and Treatment of Murine Globoid Cell Leukodystrophy" (2020). *Arts & Sciences Electronic Theses and Dissertations*. 2209.
https://openscholarship.wustl.edu/art_sci_etds/2209

This Dissertation is brought to you for free and open access by the Arts & Sciences at Washington University Open Scholarship. It has been accepted for inclusion in Arts & Sciences Electronic Theses and Dissertations by an authorized administrator of Washington University Open Scholarship. For more information, please contact digital@wumail.wustl.edu.

WASHINGTON UNIVERSITY IN ST. LOUIS

Division of Biology and Biomedical Sciences
Molecular Genetics and Genomics

Dissertation Examination Committee:
Mark S. Sands, Chair
Abhinav Diwan
Christina A. Gurnett
Robyn S. Klein
Daniel S. Ory

Pathophysiology and Treatment of Murine Globoid Cell Leukodystrophy

by

Yedda Li

A dissertation presented to
The Graduate School
of Washington University in
partial fulfillment of the
requirements for the degree
of Doctor of Philosophy

May 2020
St. Louis, Missouri

© 2020, Yedda Li

TABLE OF CONTENTS

List of Figures vii

List of Tables ix

List of Abbreviations x

Acknowledgments xii

Abstract xvi

CHAPTER 1 Introduction 1

1.1 Krabbe Disease (Globoid Cell Leukodystrophy) 2

1.2 Clinical Presentation 2

1.3 Histopathology 3

1.4 Clinical Management 4

1.5 Newborn Screening 5

1.6 Animal Models 6

1.6.1 The Twitcher mouse model 6

1.6.2 The West Highland terrier dog model 7

1.6.3 The nonhuman primate model 7

1.7 Pathophysiology 8

1.7.1 Pathogenic mechanisms in Krabbe disease 8

1.7.2 Galactosylceramidase deficiency 9

1.7.3 Psychosine 9

1.7.4 Demyelination and axonopathy 11

1.7.5 Neuroinflammation 12

1.8 Experimental Therapies 13

1.8.1 Cross correction 13
1.8.2 Hematopoietic stem cell transplantation 15
1.8.3 Gene therapies 15
1.8.4 Substrate reduction therapy 17
1.8.5 Other single therapies 18
1.8.6 Combination therapies 19
1.9 Toxicity of Adeno-Associated Viruses 21
1.10 Summary 22
1.11 Figure Legends 24
1.12 Figures 25
CHAPTER 2 Acid Ceramidase: Krabbe Disease, the 'Psychosine Hypothesis,' and a New Therapeutic Target 26
2.0 Abstract 27
2.1 Introduction 28
2.2 Results 30
2.2.1 Acid ceramidase catalyzes the catabolic formation of psychosine 30
2.2.2 Testing and confirmation of the 'Psychosine Hypothesis' 31
2.2.3 Pharmacological inhibition of acid ceramidase activity 33
2.3 Discussion 34
2.4 Methods 37
2.4.1 Experimental animals 37
2.4.2 Psychosine production *in vitro* 38
2.4.3 Lentivirus preparation 38
2.4.4 Fibroblast transduction 38
2.4.5 Mass spectrometry 39

2.4.6 Flow cytometry 39
2.4.7 Histology 39
2.4.8 Behavioral testing 40
2.4.9 Actometer testing 40
2.4.10 Immunohistochemistry 41
2.4.11 Carmofur administration 41
2.4.12 Statistical analysis 41
2.5 Tables 42
2.6 Figure Legends 43
2.7 Figures 46
CHAPTER 3 Increased Efficacy and Toxicity Associated with Combination Therapy for Murine Globoid Cell Leukodystrophy (Krabbe Disease) 59
3.0 Abstract 60
3.1 Introduction 61
3.2 Results 63
3.2.1 Lifespan 63
3.2.2 Body weight 63
3.2.3 Motor function 64
3.2.4 Biochemical analyses 65
3.2.5 Donor cell engraftment 65
3.2.6 Peripheral neuropathy 66
3.2.7 Immunohistochemistry 66
3.2.8 Cytokine levels 66
3.2.9 Hepatocellular carcinoma 67
3.3 Discussion 67

3.4 Methods 74
3.4.1 Experimental animals 74
3.4.2 Virus production 75
3.4.3 Treatment regimen 75
3.4.4 Galactosylceramidase activity assay 76
3.4.5 Mass spectrometry 76
3.4.6 Behavioral testing 76
3.4.7 Immunohistochemistry 77
3.4.8 Histology 77
3.4.9 Cytokine measurement 77
3.4.10 Statistical analysis 78
3.5 Tables 79
3.6 Figure Legends 80
3.7 Figures 85
CHAPTER 4 Conclusions and Future Directions 101
4.1 Conclusions 102
4.1.1 Outstanding questions in the field 103
4.1.2 Questions answered in chapter two 105
4.1.3 Questions answered in chapter three 107
4.2 Future directions 109
4.2.1 Small molecule inhibtors of acid ceramidase 109
4.2.2 Liver-detargeted gene therapy 109
4.2.3 Systematic study of AAV-induced hepatocellular carcinoma 110
4.2.4 *In utero* hematopoietic stem cell transplantation 111

4.3 Concluding Remarks.....111

4.4 Figure Legends.....113

4.5 Figures.....114

REFERENCES.....115

CURRICULUM VITAE.....129

LIST OF FIGURES

CHAPTER 1 Introduction

Figure 1.1 Major pathogenic mechanisms in Krabbe Disease.....25

CHAPTER 2 Acid Ceramidase: Krabbe disease, the 'Psychosine Hypothesis', and a New Therapeutic Target

Figure 2.1 Potential pathways of psychosine synthesis.....46

Figure 2.2 *In vitro* psychosine formation.....47

Figure 2.3 *In vivo* psychosine accumulation.....48

Figure 2.4 Ceramide accumulation.....49

Figure 2.5 Galactosylceramide accumulation.....50

Figure 2.6 Lifespan.....51

Figure 2.7 Body, spleen, and thymus weights.....52

Figure 2.8 Flow cytometry.....53

Figure 2.9 Tremor.....54

Figure 2.10 Motor function.....55

Figure 2.11 Histology and immunohistochemistry.....56

Figure 2.12 Lifespan of Carmofur-treated mice.....57

Figure 2.13 Biochemical changes associated with Carmofur administration.....58

CHAPTER 3 Increased Efficacy and Toxicity Associated with Combination Therapy for Murine Globoid Cell Leukodystrophy (Krabbe Disease)

Figure 3.1 Survival.....85

Figure 3.2 Body weight.....86

Figure 3.3 Rotarod performance.....87

Figure 3.4 Wirehang performance.....88

Figure 3.5 Galactosylceramidase activity.....89

Figure 3.6 Psychosine accumulation 90
Figure 3.7 GFP^+ engraftment 91
Figure 3.8 Sciatic nerve histology 92
Figure 3.9 $CD68^+$ microgliosis 93
Figure 3.10 $GFAP^+$ astrocytosis 94
Figure 3.11 Cytokine expression 95
Figure 3.12 Gross pathology of normal-appearing vs. HCC liver 96
Figure 3.13 Frequency of AAV-induced HCC 97
Figure 3.14 Ceramide levels in normal-appearing vs. HCC liver tissue 98
Figure 3.15 Chromosomal breakdown of unique AAV integration sites 99
Figure 3.16 Functional breakdown of unique AAV integration sites 100

CHAPTER 4 Conclusions and Future Directions

Figure 4.1 Potential improvements to the current triple combination therapy 114

LIST OF TABLES

CHAPTER 2 Acid Ceramidase: Krabbe disease, the 'Psychosine Hypothesis', and a New Therapeutic Target

Table 2.1 Comparison of the Twitcher vs. Farber murine phenotypes.....42

CHAPTER 3 Increased Efficacy and Toxicity Associated with Combination Therapy for Murine Globoid Cell Leukodystrophy (Krabbe Disease)

Table 3.1 Unique integration sites in normal vs. HCC tissue.....79

LIST OF ABBREVIATIONS

2xRx: Double combination therapy (AAV2/9-GALC + HSCT)

3xRx: Triple combination therapy (AAV2/9-GALC + HSCT + L-cycloserine)

AAV: Adeno-associated virus

ACDase: Acid ceramidase

Arg1: Arginase-1

CGT: Ceramide galatosyltransferase

CNS: Central nervous system

FD: Farber disease

GALC: Galactosylceramidase

GLD: Globoid cell leukodystrophy

HCC: Hepatocellular carcinoma

HSCT: Hematopoietic stem cell transplantation

IUHCT: Intra-uterine hematopoietic stem cell transplantation

IV: Intravenous

LFB/PAS: Luxol fast blue and periodic Acid-Schiff

M6PR: Mannose-6-phosphate receptor

MS: Multiple sclerosis

Op: Osteopetrotic (*CSF1*$^{-/-}$) mouse

PNS: Peripheral nervous system

PTF: Peak tremor frequency

SMN: Survival of motor neuron

SRT: Substrate reduction therapy

Twi: Twitcher

Twi/FD: Twitcher/Farber mouse (*GALC*$^{-/-}$*ASAH1*$^{P361R/P361R}$)

Twi/FDH: Twitcher/Farber heterozygous mouse (*GALC*$^{-/-}$*ASAH1*$^{+/P361R}$)

WT: Wild type

ACKNOWLEDGMENTS

First and foremost, I would like to acknowledge my advisor, Dr. Mark Sands. Mark, you never heard it from me, but you are an exceptional scientist, and an equally exceptional person. You really showed me what open-door policy means: not only are we welcome to interrupt you at any moment throughout the day, we are also welcome to eat lunch in your office. Many times have I sat down to eat, only to be met with your extemporaneous lesson on how to run a lab, or your discussion on the newest data, or your somewhat wistful glance into my very Chinese food, followed by the growl, "You're makin' me hungry! You're not supposed to do that!" Your dedication to your research, to your students, and to the patients who suffer from the diseases we study is truly inspiring, and I am extremely lucky to be your mentee.

I would also like to acknowledge my wonderful committee. Many of them have met with me one-on-one, some before my committee was officially formed, and their invaluable advice and encouragement were critical for my success. Special thanks go to Dr. Dan Ory and his lab, especially Dr. Xuntian Jiang, who processed all the metabolomics data which were important to both projects and especially critical for chapter 2. Both helped me immeasurably in designing new experiments, and lent me their expertise on lipid biology.

Special thanks also go to Dr. Robyn Klein and her lab, who helped me as I struggled with the intricacies of neuroimmunology. Dr. Kristen Funk in the Klein lab patiently taught me how to culture primary microglial cells. Although that project did not pan out in the end, they were generous with their time and resources, and I would never have brought the project as far along as I had without their guidance.

Special thanks to Dr. Mike Rettig and Julie Ritchey for helping me with obtaining the flow cytometry data in chapter 2. I will forever be in awe of Julie's superhuman techniques in all things

mouse. I am also forever indebted to Mike, who in addition to providing us with a great deal of expensive reagents for free, showed us real dedication and kindness by pulling a few all-nighters running flow cytometry for us.

The cytokine data in chapter 3 were obtained with the help of Dr. Camaron Hole and his PI, Dr. Tamara Doering. Camaron invited me to his lab and patiently walked me through the entire process, step by step. All the pathology in chapters 2 and 3 were processed and analyzed by Dr. Carole Vogler and Dr. Miguel Guzman at St. Louis University. I am especially grateful for their patience in helping me to interpret all the slides that went into these studies. Many thanks to our collaborator at NIH, Dr. Charles Venditti and his lab, for their help in producing and analyzing the deluge of AAV integration data, some of which are presented in chapter 3. Thanks as well to our collaborator at the Medical College of Wisconsin, Dr. Jeffrey Medin and his lab, for generously providing us with the murine model of Farber disease.

My heartfelt thanks to all members of the Sands Lab, who have all contributed, in small ways and large, to this dissertation. Dr. Josh Dearborn and Dr. Bruno Benitez, in particular, helped out with tremor testing and *in vitro* experiments for chapter 2, respectively. Marie Nunez helped out with collection of behavioral data for chapter 3. Without them, I would never have been able to complete my dissertation in time. My gratitude goes to Marie, who forgives me for all the messes I make in lab (and for the Sour Patch Kids); to Christina, who forgives me for hogging the mouse house; to Bruno, for giving me a nickname – "High Throughput PCR Machine" – that would look good on my CV; to Josh, for keeping me sane with cute animal videos; and to Kevin, who is a constant source of entertainment.

Special acknowledgment to Dr. Lauren Shea, who taught me numerous mouse house techniques, helped me to set up the experiments in chapter 3, and always had words of

encouragement for me. Lauren, I will always look up to your extraordinary work ethic and dedication, your true love for patients and all things medicine, and your never-ending compassion. I am very lucky to call you my friend.

I am also indebted to Greg Avant, Anthony Hopkins, and the rest of the mouse facility team at CID for taking wonderful care of all my mice, and for tolerating my mouse-breeding insanity. I can honestly say that without their dedication and hard work, there would be no mice, and hence, no dissertation.

I would not be where I am without my wonderful friends for their constant support. Thanks especially to Lucy Li, my "twin" MSTP compatriot, who has always been there with her humor and sarcasm to celebrate the highs and offer comfort during the lows. Lucy, I think I may have dislocated my jaw once or twice laughing so hard with you. Thanks as well to my many wonderful friends at Light of Christ church and Immanuel Lutheran Church. A complete list of all your names would fill up this entire page, so thank you all for showing me what it means to be "a family in Christ."

Finally, a very special acknowledgment to my dear teacher and friend, Professor Seth Carlin. It breaks my heart to know that you are no longer with us. Yet I know that you are always with me, because your lessons remain and the memories and the music will live on forever. Thank you.

Yedda Li

Washington University in St. Louis

May 2020

This thesis dedication extends two ways.

To my grandparents, for passing on their love of medicine
and
To Mom, for everything

ABSTRACT OF THE DISSERTATION

Pathophysiology and Treatment of Murine Globoid Cell Leukodystrophy

by

Yedda Li

Doctor of Philosophy in Biology and Biomedical Sciences

Genetics and Genomics

Washington University in St. Louis, 2020

Professor Mark S. Sands, Chair

Infantile globoid cell leukodystrophy (GLD, Krabbe disease) is a rapidly progressing, invariably fatal pediatric disorder first described in 1916. Krabbe disease is caused by a deficiency in the lysosomal enzyme, galactosylceramidase (GALC), and is characterized clinically by failure to thrive, limb stiffness, seizures, developmental regression, and death by 2-4 years of age. Galactosylceramidase degrades the cytotoxic glycolipid, galactosylsphingosine (psychosine). In the absence of GALC activity, psychosine accumulates primarily in oligodendrocytes and Schwann cells, resulting in profound demyelination. In 1972, psychosine was hypothesized to be responsible for the clinical signs associated with Krabbe disease. However, the 'Psychosine Hypothesis' has never been tested, due to the inability to dissociate GALC deficiency from psychosine accumulation. This is due, in part, to a limited understanding of psychosine biosynthesis. Two studies published in 1960 and 1973 provided complementary evidence suggesting that psychosine is synthesized via an anabolic pathway. However, neither the cDNA nor the enzyme catalyzing that reaction has been identified. In the first part of this dissertation, we overturn those studies and show that psychosine is generated catabolically through the deacylation of galactosylceramide by acid ceramidase (ACDase). This reaction effectively dissociates GALC

deficiency from psychosine accumulation, allowing us to test and confirm the 'Psychosine Hypothesis.' These data also identify ACDase as a potential target for substrate reduction therapy (SRT). We show that pharmacological inhibition of ACDase activity significantly prolongs the lifespan of the Twitcher (Twi) mouse, a GALC-deficient model that faithfully mimics the biochemical, histological, and clinicobehavioral features of Krabbe disease. These data clarify our understanding of psychosine synthesis, confirm the long-held 'Psychosine Hypothesis,' and provide the impetus to discover safe and effective inhibitors of ACDase to treat Krabbe disease.

Although Krabbe disease is a monogenic disorder, it is remarkably refractory to treatment, and single modality therapies are minimally effective. However, combining CNS-directed, adeno-associated virus (AAV) 2/5-mediated gene therapy, hematopoietic stem cell transplantation, and SRT greatly increases efficacy in the Twi mouse. In the second part of this dissertation, we incorporated a newer generation vector, AAV2/9, into this combination therapy regimen. This single change significantly increased the lifespan of Twi mice. Importantly, it also dramatically improved, and in some cases, normalized, the clinicobehavioral deficits that remained uncorrected in mice treated with the AAV2/5-combination therapy. Unfortunately, nearly all of the AAV2/9-combination-treated Twi mice and all combination-treated wild type control mice died from hepatocellular carcinoma (HCC). Integration site analysis confirmed AAV sequence incorporation into the mouse genome. These data demonstrate the value of targeting multiple pathogenic mechanisms for complex metabolic diseases, but highlight the potential risks associated with these approaches.

Taken together, the data presented in this dissertation greatly advance the field of Krabbe research by increasing our fundamental understanding of Krabbe pathogenesis, and by making significant progress in the treatment of this fatal disease. Modification of the combination therapy

regimen to include a safe, ACDase-inhibiting SRT to target psychosine synthesis, as well as a liver de-targeted gene therapy to minimize HCC penetrance will likely bring us even closer to a cure.

CHAPTER ONE

Introduction

1.1 Krabbe Disease (Globoid Cell Leukodystrophy)

Krabbe disease (globoid cell leukodystrophy, GLD) is a rapidly progressing, invariably fatal, pediatric lysosomal storage disorder. Krabbe was first described in 1916 by the German pediatrician, Dr. Knud Krabbe, as a "diffuse sclerosis of the brain" (Krabbe, 1916). It is caused by a deficiency in the lysosomal enzyme galactosylceramidase (GALC), which is responsible for cleaving the terminal galactose from galactosylated lipids such as galactosylceramide and galactosylsphingosine. Galactosylsphingosine, more commonly known as psychosine, is a toxic metabolite that accumulates quickly in oligodendrocytes and Schwann cells in the absence of GALC activity. Death of these myelinating cells results in a demyelinating phenotype that is characterized primarily by stiffness, spastic paralysis, hyperreactivity, and blindness.

1.2 Clinical Presentation

There is a very wide range of presentation and clinical progression for Krabbe disease. Early infantile Krabbe disease, the most severe form of GLD, is also the most common form. Children with the early infantile form present during the first year of life most noticeably with difficulty feeding and hyperirritability. Feeding difficulties include difficulty latching on, uncoordinated sucking and swallowing, coughing and gagging, and fatigue. Infants also exhibit signs of gastrointestinal dysmotility, including gastroparesis, vomiting, and constipation (Escolar et al., 2006). Disease progression occurs rapidly, with children developing hypertonicity, hyperreactivity, opisthoclonus, and mental/motor regression. Patients are also unusually prone to pneumonia, ear infections, and urinary tract infections, most likely due to an unidentified immune defect (Anderson et al., 2014). Optic nerve atrophy is often observed, resulting in vision loss. In

the final stages of disease, patients are decerebrate, blind, and often also deaf (Hagberg et al., 1963). Signs of autonomic dysfunction are observed, including hyperthermia and hypothermia, vascular leakage, and widening blood pressure variations (Escolar et al., 2016). Most patients with early infantile Krabbe die before age two.

The later-onset forms of Krabbe disease present with a milder clinical picture and have a more protracted disease course. Children with the late infantile form present at 6 months to 3 years, whereas the children with the juvenile form present from 3-8 years of age. Unlike early infantile Krabbe patients, who present most commonly with hyperirritability and gastrointestinal problems, patients with later-onset Krabbe disease often present with loss of vision and ataxia (Lyon et al., 1991).

The least common form of Krabbe disease is adult-onset Krabbe. These patients are often misdiagnosed with multiple sclerosis (MS), because symptoms at presentation are indistinguishable from those of MS patients. Unlike patients with childhood-onset Krabbe, patients with adult-onset Krabbe can be stable for long periods of time without treatment, although some patients experience a steady decline in function, ultimately resulting in death (Debs et al., 2013).

1.3 Histopathology

Long before the enzyme deficiency responsible for causing Krabbe disease was ever identified, pathological characterization of this disease revealed the existence of multinucleated, distended "globoid cells" in the central nervous system (CNS) (Collier and Greenfield, 1924). Lipid content characterization of brains from Krabbe patients later identified the buildup of galactosylceramide in globoid cells (Blackwood and Cumings, 1954). Interestingly, this elevation in galactosylceramide was not observed in whole brain. Because galactosylceramide is a major

component of myelin, it was hypothesized that the eponymous "globoid cells" were fused macrophages working in futility to phagocytose and degrade the myelin debris that accumulated in a chronically and profoundly demyelinated state (Austin and Lehfeldt, 1965). More recently, it has been shown that microglia, but not macrophages, transform into globoid cells when exposed to psychosine *in vitro* (Ijichi et al., 2013), suggesting that these eponymous cells may actually be of microglial origin.

1.4 Clinical Management

Currently, there is no cure for Krabbe disease. The standard of care is hematopoietic stem cell transplantation (HSCT), either in the form of bone marrow transplantation or umbilical cord blood transplantation. HSCT can delay symptom onset and disease progression, but is not a cure (Wright et al., 2017). Furthermore, HSCT is effective only if administered prior to symptom onset, which necessitates the detection of disease through genetic testing. Because New York and Missouri are the only states that provide newborn screening for Krabbe, most children treated for Krabbe disease are siblings of another affected sibling, and many children are no longer able to receive treatment by the time they are diagnosed. In fact, there is evidence suggesting that some infants as young as one month can no longer benefit from HSCT therapy (Orsini et al., 2016). Since HSCT carries significant risk and is associated with significant mortality and morbidity, we are greatly in need of a better therapy.

1.5 Newborn Screening

Newborn screening for Krabbe disease was initiated in the United States in 2006, and continues to be very controversial. This is due in part to the unclear genotype-phenotype associations in Krabbe disease, especially for patients with later-onset Krabbe disease (Debs et al., 2013). Only five of fourteen children who were categorized as "high risk" for having Krabbe disease have developed clinical signs and symptoms consistent with the disease (Orsini et al., 2016). Furthermore, there is significant overlap in GALC activity between patients who have Krabbe disease, carriers, and normal individuals. Because the current treatment for Krabbe disease, HSCT, is associated with significant risks, it is unclear how high-risk patients should be treated, as it is unclear whether or not they will go on to develop symptomatic Krabbe.

Currently, newborn screening assays for GALC activity in dried blood spots are done by mass spectrometry or by fluorometry. Although this gives a direct readout for the genetic determinant of Krabbe disease, GALC activity alone is not a very specific predictor for Krabbe disease. A significant fraction of patients with very low GALC activity have yet to develop any signs or symptoms of Krabbe disease. Quantification of the buildup of psychosine, the toxic metabolite that accumulates in Krabbe disease, is a secondary measure by which the specificity of newborn Krabbe screening can be increased. In fact, psychosine measurements are already being used to quantify treatment effect and disease progression in Krabbe disease (Escolar et al., 2017). Recent studies that quantified psychosine in dried blood spots showed psychosine elevation in patients affected by Krabbe disease compared to carriers and normal control patients (Turgeon et al., 2015). It remains to be seen whether psychosine accumulation can be used as a secondary, or even primary, screening tool for Krabbe disease.

1.6 Animal models

There are several naturally-occurring animal models of Krabbe disease: the mouse (Kobayashi et al., 1980; Duchen et al., 1980), the terrier dog (Victoria et al., 1996), the Australian Kelpie dog (Fletcher et al., 2010), the nonhuman primate (Baskin et al., 1998), the cat (Sigurdson et al., 2002), and the sheep (Pitchard et al., 1980).

1.6.1 The Twitcher mouse model

First observed in 1976 at the Jackson Laboratory in Bar Harbor, Maine, the Twitcher (Twi) mouse is the oldest, most studied model of Krabbe disease (Kobayashi et al., 1980; Duchen et al., 1980). The Twi mouse has a premature termination codon (W339X) in the *GALC* gene, which results in nonsense-mediated decay of the *GALC* mRNA (Lee et al., 2006). As such, Twi mice have complete absence of GALC expression, which parallels the most common 30 kB deletion resulting in complete absence of GALC activity in human Krabbe patients (Luzi et al., 1995). All patients with this mutation develop infantile Krabbe disease. In addition to the genetics, Twi mice also mirror the biochemistry, histology, and clinicopathological features of infantile Krabbe disease. Twitcher mice have a very profound phenotype consisting of severe tremor, failure to thrive, ataxia, hind limb atrophy, and kyphosis. Mice first develop symptoms at postnatal day 15, and disease progression occurs rapidly, with death occurring at ~40 days (Taniike and Suzuki, 1994). Histologically, the eponymous globoid cells are observed in Twi brains, accompanied by massive microgliosis and astrocytosis (Reddy et al., 2011). Because of its relative availability and low cost, the Twi mouse is the most frequently used model in the study of Krabbe pathophysiology and treatment.

1.6.2 The West Highland terrier dog model

Another important model of Krabbe disease is canine GLD in West Highland white terriers. This disease manifests as profound CNS demyelination, psychosine accumulation, and presence of globoid cells in the white matter of affected animals (Wenger et al., 1999). More recently, another naturally-occurring canine model of Krabbe disease was discovered in Australian Kelpies. Krabbe disease in Australian Kelpies manifests as a demyelinating disease with ataxia, tremors, paralysis, and a severely shortened lifespan. Histologically, the disease is characterized by microglial and astrocytic activation, as well as axonal spheroid formation (Fletcher et al., 2010).

Canine Krabbe disease is a large animal model of Krabbe disease that is integral for translating experimental therapies into the clinic. The canine West Highland white terrier model of Krabbe disease has been used to determine the effectiveness of gene therapy in correcting the Krabbe phenotype (Bradbury et al., 2018). These data are particularly important, because the dog is closer to the human than the mouse in brain size, and will likely more accurately predict treatment efficacy for the human disease.

1.6.3 The nonhuman primate model

The only nonhuman primate model of Krabbe disease is the rhesus macaque (Baskin et al., 1998). Like the mouse and canine models of Krabbe, this is a naturally-occurring model with a 2bp deletion in exon 4 of the *GALC* gene. This results in frameshift and a premature termination codon in the mRNA (Luzi et al., 1997). Macaques homozygous for this mutation present with severe tremors, ataxia, hypermetria, respiratory difficulties, nerve conduction abnormalities, and significantly shortened lifespan (Borda et al., 2008). Nonhuman primate Krabbe is characterized histologically by presence of globoid cells and profound microgliosis (Borda et al., 2008). Although primate models are expensive to maintain, these models are critical for drug

development and translation of experimental therapies into the clinic. A case study of mesenchymal stem cell transplantation in a one-month old rhesus macaque with early infantile Krabbe disease transiently improved coordination, ambulation, cognition, and gross motor skills (Isakova et al., 2017). Although the benefits of this treatment were temporary, the findings in this study suggest that rhesus macaques have a Krabbe phenotype most closely representative of human Krabbe. Because non-human primates are also more similar in anatomy and physiology than other mammalian species, they are an ideal model to evaluate experimental therapies before they can be moved to human study. In another case study, the feasibility of primate gene therapy administration has been confirmed (Meneghini et al., 2016). The results from this study will likely directly influence which experimental therapies will be approved for future use in human Krabbe patients.

1.7 Pathophysiology

1.7.1 Pathogenic mechanisms in Krabbe disease

Although Krabbe is a monogenic disease, it is also a very complex disease. Multiple pathogenic mechanisms interact to contribute to disease progression (Figure 1.1). The inherent deficiency in GALC activity is the very tip of the iceberg. Galactosylceramidase deficiency directly results in psychosine accumulation. Psychosine accumulation in turn, results in death of Schwann cells and oligodendrocytes, which leads to demyelination. Additionally, there have been some data suggesting a dysmyelinating phenotype in addition to the demyelinating one (Potter et al., 2013). Demyelination activates microglia and astrocytes, and recruits macrophages to the CNS to clean up myelin debris. The result is profound neuroinflammation, oxidative stress, and free radical generation. Unlike the glial activation observed in ordinary CNS maintenance, the

neuroinflammation in Krabbe is chronic and unattenuable, because the microglia are unable to clean up the myelin debris due to the inherent GALC deficiency. Deficiency of GALC activity, psychosine accumulation, demyelination/dysmyelination, oxidative stress, and neuroinflammation all coexist and interact in the Krabbe nervous system to wreak havoc and create the momentum for disease progression. The coexistence and interactions between these pathogenic mechanisms become critically important when considering the potential therapies for this complex disease.

1.7.2 Galactosylceramidase deficiency

In 1970, two separate groups identified the enzyme defect associated with Krabbe disease as that of the lysosomal enzyme galactosylceramidase (Malone, 1970; Suzuki and Suzuki, 1970). The cDNA for the human *GALC* gene was identified and cloned in 1993 (Chen et al., 1993) after the mutation responsible for Krabbe disease was mapped to human chromosome 14 (Zoglotora et al., 1990).

1.7.3 Psychosine

After *GALC* was identified as the disease-causing gene in Krabbe disease, another substrate for GALC was identified – psychosine (Miyatake and Suzuki, 1972). Unlike galactosylceramide, which was only elevated in globoid cells and not elevated in whole brain, psychosine was found to be massively elevated in the brains of Krabbe patients (Svennerholm et al., 1980). Studies of the properties of psychosine revealed it to be severely toxic to all cell types, with especially rapid effects on oligodendrocytes (Cho et al., 1997), Schwann cells (Tanaka and Webster, 1993), and glial cells (Jatana et al., 2002). In addition, psychosine promotes DNA fragmentation, increases proapoptotic factors, inhibits oligodendrocyte maturation, and promotes peripheral axonal demyelination (Yamada and Suzuki, 1999; Jatana et al., 2002; Haq et al., 2003; Khan et al., 2005; Contreras et al., 2008; Giri et al., 2008). In light of its toxicity, Miyatake and Suzuki proposed the

'Psychosine Hypothesis' in 1972, which states that psychosine, not GALC deficiency, is the primary cause of the Krabbe phenotype (Miyatake and Suzuki, 1972). Although this hypothesis has been generally accepted within the field for many years, it has never been formally tested, due to the inability to dissociate psychosine accumulation from GALC deficiency.

Figuratively speaking, psychosine has been a thorn in the side for the Krabbe research community. Other than the unproven 'Psychosine Hypothesis,' there are many other unanswered questions regarding this toxic compound. Until very recently, even the mechanism by which psychosine exerts its toxic effect was unknown. Psychosine is a relatively small, amphipathic molecule. It has been unclear how psychosine could have so many wide-ranging effects without interacting with a great number of different proteins. Although both receptor-mediated and membrane-disrupting mechanisms for toxicity have been proposed (Im et al., 2001); White et al., 2009), there is now compelling evidence to suggest that membrane disruption is the main mechanism by which psychosine effects its toxicity. In 2013, it was shown that both naturally-occurring psychosine and its enantiomer, *ent*-psychosine, were equally toxic. Because protein interactions in the natural world are specific for chirality, these results suggested that psychosine mediates its toxic effects not through protein interactions, but by disrupting the lipid rafts in cellular membranes (Hawkins-Salsbury et al., 2013).

How psychosine is produced is also unclear. There are two potential pathways of psychosine synthesis *in vivo*: 1. the anabolic dehydration of galactose and sphingosine and 2. the catabolic deacylation of galactosylceramide. It was shown in 1960 that psychosine could be produced *in vitro* by the anabolic dehydration of galactose and sphingosine (Cleland and Kennedy, 1960). In 1973, an independent group indirectly confirmed these results by concluding that the catabolic reaction does not occur *in vitro* (Lin and Radin, 1973). Together, these studies established

the dogma that psychosine is synthesized via the anabolic pathway. However, the enzyme catalyzing this reaction *in vivo* has never been identified, and the cDNA encoding such an enzyme has never been cloned. The existence of such an enzyme remains an open question to this day.

1.7.4 Demyelination and axonopathy

Demyelination and axonopathy are major pathogenic mechanisms of Krabbe disease. It is well known that psychosine induces demyelination indirectly by causing the death of oligodendrocytes and Schwann cells. However, psychosine also directly induces myelin breakdown (White et al., 2009). In addition to myelin destruction, defects in protein phosphatase signaling (Cantuti-Castelvetri et al., 2012), increases in caspase-3 expression (Smith et al., 2011), and abnormal axonal transport (Cantuti-Castelvetri et al., 2013) all contribute to axonal dysfunction.

Axonopathy manifests in Krabbe disease in many ways. Most easily observed are the defects in neuromuscular function. Axonopathy contributes to ataxia and other gross motor dysfunction in human Krabbe patients as well as in Twi mice. Less obvious are the problems in autonomic function that are the result of axonopathy in the autonomic nervous system (ANS). Autonomic denervation of lymphoid organs results in thymic atrophy in Twi mice (Galbiati et al., 2007).

Although the ANS has not been formally studied in human Krabbe patients, patients do exhibit signs of ANS dysfunction, including unstable blood pressure, increased vascular permeability, and poor gastrointestinal motility. Krabbe patients are also predisposed to infections, a finding that may reflect the abnormal thymic atrophy and T cell production observed in Twi mice.

Although a very important component of Krabbe disease, peripheral neuropathy is nevertheless very difficult to treat. To date, no published experimental therapies effectively and

consistently corrects the motor defects observed in Twi mice, even if they significantly increase Twi lifespan (Hawkins-Salsbury et al., 2015; Rafi et al., 2015). Future therapies that successfully target peripheral neuropathy will likely greatly increase the quality of life for Krabbe patients.

1.7.5 Neuroinflammation

Fever of unknown origin is one of the early manifestations of Krabbe disease, suggesting the activation of the innate immune response in these patients (Hagberg et al., 1963). The presence of phagocytic globoid cells in the brain also points to an inflammatory etiology (Krabbe, 1916). Neuroinflammation has further been characterized as a prominent feature of Krabbe disease. Human Krabbe disease, as well as all animal Krabbe models, are characterized by profound microgliosis and astrocytosis. The dogma in the field has been that the death of oligodendrocytes and demyelination directly causes neuroinflammation. While this is certainly true, more recently published data suggest that neuroinflammation is an independent pathogenic mechanism, with microgliosis beginning as early as two weeks in the mouse (Snook et al., 2014) and perturbations in cytokine and chemokine expression occurring as early as postnatal day 2 (Santambrogio et al., 2012).

The cause of neuroinflammation in the early stages of Krabbe disease is unclear. Several hypotheses have been proposed. Expression of cytokines and cellular markers of inflammation increases with psychosine accumulation (Santambrogio et al., 2012), but it is unclear whether psychosine accumulates to a significant extent so early on in the disease course. Because it is difficult to measure psychosine levels on a single-cell level, it is unclear whether microglia and astrocytes accumulate psychosine at all. The only cell types known to accumulate psychosine at a pathological level are myelinating cells – oligodendrocytes and Schwann cells (White et al., 2011). It has been suggested that GALC-deficient oligodendrocytes may trigger neuroinflammation

through contact-dependent or independent means (Potter and Petryniak, 2016). Finally, it has been hypothesized that GALC-deficient microglia and astrocytes may self-activate, but this hypothesis has yet to be experimentally tested.

Regardless of the etiology of neuroinflammation in Krabbe disease, it has been confirmed to be a critical pathogenic mechanism contributing to disease progression. Although the cytokine expression profile in the Twi CNS is predominantly pro-inflammatory (Higashi et al., 1992; Ohno et al., 1993; LeVine and Brown, 1997; Pedchenko et al., 1999; Pedchenko et al., 2000; Wu et al., 2001; Formichi et al., 2007; Pasqui et al., 2007; Luzi et al., 2009; Ripoll et al., 2011), a reduction of microglia and circulating monocytes in CSF1-deficient (*CSF1*$^{-/-}$) Twi/Osteopetrotic (Op) mice impairs myelin phagocytosis and remyelination, exacerbates neurologic symptoms, and shortens Twi lifespan (Wiktor-Jedrzejczak et al., 1990; Kondo et al., 2011). Expression of arginase-1 (Arg1), an anti-inflammatory microglial marker, is increased in Twi CNS but not in Twi/Op CNS (Kondo et al., 2011), suggesting that a subpopulation of microglia in the Twi CNS inhibits GLD disease progression. Given the global pro-inflammatory environment in the Twi CNS, it is likely that microglia with opposing functional roles coexist in the Twi CNS, and that subtle, localized changes in cytokine signaling can change microglial function in a particular area.

1.8 Experimental Therapies

1.8.1 Cross correction

Cross correction is a well-described phenomenon by which an enzyme-producing cell can correct the enzyme deficiency of a neighboring cell (Neufeld and Fratantoni, 1970). This mechanism is critically important for the effect of many therapies, including hematopoietic stem

cell transplantation and experimental therapies directly targeting the underlying genetic deficiency in Krabbe disease.

In cross correction, nascent lysosomal enzymes of GALC-expressing donor cells are glycosylated in the endoplasmic reticulum. They are then transported to the Golgi apparatus, where they acquire the mannose-6-phosphate modification. The majority of the modified enzyme is then bound to mannose-6-phosphate receptor (M6PR) and targeted to the lysosome. However, a small proportion of enzyme is secreted from the cell. These enzymes can be taken up by neighboring *GALC*$^{-/-}$ recipient cells through the ubiquitously expressed M6PR or the mannose receptor, which is expressed in cells of the reticuloendothelial system. Once taken up, these enzymes are targeted to the recipient cell's lysosome, where the enzyme dissociates from the receptor (Neufeld and Fratantoni, 1970; Kornfeld, 1992). Because M6PR is expressed on every cell type, cross correction can, in theory, correct any *GALC*$^{-/-}$ cell type by providing functional GALC enzyme. In reality, however, correction of GALC deficiency is often incomplete. Hematopoietic stem cell transplantation, for example, produces ~15% GALC activity normalization in the brain, even with complete donor cell engraftment (Hoogerbrugge et al., 1988).

Despite its limitations, cross correction is an important mechanism by which therapies targeting the underlying GALC deficiency must work. Gene therapy, for example, relies heavily on cross correction, without which only a very limited population of cells closest to the injection sites would be corrected. Because viral tropism further limits the type of cell that can be transduced by viral-mediated gene therapy (Hammond et al., 2017), cross correction is especially important in that it enables transduced cells overexpressing the deficient enzyme to produce and secrete the enzyme so that it can be taken up by neighboring untransduced cells. This significantly increases the area of effect.

1.8.2 Hematopoietic stem cell transplantation

Hematopoietic stem cell transplantation (HSCT) became the standard of care for Krabbe disease after it was shown in 1984 that HSCT extended the mean lifespan of Twi mice from 36 days to 80 days (Yeager et al., 1984). This was the first breakthrough in experimental therapies since the Twi model was first published in 1980. Hematopoietic stem cell transplantation was thought to provide long term, albeit low GALC activity to the Twi CNS through cross correction from donor cells that migrate into the CNS after transplantation (Yeager et al., 1984; Hoogerbrugge et al., 1988). However, some recent HSCT studies using a non-lethal conditioning regimen with resulting incomplete engraftment have shown no increase in CNS GALC activity post-transplant (Reddy et al., 2011). Instead, data from these studies show that HSCT is profoundly immunomodulatory. In fact, when administered with gene therapy, HSCT abolishes both disease-specific microgliosis and gene therapy-specific lymphocytosis in the CNS (Reddy et al., 2011). The mechanism underlying the neuroimmunomodulatory effects of HSCT are unknown, but it is likely that immunomodulation and cross correction both play important roles in the effectiveness of HSCT in treating Krabbe disease.

1.8.3 Gene therapies

Monogenic disorders, such as lysosomal storage disorders, are very amenable to gene therapy. Thus far, CNS-directed, adeno-associated virus (AAV)-mediated gene therapy has been used to restore long-term gene expression and improve clinical outcomes in mouse models of many lysosomal storage disorders, including but not limited to mucopolysaccharidosis VII (Skorupa et al., 1999), infantile neuronal ceroid lipofuscinosis (Shyng et al., 2017), late infantile neuronal ceroid lipofuscinosis (Passini et al., 2006), Niemann Pick A (Passini et al., 2005), and Farber disease (Alayoubi et al., 2013).

Adeno-associated viruses are non-enveloped, single-stranded DNA viruses that require the presence of a helper virus for replication. They are popular as a viral vector for CNS-directed gene therapy because of the existence of capsids with CNS-directed viral tropism, their relatively benign profile, and their ability to maintain long-term gene expression in hosts (Ojala et al., 2015). Of the eleven naturally-occurring AAV capsids, AAV2, 7, 8, 9, and 10 have relatively strong neuronal cell tropism. In particular, AAV9 and AAV10 are more recently discovered capsids that have improved transduction and broader distribution in the CNS (Cearley and Wolfe, 2006). Importantly for CNS diseases that need correction during the neonatal period, such as Krabbe disease, AAV9 preferentially targets neonatal neurons and undergoes increased axonal transport (Foust et al., 2009; Aschauer et al., 2013).

The first study of gene therapy in Krabbe disease used the AAV2/1 and AAV2/5 vectors, which have the GALC cDNA cloned into the AAV2 backbone and pseudotyped with the AAV1 and AAV5 capsids, respectively. These studies showed modest improvements in histological and clinical measures of disease progression, despite supraphysiologic GALC enzyme activity in the brain (Lin et al., 2005; Rafi et al., 2005). One of the limitations of intracranial delivery of viral vectors is its limited feasibility in humans due to poor vector spread (Cunningham et al., 2008). Intravenous administration of AAV2/rh10-GALC, which has been shown to cross the blood brain barrier (Rafi et al., 2012), extended Twi lifespan to a median of about 70 days (Rafi et al., 2015).

Although Krabbe is a monogenic disorder, correcting the underlying GALC deficiency with gene therapy produces very limited improvements in clinicopathological measures. Lifespan extension with the latest generation AAV vector alone is less than the extension published in 1984 with HSCT. These results suggest that there is far more to Krabbe pathogenesis than the underlying genetic deficiency, even if it is a monogenic disorder.

1.8.4 Substrate reduction therapy

Because psychosine is generally accepted as the disease-causing agent in Krabbe disease, therapies that directly target psychosine synthesis have been proposed as an adjuvant to gene therapy. These therapies, termed substrate reduction therapies (SRT), aim to partially reduce the synthesis of substrates that accumulate in lysosomal storage disorders. Substrate reduction therapy for Krabbe disease decreases the rate of psychosine accumulation in the cell by administration of a small molecule that 1) crosses the blood brain barrier and 2) inhibits an enzyme in the pathway of psychosine synthesis.

Currently, the most commonly used SRT in Krabbe disease is L-cycloserine. L-cycloserine is a synthetic enantiomer of the naturally-occurring D-cycloserine, a compound isolated from bacteria and used pharmaceutically as an antibiotic (Lowther et al., 2010). L-cycloserine inhibits serine palmitoyl transferase, an enzyme upstream of ceramide synthesis (Sundaram and Lev, 1984). Ceramides, in turn, give rise to psychosine through an unclear pathway.

L-cycloserine administration improves the clinical course of Krabbe disease in Twi mice, increasing their median lifespan to 56.7 days (LeVine et al., 2000) by decreasing CNS psychosine accumulation (Hawkins-Salsbury et al., 2015). In dogs, however, L-cycloserine injection had no significant effect on lifespan (Duffner et al., 2009). As the dog CNS has a much larger volume compared to the mouse CNS, the dog is much more difficult to treat. Since L-cycloserine does not treat the underlying genetic defect, it is hardly surprising that L-cycloserine alone has no therapeutic effect in dogs. The results from these studies demonstrate that L-cycloserine and SRT in general have significant potential in treating Krabbe disease, and may be more effective if administered in combination with other therapies targeting the underlying genetic deficiency.

Although L-cycloserine is the most common SRT of choice in experimental therapy studies for Krabbe disease, it is highly unlikely that it will ever be approved for human use. This is because L-cycloserine is not a specific inhibitor of psychosine synthesis. By inhibiting serine palmitoyl transferase, L-cycloserine greatly perturbs many lipid pathways in the cell. Adverse effects of such a perturbation include the decreased *in vivo* synthesis of myelin, sulfatides, and gangliosides (Sundaram and Lev, 1984), increased CNS GABA levels (Chung et al., 1984), decreased neuronal firing (Haas and Wieser, 1980), and decreased expression of alanine and aspartate aminotransferases in the liver (Cornell et al., 1984).

A more specific inhibitor targeting the enzyme directly responsible for catalyzing psychosine synthesis would likely have a more favorable safety profile. However, that enzyme remains elusive, thwarting all efforts to find a specific inhibitor that targets it. Identifying the *in vivo* pathway of psychosine synthesis would likely spur the discovery of more specific and potent inhibitors of psychosine synthesis that could be translated into the clinic.

1.8.5 Other single therapies

In addition to HSCT, gene therapy, and SRT, numerous other experimental single therapies for Krabbe disease have been published. These include, but are not limited to, enzyme replacement therapy, anti-inflammatory therapies, anti-oxidant therapies, oligodendrocyte transplantation, neuronal stem cell transplantation, mesenchymal stem cell transplantation, molecular chaperones, and GALC enhancers (Mikulka and Sands, 2016). An in-depth discussion of all of these therapies is beyond the scope of this dissertation. However, it is important to note that none of the single therapies published to date, including the gene therapies, have extended Twi lifespan beyond that of the HSCT study published in 1984.

The limited efficacy of single therapies in the treatment of Krabbe disease is worth discussion. Gene therapy alone, which corrects the underlying genetic defect, is an effective therapy for many other simple monogenic disorders such as Leber's congenital amaurosis type 2 (Bainbridge et al., 2008), lipoprotein lipase deficiency (Miller, 2012), and hemophilia B (Nathwani et al., 2011). Krabbe disease, while monogenic, also has a very complex pathophysiology (see discussion in section 1.6). It is likely that targeting only one major pathogenic mechanism as single therapies do is insufficient to effectively correct the disease. With that in mind, we turn to combination therapies to simultaneously target more than one major pathogenic mechanism in Krabbe disease.

1.8.6 Combination therapies

The first combination therapy for Krabbe disease showed that HSCT and SRT synergize and increase Twi lifespan to 112 days (Biswas and LeVine, 2002). Subsequent studies have shown that combination therapies, as a whole, are much more effective than single therapies. Many therapies synergize when administered in combination, which results in significant increases in Twi lifespan. However, not all therapies synergize (Mikulka and Sands, 2016). With the exception of the initial study combining SRT with HSCT, all subsequent therapies that synergize include a combination of gene therapy and HSCT (Reddy et al., 2013; Hawkins-Salsbury et al., 2015; Rafi et al., 2017). This suggests that together, HSCT and gene therapy treat Krabbe disease through an interactive mechanism that requires the presence of both therapies.

Neuroimmunologic studies have shown that Twi mice have profound microgliosis and astrocytosis. Unsurprisingly, perhaps, intracranial and intrathecal injection of AAV2/5 induces significant lymphocytic infiltration into the CNS. In Twi mice, AAV2/5 administration also worsens microgliosis. These findings may explain why AAV2/5 alone has very limited efficacy in

increasing Twi lifespan even though it induces supraphysiologic GALC expression in the Twi CNS. Administration of HSCT with gene therapy abolishes both the disease-specific microgliosis, the AAV-associated microgliosis, and the AAV-associated lymphocytosis (Reddy et al., 2011).

A more recent study showed that intravenous (IV) administration of AAV2/rh10-GALC and HSCT also greatly extended the lifespan of Twi mice (Rafi et al., 2015). Because AAV2/rh10 crosses the blood brain barrier, it is likely that IV injection of the virus resulted in significant expression of GALC in the CNS and peripheral nervous system (PNS), as well as increasing systemic GALC expression. Although no systemic disease has ever been reported in Krabbe, these data suggest that targeting systemic GALC expression in addition to the nervous system contributes to increased Twi survival. This is not surprising, as GALC is expressed in every cell of the body, and is actually most highly expressed in the kidneys. It is likely that GALC has an as yet unknown systemic function whose disease manifestations are masked by the rapidly progressive CNS disease.

Taken together, these results show that gene therapy and HSCT work synergistically by directly targeting at least two major pathogenic mechanisms of Krabbe disease: the underlying genetic defect and neuroinflammation. Addition of L-cycloserine, which directly targets psychosine accumulation, to the gene therapy and HSCT produces an even more dramatic increase in median Twi lifespan to 298.5 days (Hawkins-Salsbury et al., 2015). The mechanism by which L-cycloserine induces synergy is unclear. However, recent studies have shown that L-cycloserine increases the expression of M6PR in the Twi CNS (Hu et al., 2016). Because cross correction relies on the M6PR to supply enzyme to enzyme-deficient cells, increased expression of M6PR would likely increase the number of GALC-deficient cells that are corrected by cross correction.

1.9 Toxicity of Adeno-Associated Viruses

Although AAV vectors have a reputation of low toxicity and low immunogenicity (Naso et al., 2017), they have recently been shown to cause severe acute and chronic toxicity in larger animal models (Hinderer et al., 2018). Rhesus macaques injected intravenously with an AAV2/9 vector encoding survival of motor neuron (SMN) at a dose of $2x10^{14}$ genome copies per kilogram of body weight displayed severe hepatotoxicity. Massive elevation of liver enzymes was observed in all injected monkeys, and one macaque expired within four days of injection from acute shock. Piglets treated with the same vector at the same dosage by weight demonstrated severe neurotoxicity, with all injected animals developing ataxia and paralysis severe enough to require euthanasia within 1-3 days.

Toxicity of adeno-associated viruses is not limited to large animal models. In 2001, the first cases of AAV-induced hepatocellular carcinoma (HCC) were reported in a long-term study of AAV administration in mice (Donsante et al., 2001). Since this publication, numerous other publications have independently shown AAV-induced HCC in mice using different models and AAV vectors. At least four factors significantly increase the penetrance of AAV-induced HCC: 1. Strong liver tropism 2. Increased promoter strength 3. Increased virus dose, and 4. Neonatal delivery of virus (Chandler et al., 2015).

Although AAV is thought of as a non-integrating virus, integration does occur at a significant frequency. *In utero* intravenous AAV2/9 administration in macaques resulted in up to 550,000 unique integration sites in liver genomic DNA (Mattar et al., 2017). The *Rian* locus is an integration hotspot in mice, and AAV integration at this site disrupts the expression of multiple microRNAs embedded within *Rian* (Donsante et al., 2007). Disruption of the *Rian* locus has been shown to cause HCC in mice (Wang et al., 2012).

The *Rian* locus lies in an area of the mouse genome that has a corresponding syntenic region in the human genome. Fortunately, 32/51 of the reported integration sites lie in a 50-bp segment that is unique to the mouse. However, 19/51 integration sites lie in regions that are highly conserved with the human genome (Chandler et al., 2016). Whether or not AAV-induced HCC will translate to humans is unclear, but currently available data suggest that this is a major area of concern. Recurrent clonal insertions of AAV2 have been found in human HCC tumors at a frequency of 5% (Nault et al., 2015). A subset of these integrations resulted in overexpression of *TERT*, a telomerase reverse transcriptase that is overexpressed in ~90% of HCC tumors (Jiao et al., 2018).

The ongoing spinal muscular atrophy type I human clinical trial (Mendell et al., 2017) may be able to determine whether a causative link between AAV administration and human HCC exists. Infants enrolled in this trial received intravenous high-dose AAV2/9 vector encoding SMN. The young age of the patients at treatment, the use of the CMV enhancer/chicken β-actin promoter to induce high levels of gene expression, the high dose of virus, and the IV route of administration make a worrisome combination of factors that may increase the penetrance of AAV-induced HCC. Long-term monitoring of these patients may determine whether AAV-induced HCC is a toxicity that translates to humans.

1.10 Summary

Infantile globoid cell leukodystrophy (Krabbe disease) is a rapidly progressive, pediatric inborn error of metabolism that is remarkably refractory to treatment. This introduction outlined the clinicopathology, the standard of care, the pathophysiology, the animal models, and the experimental therapies for Krabbe disease. Although the field of Krabbe research is advancing

rapidly, there are many unanswered questions that still need to be addressed. One of the most important unanswered questions is the *in vivo* pathway of psychosine synthesis. Although the *in vitro* pathway was putatively identified in 1960, the enzyme that catalyzes the reaction *in vivo* has not been identified. In Chapter 2 of this dissertation, we present data that irrefutably overturn the current dogma of psychosine synthesis by showing that psychosine is synthesized, not anabolically, but catabolically through the deacylation of galactosylceramide by acid ceramidase (ACDase). These data identify ACDase as a target for SRT that is much more specific for psychosine synthesis than the currently-used L-cycloserine. Through this project, we created a GALC-deficient mouse model that does not accumulate psychosine, thereby successfully dissociating GALC deficiency from psychosine accumulation. The observation that this mouse model does not have any signs of Krabbe disease suggests that the longstanding 'Psychosine Hypothesis' is correct, and that psychosine does indeed cause all the signs and symptoms associated with Krabbe. A better understanding of the perturbation of lipid pathways in Krabbe disease may also help to identify new biomarkers that would improve the sensitivity of newborn screening.

Another persistent challenge in the Krabbe field is the lack of an effective therapy. Hematopoietic stem cell transplantation, the current standard of care, is less than ideal due to its limited efficacy and significant toxicities. In recent years, combination therapies that simultaneously target more than one pathogenic mechanism have been shown to be much more effective than single therapies. Despite the progress that has been made, much more work remains to be done. Specifically, the peripheral neuropathy in the Twi mouse has thus far remained stubbornly refractory to treatment. In chapter 3 of this dissertation, we present a combination therapy that pushes the median Twi lifespan significantly beyond what has been reported to date.

Equally importantly, this combination therapy corrects the motor deficits in Twi mice such that many treated mice are still able to perform well on behavioral tests even a few days before death.

Finally, AAV-induced HCC is a challenge not only for the Krabbe community but also for the gene therapy community at large. In the latter part of chapter 3, we present data that show how combination of different therapies with AAV-mediated gene therapy can change the penetrance of AAV-induced HCC. These data are critically important, because it is likely that a cure for Krabbe disease will consist of a multimodal therapy. Only when we are armed with a better understanding of the pathogenesis of AAV-induced HCC can we hope to design viral vectors and therapies to circumvent this unintended, but potentially fatal adverse effect.

1.11 Figure Legends

Figure 1.1. Multiple major pathogenic mechanisms contribute to Krabbe disease. Lack of GALC activity is the underlying defect, which results in accumulation of the cytotoxic metabolite psychosine. Rapid psychosine accumulation in oligodendrocytes and Schwann cells results in myelin destruction and demyelination. Generation of oxidative stress further worsens CNS pathology. Unattenuated microgliosis and astrocytosis result in severe neuroinflammation.

1.12 Figures

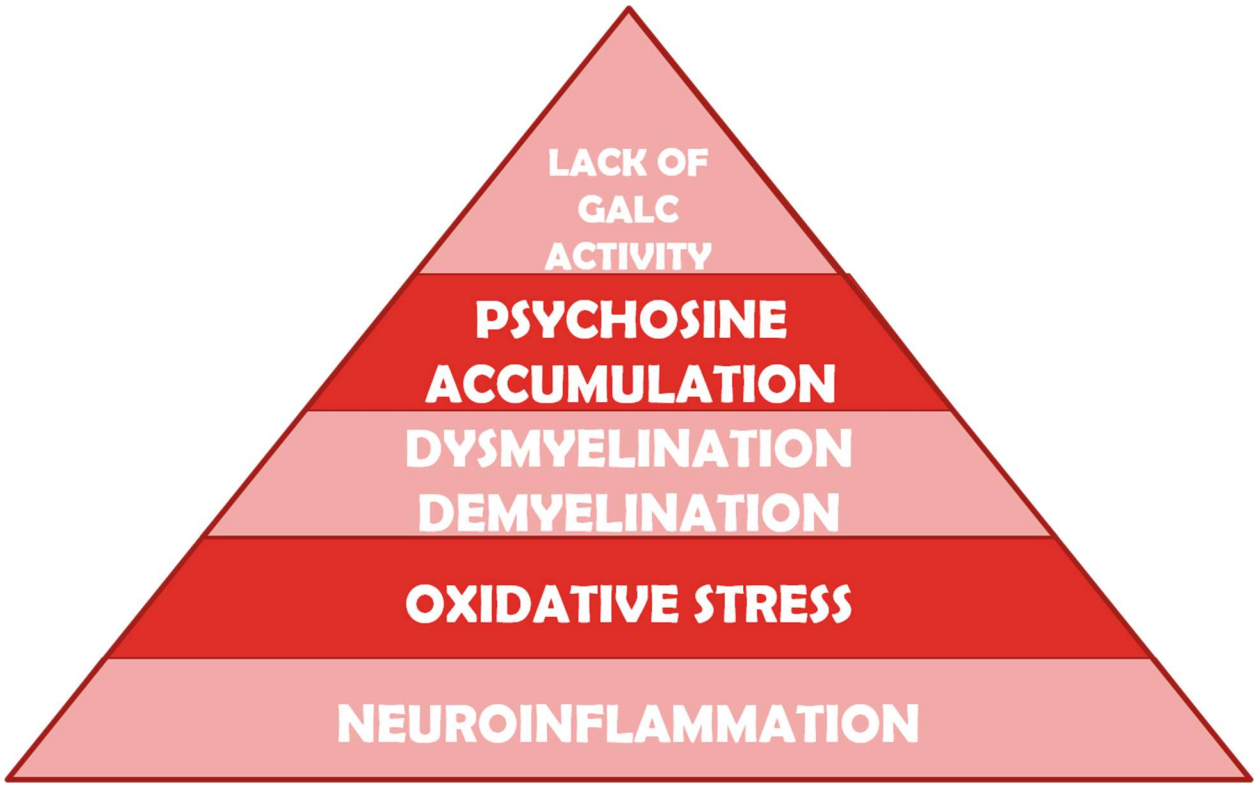

Figure 1 Major pathogenic mechanisms in Krabbe Disease

CHAPTER TWO

Acid Ceramidase: Krabbe Disease, the 'Psychosine Hypothesis,' and a New Therapeutic Target

2.0 Abstract

Infantile globoid cell leukodystrophy (Krabbe disease) is a pediatric demyelinating lysosomal disorder caused by the deficiency of galactosylceramidase (GALC) activity and characterized by the accumulation of the toxic metabolite galactosylsphingosine, commonly referred to as psychosine. Over the past six decades, psychosine was believed to be synthesized anabolically from galactose and sphingosine. However, neither the enzyme nor the cDNA encoding the enzyme responsible for this reaction has been identified. Here, we show that psychosine is generated catabolically through the deacylation of galactosylceramide by acid ceramidase (ACDase). This reaction effectively dissociates GALC deficiency from psychosine accumulation, thus allowing the long-standing 'Psychosine Hypothesis' to be directly tested. We confirm here that psychosine accumulation is the primary disease-causing mechanism in infantile Krabbe disease. Finally, these data identify ACDase as a potential target for substrate reduction therapy. Pharmacological inhibition of ACDase activity significantly prolongs the lifespan of the Twitcher mouse, a faithful model of Krabbe disease.

2.1 Introduction

Infantile globoid cell leukodystrophy (GLD, Krabbe disease) is a rapidly progressive and invariably fatal demyelinating disorder that was first described in 1916 (Krabbe). Krabbe disease is characterized clinically by failure to thrive, limb stiffness, seizures, developmental regression, and death by 2-4 years of age (Wenger et al., 2016). The disease is caused by the deficiency of the lysosomal enzyme, galactosylceramidase (GALC). Galactosylceramidase cleaves the terminal galactose from galactosylated lipids, including the myelin lipid, galactosylceramide, and the cytotoxic lipid, galactosylsphingosine (psychosine).

Psychosine is a cytotoxic metabolite that accumulates most rapidly in oligodendrocytes and Schwann cells *in vivo* (Suzuki and Suzuki, 1983). In 1972, the 'Psychosine Hypothesis' was proposed, stating that psychosine accumulation is the primary cause of disease manifestations in GLD (Miyatake and Suzuki, 1972). The 'Psychosine Hypothesis' has never been formally tested due to the inability to dissociate GALC deficiency from psychosine accumulation.

A seminal study published ~60 years ago concluded that psychosine is synthesized anabolically from sphingosine and galactose (Cleland and Kennedy, 1960). A subsequent study indirectly supported these data by suggesting that the catabolic deacylation of galactosylceramide to psychosine does not occur (Lin and Radin, 1973). Together, these studies established the paradigm that psychosine is synthesized via an anabolic pathway (Figure 2.1). However, the enzyme catalyzing this reaction *in vivo* remains elusive.

The deacylation of glucosylceramide to glucosylsphingosine by acid ceramidase (ACDase) is a reaction that closely parallels the hypothetical deacylation of galactosylceramide to galactosylsphingosine. Since neither the enzyme nor the cDNA responsible for psychosine

synthesis has ever been identified, and because galactose is the stereoisomer of glucose, we hypothesized that ACDase may also catalyze the deacylation of galactosylceramide to psychosine.

The availability of a tractable mouse model of ACDase deficiency (*Asah1*$^{P361R/P361R}$, Farber disease, FD) (Alayoubi et al., 2013) has enabled us to directly test this hypothesis *in vivo*. The Farber mouse is a model of Farber disease, an inherited pediatric lysosomal storage disorder of ceramide accumulation. Patients with Farber disease present in infancy with hoarseness, arthritis, and subcutaneous nodules due to laryngeal, joint, and subcutaneous accumulation of ceramide, respectively (Levade et al., 1995). Disease progression is characterized by severe hepatosplenomegaly, impaired growth, and psychomotor retardation, with death usually occurring before two years of age (Haraoka et al., 1997).

A number of different mutations in the *ASAH1* gene causes low acid ceramidase activity and Farber disease in human patients. The Farber mouse has a knock-in of a known human *ASAH1* mutation (P361R), which gives rise to a hypomorphic ACDase protein product. This model faithfully recapitulates many clinical features of human Farber disease, including severe hepatosplenomegaly and subcutaneous ceramide accumulation. More importantly, the Farber mouse recapitulates the lipid profile of Farber patients, with massive elevations in all ceramide species (Alayoubi et al., 2013).

We bred the *Asah1*$^{P361R/P361R}$ mutation onto the Twitcher (*GALC*$^{-/-}$, Twi) mouse, a murine model that closely mimics the biochemical, histological and clinical features of Krabbe disease (Kobayashi et al., 1980; Duchen et al., 1980; Suzuki and Suzuki, 1983). The drastic phenotypic differences between the Twi mice and the Farber mice (Table 1) facilitate the characterization of the *GALC*$^{-/-}$*Asah1*$^{P361R/P361R}$ Twitcher/Farber (Twi/FD) double mutant in reference to these mice.

We show here that Twi/FD mice have normal levels of psychosine, exhibit none of the characteristic Twi phenotypes, and appear nearly identical to Farber mice. These results demonstrate that psychosine production *in vivo* is mediated by the ACDase-catalyzed catabolic deacylation of galactosylceramide. The lack of psychosine accumulation in the context of GALC deficiency and the nearly complete absence of the Twi phenotype in the Twi/FD double mutant also confirm the long held 'Psychosine Hypothesis.'

Substrate reduction therapy (SRT) that targets psychosine accumulation can partially ameliorate the signs of Krabbe disease in the Twi mouse (Levine et al., 2000). However, current SRT compounds do not directly inhibit psychosine synthesis; rather they decrease the production of galactosylceramide by disrupting upstream synthetic pathways (Sundaram and Lev, 1984; Sundaram and Lev, 1985). The data presented here suggest that ACDase could be a novel and direct SRT target for the treatment of Krabbe disease. We show that pharmacologic inhibition of ACDase activity by the chemotherapeutic drug Carmofur decreases psychosine accumulation and significantly prolongs the lifespan of Twi mice. Taken together, these data greatly advance our understanding of the underlying pathogenic mechanisms leading to GLD and provide the impetus to search for safer and more potent ACDase inhibitors as SRT drugs in the treatment of GLD.

2.2 Results

2.2.1 Acid ceramidase catalyzes the catabolic formation of psychosine

The deacylation of glucosylceramide to glucosylsphingosine is known to be catalyzed by ACDase (Yamaguchi et al., 1994; Ferraz et al., 2016). Since galactose is structurally related to glucose, its stereoisomer, we hypothesized that ACDase may also catalyze the production of psychosine from galactosylceramide. In a pure *in vitro* system we showed that recombinant

ACDase can remove the fatty acyl chain from galactosylceramide to produce psychosine. The addition of carmofur, an inhibitor of ACDase activity (Realini et al., 2013), eliminated psychosine formation. (Fig. 2.2A) In order to determine if the same reaction occurs *in vivo*, we established a cell culture system using primary fibroblasts from GALC- and ACDase-deficient mice. Cells were cultured from Twi mice that also harbored a homozygous mutation (*Asah1*$^{P361R/P361R}$) in the ACDase gene which results in Farber disease (FD) (Alayoubi et al., 2013). Relatively high levels of psychosine and ceramide were measured in Twi and FD fibroblasts, respectively. Fibroblasts from double mutant (*GALC*$^{-/-}$/*Asah1*$^{P361R/P361R}$, Twi/FD) mice accumulated high levels of ceramide but <u>not</u> psychosine. This is consistent with the data showing that ACDase is responsible for psychosine production *in vitro*. Importantly, reconstitution of ACDase activity following lentiviral transduction of Twi/FD fibroblasts resulted in the accumulation of high levels of psychosine (Fig 2.2B).

To determine if ACDase catalyzes the formation of psychosine in an intact animal, we characterized the Twi/FD double mutant mice. The levels of psychosine in Twi/FD brain, liver, spleen, and sciatic nerve were indistinguishable from those in wild type (WT) animals and significantly lower than those in Twi mice (Fig. 2.3). Ceramide elevation due to absence of ACDase activity was observed in FD and Twi/FD mice, but not in WT or Twi mice. (Fig. 2.4). Galactosylceramides were elevated in Twi/FD mice, but not in WT, Twi or FD mice. (Fig. 2.5) Together, these data strongly suggest that the deacylation of galactosylceramide by acid ceramidase is the primary, if not only, mechanism that leads to psychosine production *in vivo*.

2.2.2 Testing and confirmation of the 'Psychosine Hypothesis'

In the Twi/FD mouse, GALC deficiency is effectively dissociated from psychosine accumulation. This allowed us to directly test the longstanding 'Psychosine Hypothesis', which

states that psychosine accumulation is the primary cause of the clinical manifestations of Krabbe disease (Miyatake and Suzuki, 1972). The median lifespan of Twi/FD mice (63d) was significantly longer than that of Twi mice (42d) and slightly shorter than that of FD mice (74d) (Fig. 2.6). The mean maximum body weight of Twi/FD mice was 18.1±1.8 g, which was virtually identical to FD mice (18.2±1.9g) and significantly greater than Twi mice (12.2±1.9g). (Fig. 2.7A) Both Twi/FD and FD mice had splenomegaly and thymic hypertrophy compared to WT and Twi mice. (Fig. 2.7B) The hematological abnormalities in Twi/FD mice were similar to those in FD mice with larger circulating monocyte ($Ly6G^{-}Ly6C^{hi}$) and neutrophil ($Ly6G^{+}Ly6C^{+}$) populations, and significantly smaller T lymphocyte ($CD3^{+}$) populations compared to WT and Twi mice. (Fig. 2.8)

Tremor is a defining characteristic of the Twi mouse (Duchen et al., 1980). At 36 days, the peak tremor frequencies (PTFs) observed in Twi/FD and FD mice (9.0±4.0 Hz and 8.6±2.2 Hz, respectively) were not different from WT animals. In contrast, 36-day-old Twi mice had a PTF of 17.4±2.2 Hz. By 63 days, tremor was observed in both Twi/FD (14.6±5.9 Hz) and FD (16.6±3.7 Hz) mice. There was no significant difference in PTF between Twi/FD and FD mice at either time point. (Fig. 2.9)

Motor function in Twi/FD mice was assessed by the rotarod (Fig. 2.10A) and wirehang (Fig. 2.10B) tests at two time points. The first, 36 days, represents a time point when Twi mice are severely affected but FD mice are virtually asymptomatic; the second, 63 days, is when all the Twi mice have died and FD mice have measurable motor deficits. At 36 days, Twi/FD and FD mice consistently performed near WT levels on both the rotarod and wirehang tests. In contrast, Twi mice exhibited significant deficits on both tests. At 63d, Twi/FD and FD mice exhibited significant motor deficits in both rotarod and wirehang performance, although they still performed the wirehang test better than 36-day-old Twi mice.

There are various differentiating histological features in the Twi and the FD mice, thus facilitating comparative histological analysis of Twi/FD mice (Figure 2.11A). Cerebellar inclusions and microgliosis were observed in Twi, FD, and Twi/FD mice, but the inclusion patterns were different for the different genotypes. In Twi mice, the macrophages had a multifocal distribution without clustering. In addition, the white matter was abnormal with evidence of myelin loss. In FD mice, the macrophages were in clusters in the white matter and perivascular spaces. Twitcher/FD mice resembled FD mice, with much less storage macrophages scattered throughout the white matter compared to Twi mice. In addition, Twi/FD mice showed no evidence of demyelination.

Microglial activation was diffuse in Twi mice, but patchy and concentrated at multiple foci in FD mice. Twitcher/FD mice had a mixed phenotype, with very low intensity, diffuse microglial activation, as well as focal areas of cerebellar microglial aggregation that were smaller than those in FD mice.

Twitcher spleens had inflammatory infiltrates, while the spleens of FD mice and Twi/FD double mutants were vacuolated. However, splenic vacuolization was less severe in Twi/FD mice. In Twi mice, destruction of sciatic nerve structure was coupled with significant inflammatory infiltrate, decreased myelination, and edema. Sciatic nerves from FD mice and Twi/FD mice, however, had significantly less inflammatory infiltrate, with mostly intact axonal structures. Quantification of axon density showed normal axon counts in Twi/FD and FD mice, compared to a profoundly decreased axon count in Twi mice. (Fig. 2.11B)

2.2.3 Pharmacological inhibition of acid ceramidase activity

Because the hypomorphic *Asah1*$^{P361R/P361R}$ mutation essentially eliminates both psychosine accumulation and the Krabbe disease phenotype, we hypothesized that pharmacologic inhibition

of ACDase activity could result in clinical benefits in the Twi mouse. Carmofur is a 5-fluorouracil-releasing chemotherapeutic agent currently used in the treatment of colorectal cancer (Kubota et al., 1991; Watanabe et al., 2006). It is also an effective inhibitor of ACDase activity when administered *in vivo* (Realini et al., 2013). Intraperitoneal Carmofur administration significantly increased the median lifespan of Twi/FDH mice compared to vehicle-treated Twi/FDH mice (46d versus 40d, respectively). (Fig. 2.12A) Interestingly, Carmofur administration did not increase the median lifespan of Twi mice that were WT at the *ASAH1* locus. (Fig. 2.12B) Importantly, Carmofur administration directly decreased psychosine synthesis (Fig. 2.13A), but did not alter ceramide levels (Fig. 2.13B) in both Twi and Twi/FDH mice.

2.3 Discussion

Psychosine plays a critical role in the pathogenesis of Krabbe disease. However, the *in vivo* synthetic pathway of this cytotoxic lipid remains unclear. Although two publications from 1960 (Cleland and Kennedy, 1960) and 1973 (Lin and Radin, 1973) independently suggested that psychosine production occurs by the anabolic dehydration of galactose and ceramide, the enzyme that catalyzes this reaction remains a mystery. In this study, we overturn those data and provide incontrovertible evidence showing that psychosine is synthesized through the catabolic deacylation of galactosylceramide. We further identify the enzyme catalyzing this reaction *in vivo* as ACDase.

The Twi/FD mouse is an experimental system that dissociates GALC deficiency from psychosine accumulation. This allows the testing of the longstanding ‘Psychosine Hypothesis.’ Clinicobehavioral and histological analysis of the Twi/FD mouse show that the absence of

psychosine accumulation in GALC deficient mice essentially eliminates the Twi phenotype. These data confirm the 'Psychosine Hypothesis,' at least within the lifespan of the Twi/FD mouse.

We believe that the slight but significant shortening of lifespan in Twi/FD mice is due to the unique accumulation of galactosylceramide, which is a secondary consequence of concurrent GALC and ACDase deficiency. These data clarify that both GALC and ACDase participate in the *in vivo* metabolism of galactosylceramide, which explains the confounding observation that Twi mice do not accumulate high levels of galactosylceramide (Eto et al., 1970). Given the shortened lifespan of Twi/ACD mice, it is likely that supraphysiologic levels of galactosylceramide accumulation is toxic, albeit to a lesser extent than psychosine. A detailed description of the pathological effects of galactosylceramide accumulation remains to be determined.

Absence of the classic Twi phenotype in Twi/FD mice suggests that ACDase might be a novel target of SRT for Krabbe disease. Experimental SRT for Krabbe disease has been limited to L-cycloserine, which indirectly reduces psychosine accumulation by inhibiting serine palmitoyl transferase, an enzyme several steps upstream of psychosine synthesis (LeVine et al., 2000). As such, it disrupts many other critical sphingolipid pathways (Sundaram and Lev, 1984; Sundaram and Lev, 1985). Although L-cycloserine has been instrumental for proof-of-concept experiments in the Twi mouse, it is neither efficient nor specific. We hypothesized that decreasing psychosine accumulation directly by pharmacological inhibition of ACDase activity could provide clinical benefits to the Twi mouse. We performed a proof-of-concept experiment by pharmacologically inhibiting ACDase activity in the Twi mouse via Carmofur administration. Although Carmofur administration significantly increased the median lifespan of Twi/FDH, this effect was not observed in Twi mice. The increased therapeutic efficacy of Carmofur administration in Twi/FDH mice suggests that there is a threshold of ACDase activity inhibition that must be reached to

produce therapeutic efficacy for Krabbe disease. Importantly, Carmofur administration did not increase ceramide accumulation in the liver even though psychosine levels were decreased by nearly 90% compared to vehicle-treated Twi mice. This suggests that there may be an acceptable therapeutic window in which ACDase activity can be sufficiently inhibited to decrease psychosine accumulation without inducing concurrent ceramide accumulation and Farber disease.

By its very nature, SRT should slow disease progression, not provide a cure. Therefore, it is not surprising that Carmofur partially corrects the Krabbe phenotype, even in Twi/FDH mice. We used Carmofur as a commercially-available, proof-of-concept tool to demonstrate the viability of pharmacologic ACDase inhibition as an SRT target in Krabbe disease. Carmofur was not designed as a specific inhibitor of ACDase activity. Therefore, it seems likely that a more specific and potent inhibitor of ACDase activity could increase therapeutic efficacy in Krabbe disease. Substrate reduction therapy has been shown to synergize dramatically with other therapies in the treatment of Krabbe disease (Biswas and LeVine, 2002; Hawkins-Salsbury et al., 2015), and the incorporation of a potent ACDase inhibitor into a combination therapy regimen would likely greatly enhance therapeutic efficacy.

Finally, it is important to note that in all clinicobehavioral and histological phenotypes, Twi mice heterozygous at the *ASAH1* locus (*GALC*$^{-/-}$/*Asah1*$^{+/P361R}$, Twi/FDH) were indistinguishable from Twi mice. Conversely, FD mice heterozygous at the *GALC* locus (*GALC*$^{+/-}$/*Asah1*$^{P361R/P361R}$) were indistinguishable from FD mice. These observations suggest that heterozygosity at the *GALC* and the *ASAH1* loci do not affect the phenotypes of FD and Twi mice, respectively, at least within the ages at which these mice were examined. This is not surprising, as most heterozygous carriers of inborn errors of metabolism are phenotypically normal. Those who

do develop phenotypic abnormalities generally do so at an advanced age that would be well beyond the ages of the mice that were analyzed in this study (Liu et al., 2011; Lee et al., 2015).

Taken together, the results from this study overturn the nearly 60-year-old dogma stating that psychosine is produced through an anabolic pathway. We show instead that psychosine is generated catabolically *in vitro* and *in vivo* by the deacylation of galactosylceramide by ACDase. These data also explain the lack of galactosylceramide accumulation in the human and murine Krabbe brains (Eto et al., 1970; Svennerholm et al., 1980). Here, we also confirm the longstanding 'Psychosine Hypothesis,' by demonstrating that GALC-deficient mice do not develop the Krabbe phenotypes in the absence of psychosine accumulation. Finally, we identify ACDase as a novel SRT target, providing the impetus to discover safer and more effective inhibitors for the treatment of Krabbe disease.

2.4 Methods

2.4.1 Experimental animals

Animals were housed at Washington University in St. Louis under the supervision of MSS. Heterozygous Twi ($GALC^{+/-}$) mice on a C57BL6 background (Jackson Laboratory, Maine, USA) were bred with heterozygous FD ($Asah1^{+/-}$) mice on a mixed C57BL6 and 129S6 background. Genotypes of all experimental mice were determined by PCR, as previously described for the Twi mouse (Sakai et al., 1996; Lin et al., 2005) and the FD mouse (Alayoubi et al., 2013). Mice were housed under standard conditions with *ad libitum* access to food and water. Mice were maintained on a 12 hr/12 hr light/dark cycle. All animal procedures were approved by the Institutional Animal Studies Committee at Washington University School of Medicine and were in accordance with the guidelines of the National Institutes of Health.

2.4.2 Psychosine production in vitro

To determine whether ACDase could directly cleave glycosphingolipids, 20uM of C12-NBD-galactosylceramides (Cayman Chemical) were incubated with 5-10ug of purified acid ceramidase in a 30 ul of reaction containing 15 ul of 0.2M citrate phosphate buffer (pH 4.5), 2.25 ul of 2M NaCl, 1.5ul of 10 mg/ml BSA, and 0.3 ul 10% IGEPAL CA630. The reaction was incubated at 37ºC for 18 hours without agitation and then stopped by adding 60 uL methanol. The amount of NBD-psychosine released by the action of the enzyme was determined by Acquity UPLC (excitation, 435nm; emission, 525nm).

2.4.3 Lentivirus preparation

The ASAH1 and α-galactosidase A (AGA) cDNAs were cloned into the lentiviral transfer plasmid (pDY) to generate pDY-hASAH1 and pDY-AGA as previously described (Alayoubi et al., 2013). Lentiviral stocks were prepared by transient transfection of HEK293T cells using a four-plasmid system (pCMVΔR8.91, pMD.G, pAdV and the transfer plasmids) and concentrated by centrifugation. Concentrated viral stocks were titered on HEK293T cells and vector copy number was determined by quantitative PCR.

2.4.4 Fibroblast transduction

Primary subdermal fibroblasts from FD and Twi mice were isolated from newborn animals and grown in DMEM supplemented with 10% heat-inactivated FBS, 10 mM HEPES buffer, MEM non-essential amino acid solution, 1mM sodium pyruvate, and 1% penicillin/streptomycin under 5% pCO2 at 37°C. Cells were transduced with lentivirus expressing acid ceramidase (*Asah1*) or aspartylglucosaminidase (control) with a multiplicity of infection of 50. Serum level was dropped to 1% 72 hours after transduction. Fibroblasts were maintained at 1% serum level for one week, after which they were harvested, pelleted, and stored at -70°C for metabolic analyses.

2.4.5 Mass spectrometry

Galactosylsphingosine (psychosine), galactosylceramide, and ceramides were measured in brain, liver, sciatic nerve, and spleen, essentially as previously described (Sikora et al., 2017). Galactosylsphingosine and galactosylceramide were separated from glucosylsphingosine and glucosylceramide by hydrophilic interaction liquid chromatography (HILIC) columns. Ceramides were separated on two-dimensional chromatography by HILIC column in the first dimension and by reversed phase column in the second dimension. Multiple reaction monitoring (MRM) was used to detect galactosylsphingosine, ceramide, and galactosylceramide on an AB SCIEX 4000QTRAP tandem mass spectrometer in positive ESI mode. Data processing was conducted with Analyst 1.5.2 (Applied Biosystems). Data are reported as the peak area ratios of lipids to their internal standards.

2.4.6 Flow cytometry

Circulating hematopoietic-derived cells from experimental and control animals were identified and quantified by fluorescence-activated cell sorting. Red blood cells were lysed, and cells were stained with 7AAD (vital stain) and fluorophore-conjugated antibodies after blocking with Fc receptor. The following antibodies were used: FITC rat anti-mouse CD3 (T-cells, BD Biosciences), APC rat anti-mouse CD11b (monocytes, BD Biosciences), PEcy7 anti-mouse Ly6G (monocytes, neutrophils), and eFluor 450 rat anti-mouse Ly6C (monocytes, neutrophils, E-Biosciences). Data were acquired on the Gallios flow cytometer (Beckman Coulter), and analyzed using FlowJo software (Tree Star).

2.4.7 Histology

After mice were deeply anesthetized and perfused with phosphate-buffered saline, spleen, liver, and one sagittal half of brain were harvested immediately. Tissue samples were

cryoprotected in 30% sucrose after being fixed in 4% paraformaldehyde in phosphate buffer for 24-48 hours at 4°C. Tissues were embedded in paraffin for Luxol fast blue and periodic Acid-Schiff (LFB/PAS) staining. Ten micron sections were mounted on slides for analysis.

Sciatic nerves were isolated following perfusion with phosphate buffer and fixed in 4% paraformaldehyde/2% glutaraldehyde in phosphate buffer. Nerves were incubated in osmium tetroxide and then dehydrated in ethanol. After embedding in Araldite 502 (Polysciences), one μm sections were prepared using an ultramicrotome and stained with toluidine blue. After mounting on slides, images were acquired using the Hitachi CCD KP-MIAN digitizing camera mounted on a Leitz Laborlux S microscope. Histomorphometric analysis was carried out using the Leco IA32 Image Analysis System.

2.4.8 Behavioral testing

Behavioral testing consisted of the rotarod and wirehang tests, which were conducted as previously reported (Hawkins-Salsbury et al., 2015). Mice were tested once every other week on the rotarod and once every week on the wirehang. Performance was measured as the time it took the mouse to fall from either apparatus. Three trials were run for each test, and the average of the three trials was reported. For both tests, the maximum tested time was 60 seconds. Each group contained at least n=10 animals.

2.4.9 Actometer testing

Tremor severity was quantified using a custom-made force-plate actometer as previously described (Fowler et al., 2001; Reddy et al., 2011). Maximum tremor frequency was reported for each mouse. At least 10 mice per experimental group were tested.

2.4.10 Immunohistochemistry

One sagittal half of each brain was harvested immediately following perfusion with phosphate-buffered saline and fixed in 4% paraformaldehyde for 24-48 hours at 4°C and cryoprotected in 30% sucrose. Sixteen micron sections were blocked in normal goat serum then incubated with primary rabbit anti-mouse GFAP (Immunostar) antibody or rat anti-mouse CD68 (BioRad), as previously described (Reddy et al., 2011). The sections were then incubated in the appropriate horse radish peroxidase-conjugated secondary antibody and developed with a commercially available DAB kit (Vector Laboratories).

2.4.11 Carmofur administration

Carmofur was obtained from LKT Laboratories. A stock solution of 300 mg/kg solution was made in dimethylsulfoxide (DMSO) and stored at -20°C. Stock solutions were diluted in Solutol (Sigma-Aldrich) and citrate buffer to make the 30 mg/kg working solution immediately prior to each injection. Starting at postnatal day 10, all experimental animals received intraperitoneal injections of 30 mg/kg Carmofur every 12 hours for the remainder of their lives. Control animals received the same dose of DMSO, Solutol citrate solution.

2.4.12 Statistical analysis

Statistical significance was calculated using the one-way ANOVA with a Bonferroni correction for multiple comparisons, unless otherwise specified. P values are denoted as follows: *$p < 0.05$; **$p < 0.01$; ***$p < 0.001$; n.s. denotes not significant, $p \geq 0.05$.

2.5 Tables

Table 2.1 Comparison of the Twitcher vs. Farber murine phenotypes

Attribute	Twitcher	Farber
Average lifespan	~40 days	~70 days
Max weight	~12 g	~20 g
Spleen size	No Δ	↑↑↑
Thymus size	No Δ	↑↑↑
Ceramides	No Δ	↑↑↑↑
Psychosine	↑↑↑↑	No Δ

Table 2.1 Phenotypes that differ significantly between Twi mice and FD mice include average lifespan, body weight, spleen and thymus size, ceramide accumulation, and psychosine accumulation.

2.6 Figure Legends

Figure 2.1. Potential pathways of psychosine synthesis. Psychosine can be synthesized either through the anabolic dehydration of sphingosine and galactose (left), or through the catabolic deacylation of galactosylceramide (right). Two studies have directly (Cleland and Kennedy, 1960) or indirectly (Lin and Radin, 1973) supported the anabolic pathway. We show here that acid ceramidase (ACDase) catalyzes the catabolic production of psychosine *in vitro* and *in vivo*.

Figure 2.2. Acid ceramidase catalyzes the *in vitro* formation of psychosine.** (A) Recombinant ACDase catalyzes the conversion of galactosylceramide (GalCer) to psychosine *in vitro*. Addition of Carmofur, an inhibitor of ACDase activity, prevents psychosine formation. (B) Twitcher (Twi) fibroblasts accumulate psychosine compared to WT, FD, and Twi/FD (Twi/FD untransduced) fibroblasts. Reconstitution of ACDase activity following lentiviral transduction of Twi/FD fibroblasts dramatically increases psychosine accumulation in these cells (Twi/FD LV-ACDase).

Figure 2.3. Acid ceramidase catalyzes the *in vivo* formation of psychosine.** Psychosine is elevated in brain, sciatic nerve, liver, and spleen in Twi and Twi/FDH mice at 36d and terminal age. There is no elevation of psychosine in WT, FD, or Twi/FD mice at either time point.

Figure 2.4. Ceramides* are elevated in FD and Twi/FD mice at 36d and terminal age** in brain, liver, and spleen. In contrast, elevations in ceramide species are not observed in WT, Twi, or Twi/FDH mice at either time point.

Figure 2.5. Accumulation of galactosylceramides* is unique to Twi/FD double mutant mice.** Galactosylceramide elevation is observed in brain, liver, and spleen of Twi/FD mice, but not in Twi, FD, or WT mice.

Figure 2.6. Acid ceramidase deficiency significantly increases lifespan of Twi/FD. Median lifespan of Twi/FD mice (63d) is significantly longer than that of Twi mice (42d) and slightly shorter than that of FD mice (74d). No WT mice died during the course of this study.

Figure 2.7. Acid ceramidase deficiency significantly increases body weight, spleen weight, and thymus weight in Twi/FD mice. The **(A)** mean maximum body weight and normalized **(B)** spleen and **(C)** thymus weights in Twi/FD mice are not significantly different from those in FD mice, but are significantly greater than those in Twi mice.

Figure 2.8. Twitcher/FD and FD mice have fewer increased blood neutrophil and monocytes, and fewer blood T cells than WT mice. (A) Blood neutrophil and **(B)** monocyte populations are increased in Twi/FD and FD mice compared to WT mice. **(C)** The blood T cell population is decreased in Twi/FD and FD mice than in WT mice.

Figure 2.9. Acid ceramidase deficiency attenuates tremor in Twi/FD mice. Peak tremor frequencies show that there is prominent tremor in Twi mice but not in WT, Twi/FD or FD mice at 5 weeks of age. Tremor is more pronounced in FD and Twi/FD at 9 weeks of age.

Figure 2.10. Acid ceramidase deficiency normalizes motor function in Twi/FD mice. Twi mice have significant motor deficits as measured by the **(A)** rotarod and the **(B)** wirehang tests compared to WT, FD, and Twi/FD mice at 5 weeks of age. Functional impairment in both behavioral tests becomes more severe in FD and Twi/FD mice at 9 weeks of age.

Figure 2.11. Histology of Twi/FD mice is virtually indistinguishable from that of FD mice. (A) Cerebellar inclusions are present in Twi, FD, and Twi/FD mice (black arrows). Twi mice have diffuse distribution of macrophages and abnormal myelination in white matter. In FD mice, macrophages (PAS-positive globoid cells) cluster in white matter and perivascular spaces. Twitcher/FD mice resemble FD mice, and have much fewer storage macrophages scattered

throughout the white matter than Twi mice. Furthermore, Twi/FD mice also have less demyelination than Twi mice. **(B)** $CD68^+$ microgliosis (brown staining) is widespread and more uniform in Twi mice than in Twi/FD and FD mice. There are focal areas of $CD68^+$ microgliosis in FD cerebellum. Twitcher/FD mice also have a hybrid phenotype, with mild and diffuse $CD68^+$ microgliosis throughout the cerebellum with small focal areas of microglial activation (purple arrows). Microglial aggregates in Twi/FD mice are also smaller than those seen in FD mice. **(C)** Twitcher spleens are characterized by dense inflammatory infiltrate, whereas the spleens of FD mice and Twi/FD double mutants are vacuolated (vacuolization outlined by red arrows). Splenic vacuolization is less severe in Twi/FD mice. **(D)** Sciatic nerve structural integrity is severely compromised in Twi mice. Significant inflammatory infiltrate, decreased myelination, and edema are also observed. In FD and Twi/FD mice, sciatic nerve structure is preserved, although there is mild inflammatory infiltrate (green arrows). **(E)** Axon quantification shows low axon count in Twi mice compared to WT, Twi/FD, and FD mice.

Figure 2.12. Pharmacologic inhibition of acid ceramidase activity increases the lifespan of Twi/FDH mice. Carmofur administration significantly increases the median lifespan of **(A)** Twi/FDH mice but not of **(B)** Twi mice compared to vehicle controls.

Figure 2.13. Carmofur administration reduces psychosine accumulation but does not increase ceramide* levels.** Carmofur administration significantly reduces **(A)** CNS psychosine accumulation in Twi and Twi/FDH mice, but does not alter **(B)** liver ceramide levels in Twi or Twi/FDH mice.

* Only data for 16:0 species of ceramides and galactosylceramides are shown. The other species show similar expression patterns amongst the different genotypes.

** Data are reported as the peak area ratios of lipids to their internal standards.

2.7 Figures

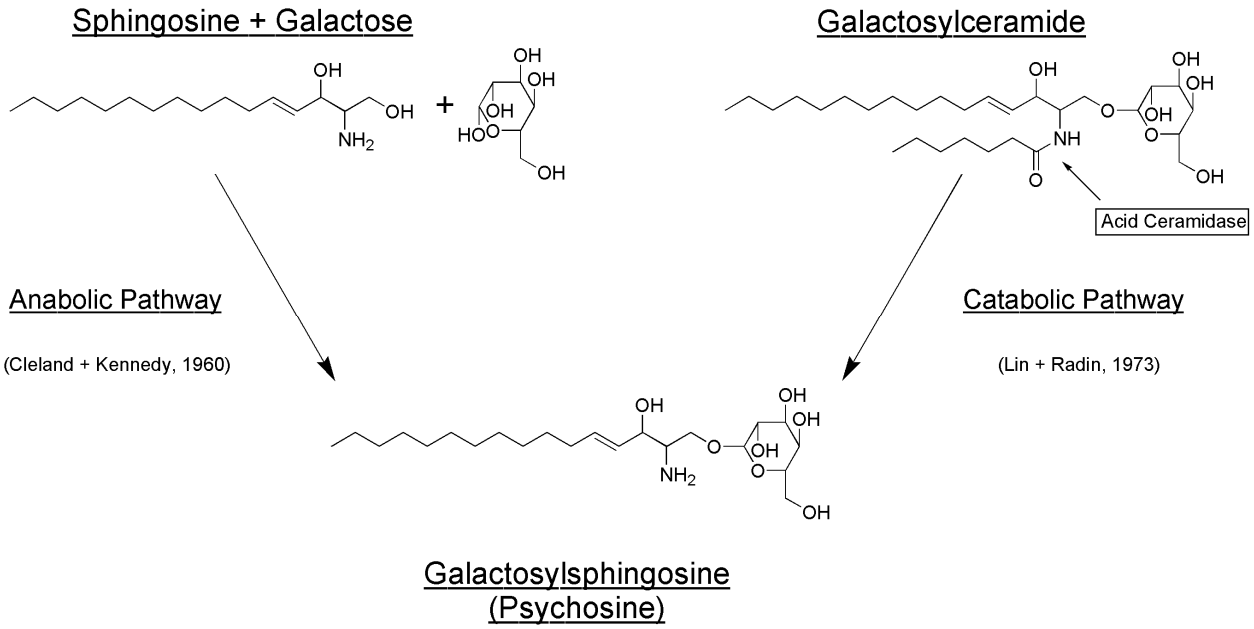

Figure 2.1 Potential pathways of psychosine synthesis

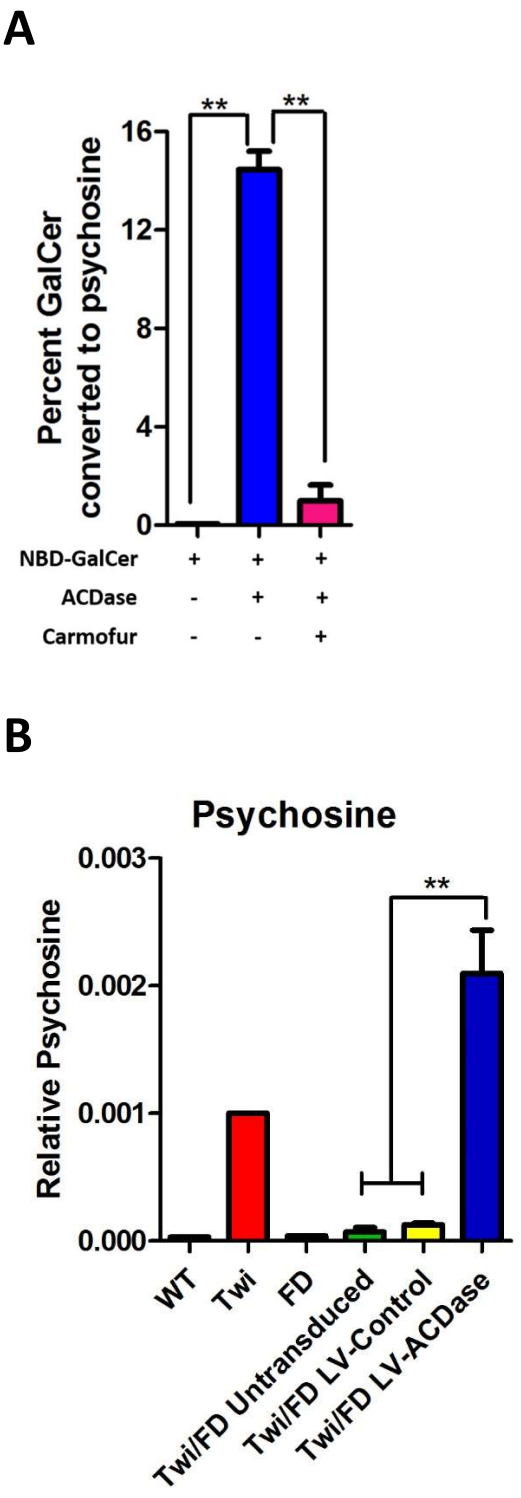

Figure 2.2 *In vitro* psychosine formation**

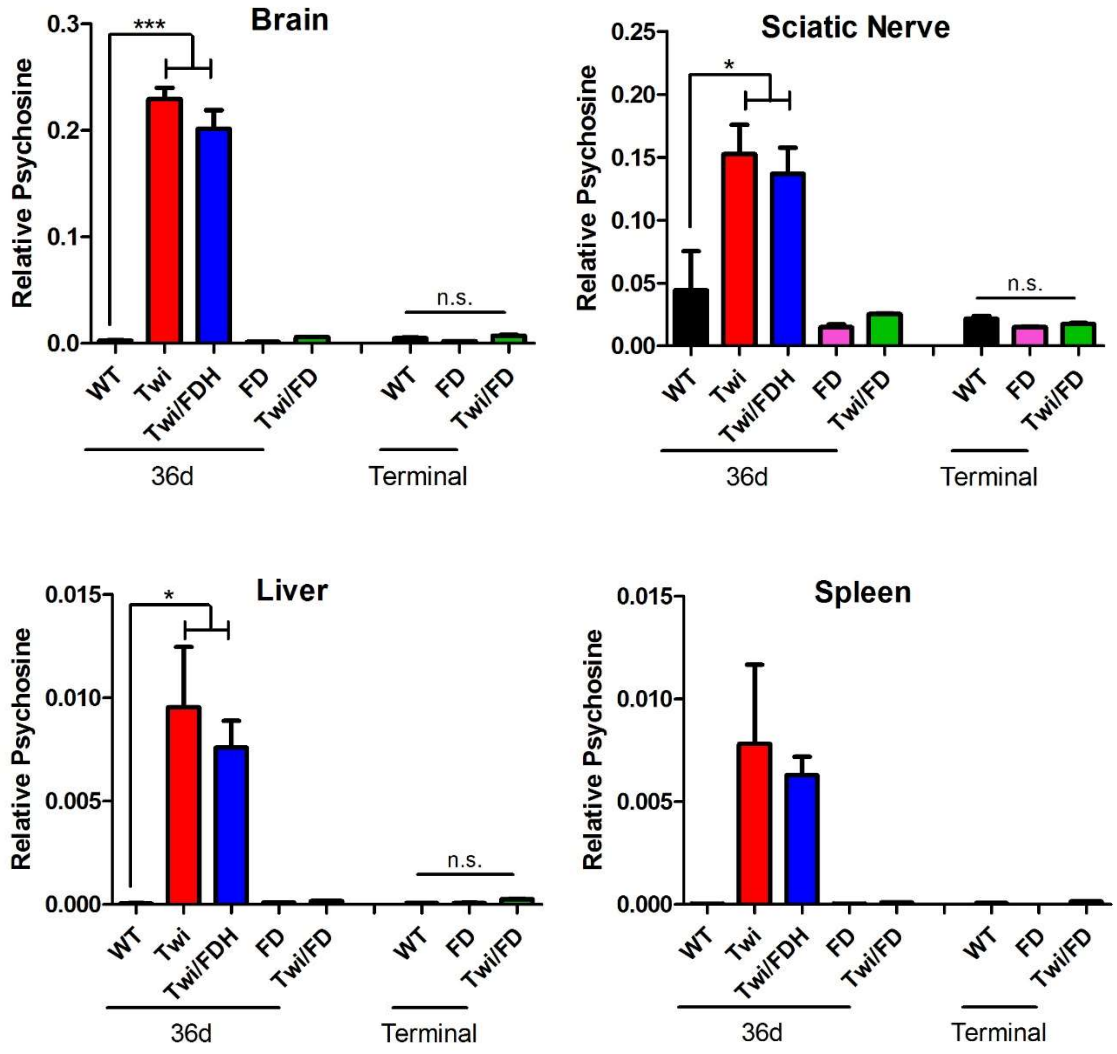

Figure 2.3 *In vivo* psychosine accumulation**

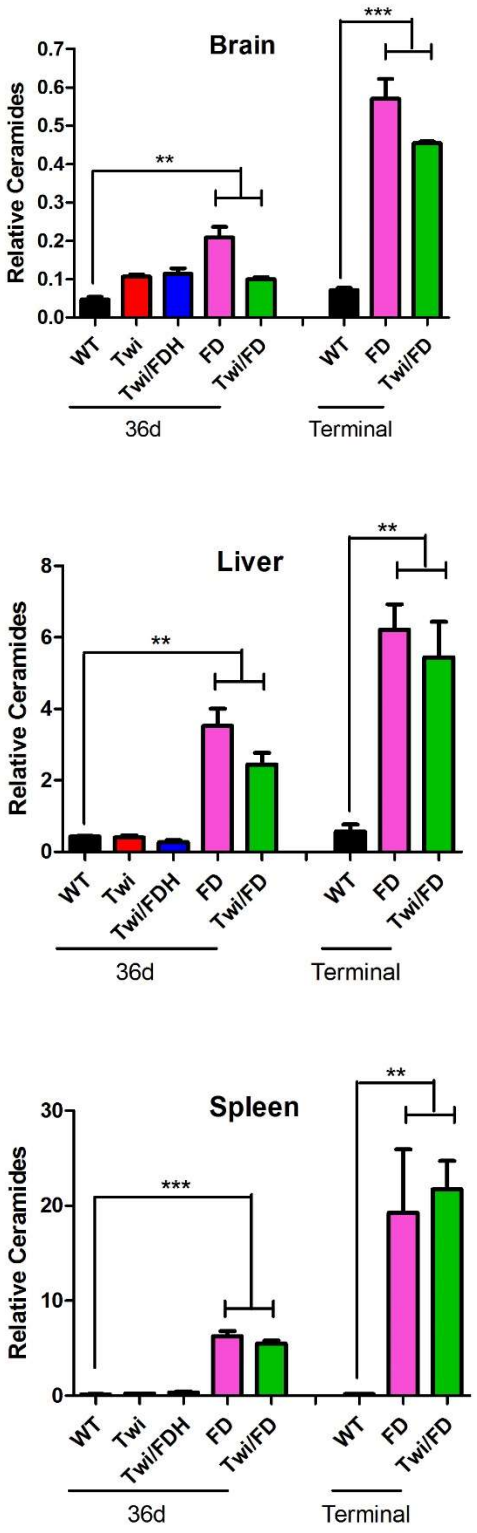

Figure 2.4 Ceramide accumulation*, **

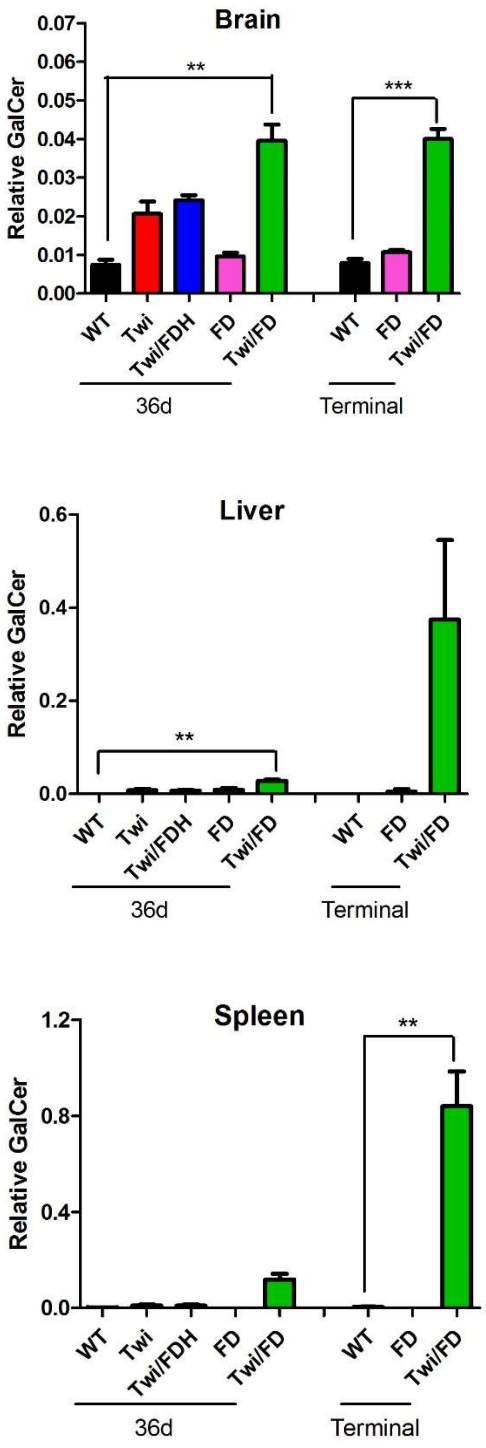

Figure 2.5 Galactosylceramide accumulation*, **

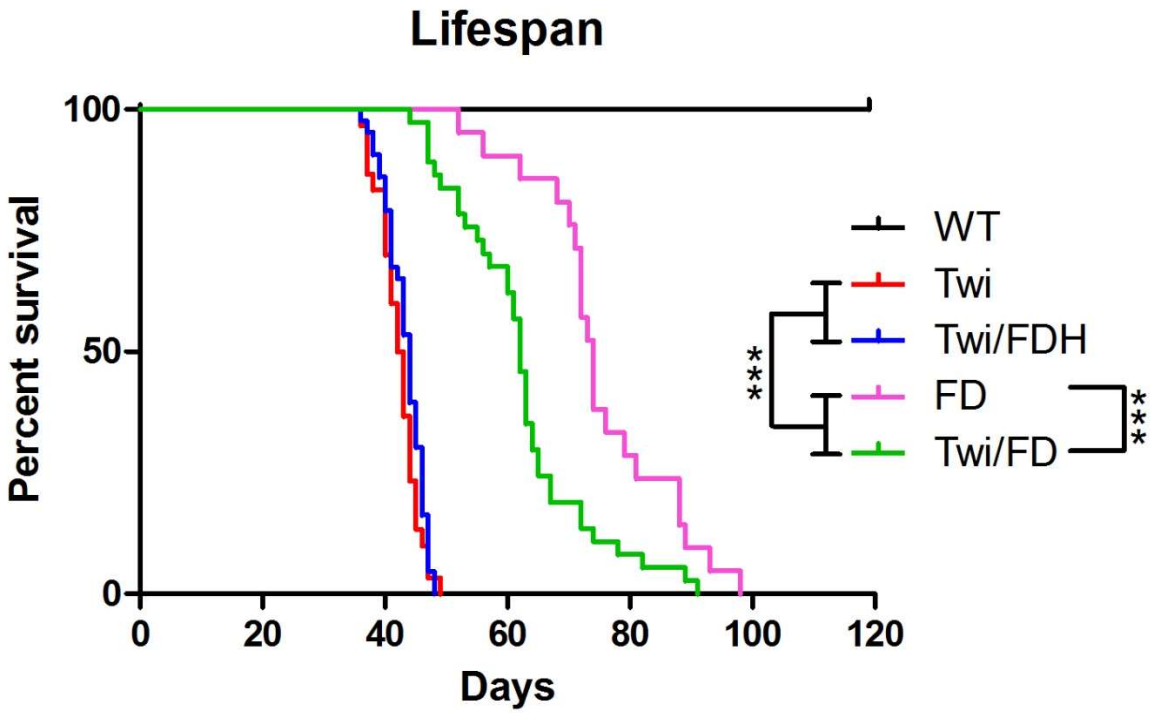

Figure 2.6 Lifespan

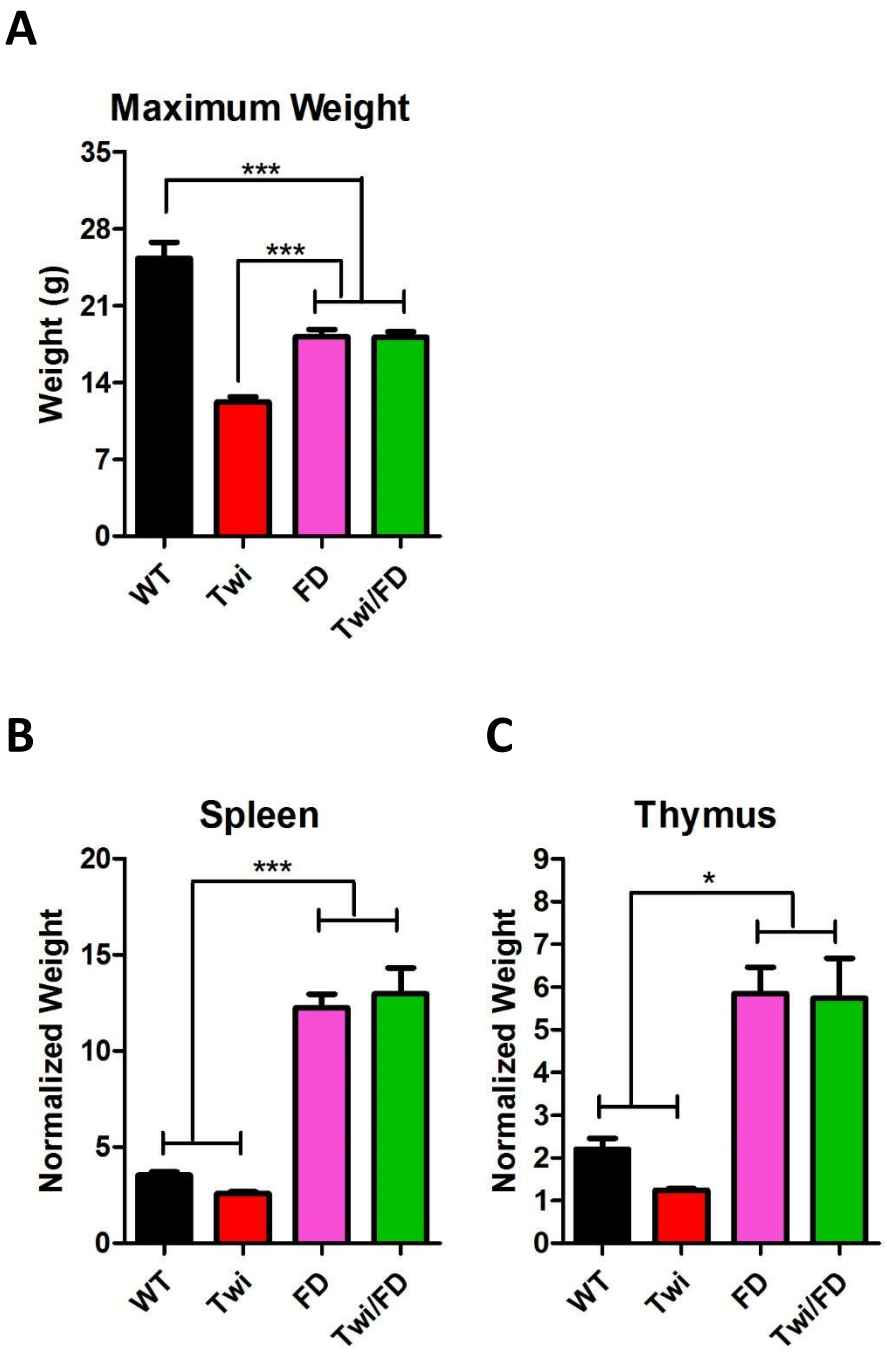

Figure 2.7 Body, spleen, and thymus weights

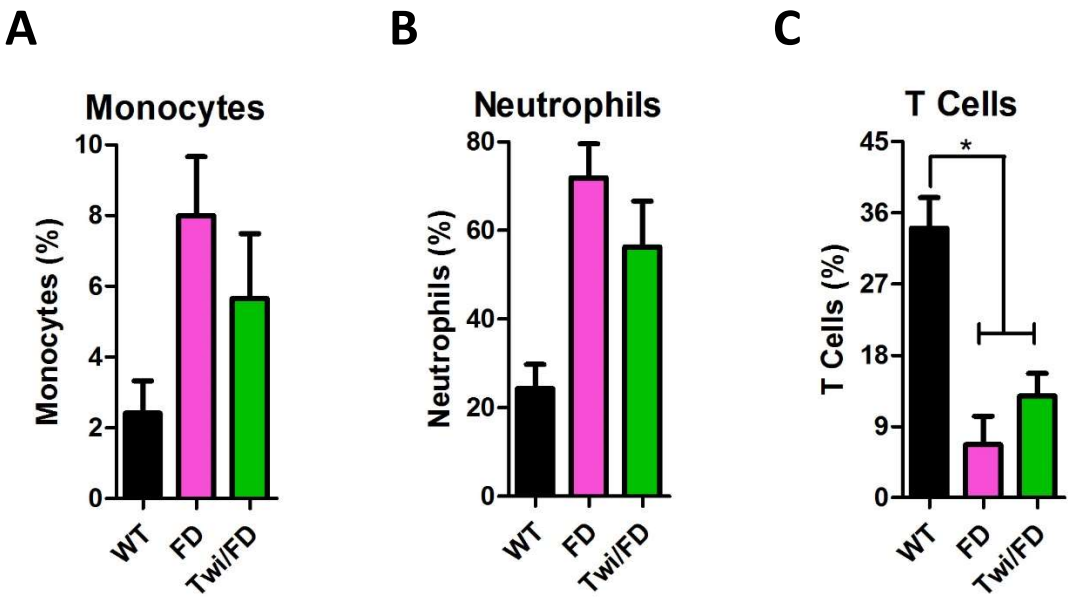

Figure 2.8 Flow cytometry

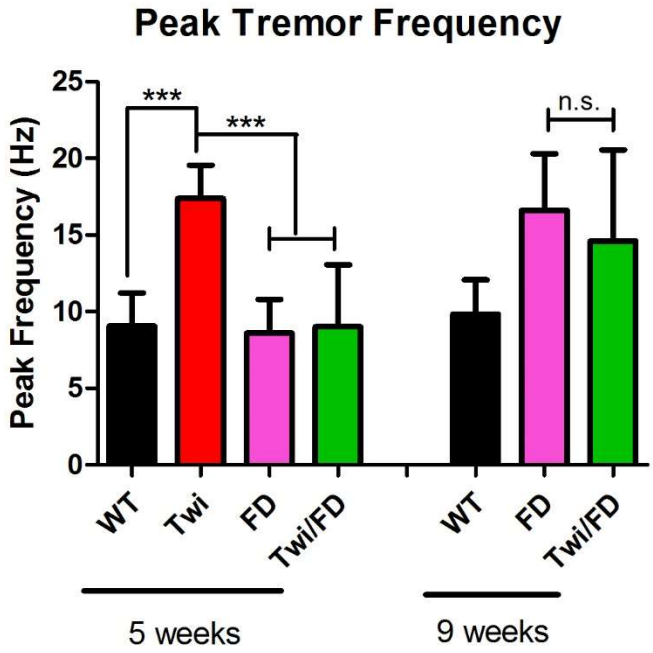

Figure 2.9 Tremor

A

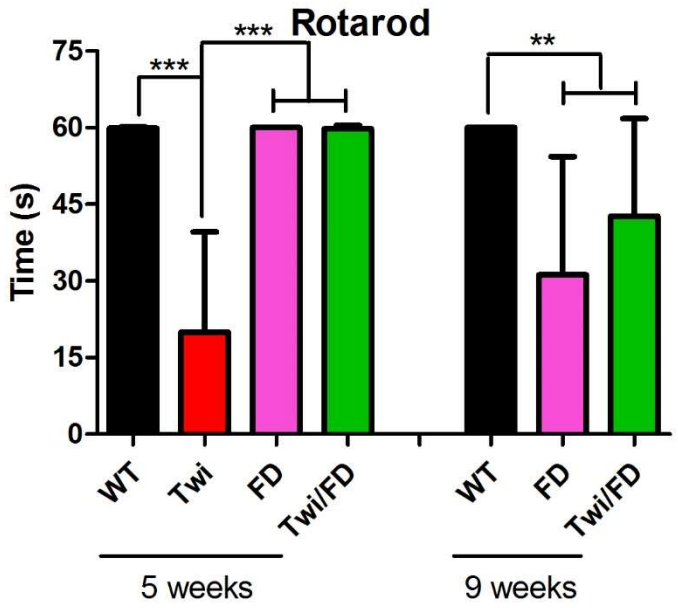

B

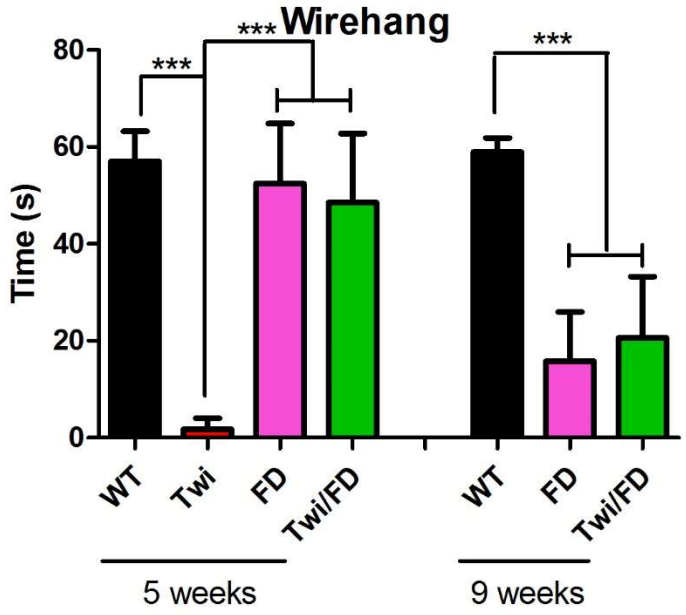

Figure 2.10 Motor function

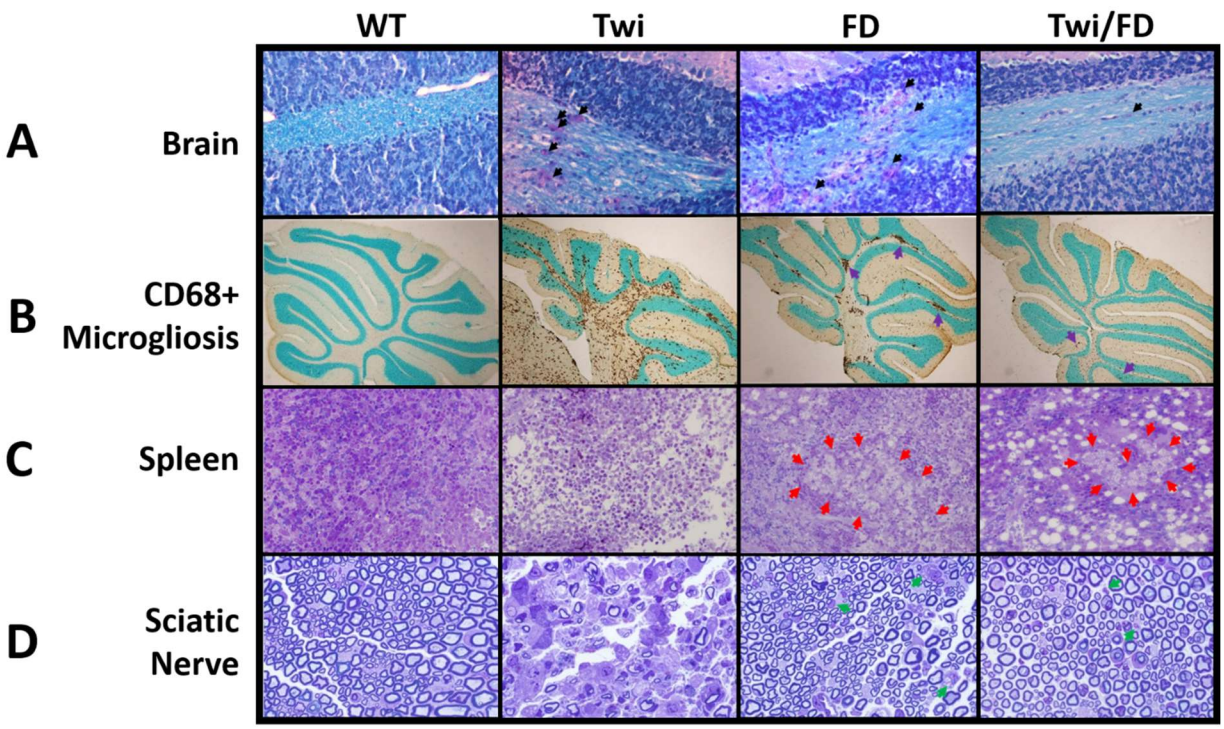

E

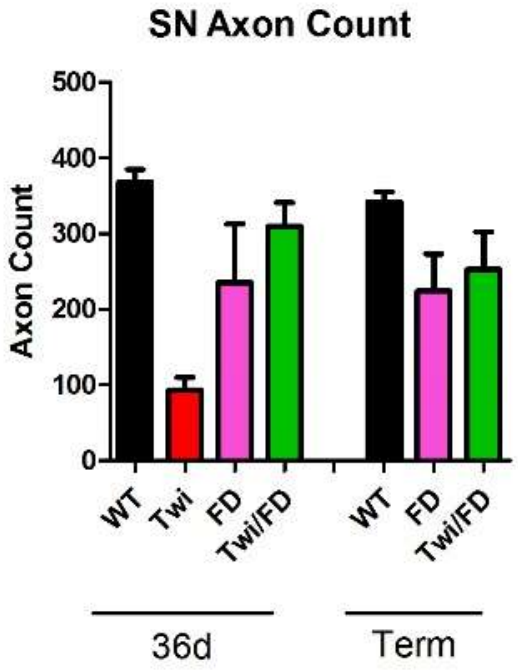

Figure 2.11 Histology and immunohistochemistry

A

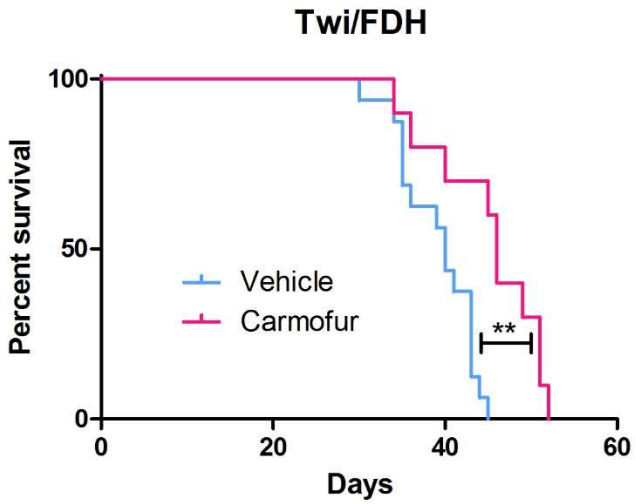

B

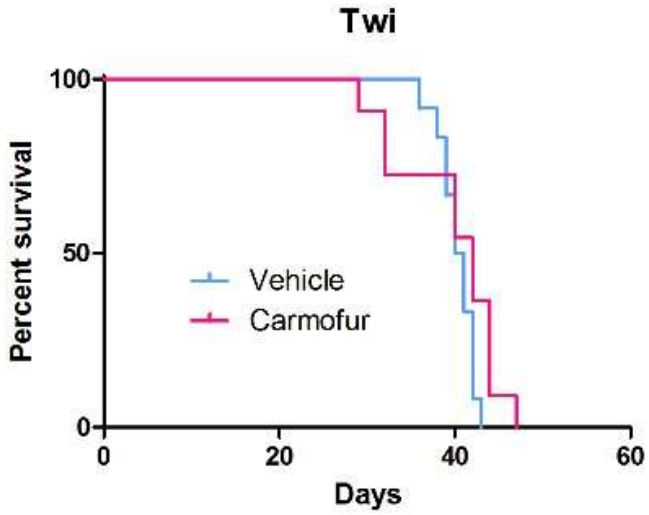

Figure 2.12 Lifespan of Carmofur-treated mice

A

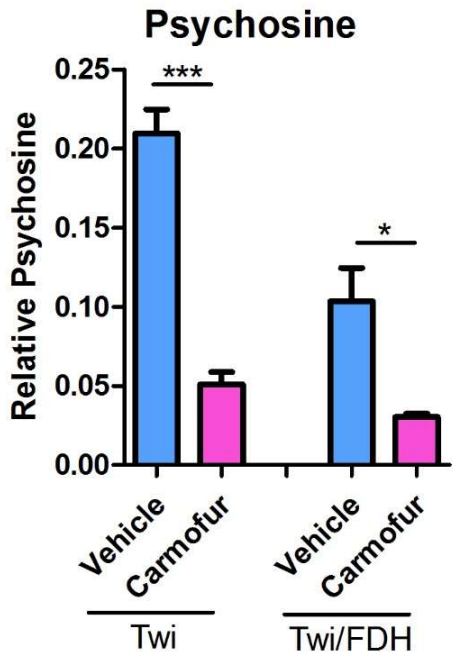

B

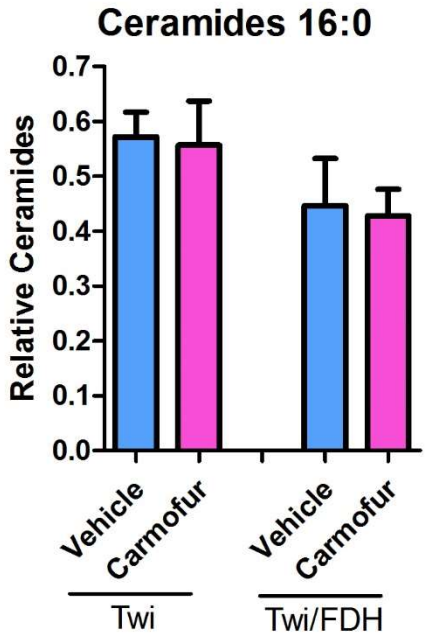

Figure 2.13 Biochemical changes associated with Carmofur injections*, **

CHAPTER THREE

Increased Efficacy and Toxicty Associated with Combination Therapy for Murine Globoid Cell Leukodystrophy (Krabbe Disease)

3.0 Abstract

Infantile globoid cell leukodystrophy (GLD, Krabbe disease) is a rapidly progressive, invariably fatal pediatric disorder caused by the deficiency of the lysosomal enzyme, galactosylceramidase (GALC). Absence of GALC activity results in the accumulation of the toxic glycolipid, galactosylsphingosine (psychosine). Accumulation of psychosine in the central and peripheral nervous systems results in profound demyelination. Although GLD is a monogenic disorder, single modality therapies are minimally effective. However, combining central nervous system (CNS)-directed, AAV2/5-mediated gene therapy, hematopoietic stem cell transplantation, and substrate reduction therapy greatly increased efficacy in the Twitcher (Twi) mouse, a faithful model of GLD. In the current study, we replaced AAV2/5 with a newer generation vector, AAV2/9. This single change significantly increased the lifespan and dramatically improved, and in some cases normalized, the clinical/behavioral deficits compared with the animals treated with the combination using the AAV2/5 vector. Unfortunately, nearly all of the combination-treated Twi mice and all combination-treated wild type control mice died from hepatocellular carcinoma. Integration site analysis confirms a high rate of AAV sequence integration into the mouse genome. These data demonstrate the value of targeting multiple pathogenic mechanisms for complex metabolic diseases, but highlights the potential risks associated with these approaches.

3.1 Introduction

Infantile globoid cell leukodystrophy (GLD, Krabbe disease) is a rapidly progressing and invariably fatal lysosomal storage disorder caused by the deficiency of galactosylceramidase (GALC) activity (Krabbe, 1916; Wenger et al., 2016). This deficiency results in the rapid accumulation of psychosine, a toxic glycolipid normally degraded exclusively by GALC. Psychosine accumulates rapidly in oligodendrocytes and Schwann cells, leading to a profoundly demyelinating phenotype characterized by failure to thrive, limb stiffness, weakness, paralysis, blindness, and developmental regression and delay. Symptoms typically appear by 3-6 months of age, and death occurs by 2-4 years of age (Wenger et al., 2016). Currently, the only available therapy is hematopoietic stem cell transplantation (HSCT), which must be administered prior to symptom onset to delay symptom progression (Wright et al., 2017). This treatment is not curative.

The Twitcher (Twi) mouse is a genetically faithful model of Krabbe disease that closely parallels the biochemistry, histology, and clinical progression of the human disease. Twitcher mice experience a rapidly progressive disease course, with tremors and ataxia starting at ~21 days, and death occurring by ~40 days (Kobayashi et al., 1980; Duchen et al., 1980; Suzuki and Suzuki, 1983). The Twi mouse has been an indispensable tool for testing new therapies since its publication in 1980, but finding an effective therapy has been a challenge. Single modality therapies, including gene therapies, HSCT, stem cell therapies, substrate reduction therapies (SRT), and anti-inflammatories provide only limited clinical benefit, and none are curative. Several groups have now shown that combination therapies targeting multiple pathogenic mechanisms are significantly more efficacious (Mikulka and Sands, 2016).

We showed previously that CNS-directed, AAV2/5-mediated gene therapy synergized with HSCT to increase the median life span (~110 days) of Twi mice to a greater extent than the

sum of the increases from the individual treatments. We subsequently showed that the synergy was likely due to AAV-mediated gene therapy supplying a persistent source of the deficient enzyme while HSCT provided a significant immunomodulatory effect (Reddy et al., 2011). Although this improvement was a major advance, the increase in lifespan was modest compared to the lifespan of a normal laboratory mouse (2-3 years). Therefore, we added a small molecule SRT drug, L-cycloserine, to the gene therapy/HSCT regimen in an attempt to further decrease psychosine levels by inhibiting its synthesis. The addition of thrice weekly injections of L-cycloserine significantly and synergistically increased the median life span (~300 days) and dramatically improved the clinical/behavioral (rotarod and wirehang) deficits observed in the Twi mouse (Hawkins-Salsbury et al., 2015).

As we systematically tested these various combination approaches, we kept the second generation AAV2/5 vector constant. In the current study, we performed the same triple-treatment (3xRx) experiment as described above using the same recombinant AAV genome but packaged with an AAV9 capsid. The newer generation AAV vector increased efficacy even further. The median lifespan of 3xRx Twi mice was increased to ~400 days and the clinical/behavioral deficits were dramatically improved, and in some cases completely normalized for the entire life of the animal. Unfortunately, >90% of the 3xRx Twi mice and 100% of the 3xRx normal control mice died of hepatocellular carcinoma (HCC) that was observed as early as 8 months of age. In fact, most of the 3xRx Twi mice, even the ones >300 days of age, did not appear to die from Krabbe disease. Rather, they succumbed to HCC.

A high incidence (30-50%) of HCC at ≥1 year of age following intravenous injection of AAV vectors in newborn mice has been reported previously by several groups (Chandler et al., 2016). Although the exact cause of the increased incidence (100%) and decreased latency of HCC

in the current study is not known, we hypothesize that AAV integration sites may disrupt oncogenes, tumor suppressor genes, and other genes that regulate cell survival and proliferation. It is highly likely that the conditioning radiation associated with the HSCT and the L-cycloserine also contributed to the increased penetrance of HCC.

Despite the high penetrance of HCC, these data show that combination therapy is a highly effective treatment of murine GLD. Detailed analyses of the tumor and normal-appearing liver tissue will undoubtedly provide insights into the potential of these therapies to interact to increase the penetrance of HCC.

3.2 Results

3.2.1 Lifespan

Untreated Twi mice had a median lifespan of 41 days (d) (range: 24-46d) (Figure 3.1). Adeno-associated virus 2/9-GALC treated Twi mice had a median lifespan of 66.5d (range: 50-83d). Twitcher mice treated with AAV2/9-GALC and HSCT (2xRx) or AAV2/9-GALC, HSCT, and L-cycloserine (3xRx) had median lifespans of 269d (range: 180-673d) and 404d (range: 157-569d), respectively. Although the median lifespan of the 2xRx-treated Twi mice was 135d less than the 3xRx-treated Twi mice, the lifespans were not significantly different. Wild type mice treated with the same triple therapy regimen had a median lifespan of 440d (range: 347-507d). All untreated WT mice lived to be at least 673d, at which point they were sacrificed to terminate the study.

3.2.2 Body weight

Untreated Twi mice experience failure to thrive, as indicated by severely impaired weight gain, with a mean maximum weight of 7.8±0.5 grams (g). (Figure 3.2) Both 2xRx and 3xRx

combination therapy improve weight gain, with body weight plateauing at an average of ~18 g for both groups. In contrast, untreated WT mice surpass 30 g on average. WT mice receiving 3xRx therapy gain more weight than combination therapy treated Twi mice, but they are significantly smaller than untreated WT mice, only reaching an average weight of ~21 g.

3.2.3 Motor function

Motor function was assessed by the rotarod and wirehang tests. Untreated Twi mice were unable to complete the rotarod or the wirehang test at 4 weeks of age. Untreated WT mice performed both rotarod and wirehang for the maximal 60 seconds of testing throughout life. Twitcher mice treated with 2xRx therapy were able to perform rotarod near WT levels until approximately one month prior to death. Nearly all 3xRx-treated Twi mice performed the rotarod test at WT levels throughout life (Figure 3.3A), and were able to maintain a 60s performance until they were moribund (Figure 3.3B).

Twitcher mice receiving 2xRx therapy were able to perform the wirehang test near WT levels until 10 weeks of age, after which wirehang performance quickly deteriorated. No 2xRx Twi mouse was able to stay on the inverted wire for 60 seconds past 90 days. At 10 weeks of age, Twi mice receiving 3xRx therapy were also able to perform wirehang near WT levels; at twenty weeks of age, half of all 3xRx-treated Twi mice remained on the wirehang for 60 seconds, whereas the other 3xRx-treated Twi mice were not able to perform the test at all (Figure 3.4A). This bimodal distribution was observed at all subsequent testing time points with some 3xRx-treated Twi mice able to perform the wirehang test for the full 60 seconds at 455 days of age.

Wirehang performance at 20 weeks was only weakly predictive of lifespan (Figure 3.4B). Specifically, 3xRx-treated Twi mice with lifespan <300 days performed poorly on wirehang at 20 weeks, and 3xRx-treated Twi mice with lifespan >435 days performed well on wirehang at 20

weeks. Between 300 and 435 days, however, wirehang performance was poorly predictive of lifespan, with some Twi mice performing for the full 60 seconds of testing and some Twi mice falling off the wirehang as soon as it was inverted.

3.2.4 Biochemical analyses

The brains of Twi mice had virtually undetectable levels of GALC activity when compared to that of their WT littermates (Figure 3.5). All mice treated with AAV2/9-GALC gene therapy, either as a single therapy, 2xRx or 3xRx, had at least WT levels of GALC activity. Some mice treated with AAV2/9-GALC gene therapy had up to 2.5 times WT levels of GALC activity. GALC activity remained high throughout the lifetime of the treated mice. There was no significant difference in brain GALC activity between animals receiving AAV2/9-GALC single therapy, 2xRx therapy, or 3xRx therapy.

For both brains (Figure 3.6A) and sciatic nerves (Figure 3.6B), psychosine levels were significantly decreased in AAV2/9-GALC only and combination therapy treated mice, compared to untreated Twi mice. There was no significant difference in brain or sciatic nerve psychosine levels between mice treated with AAV2/9-GALC single therapy, 2xRx therapy, or 3xRx therapy. Psychosine levels remained low throughout the lifetime of single and combination therapy treated mice. However, there remained a slight elevation in psychosine compared to WT levels at nearly every time point in treated whole brain lysate and sciatic nerves.

3.2.5 Donor cell engraftment

Twitcher mice treated with 2xRx or 3xRx combination therapy had mean GFP+ donor engraftment levels of 52.9±19.9% and 46.9±20.2%, respectively. WT mice treated with 3xRx therapy had a mean engraftment level of 44.6±18.0%. There is no significant difference in engraftment amongst these three groups. (Figure 3.7)

3.2.6 Peripheral neuropathy

Untreated Twi mice had fewer axons, significant edema and macrophage infiltration in the sciatic nerve compared to WT mice. (Figure 3.8A) In Twi mice receiving 3xRx therapy, there were fewer infiltrating monocytes/macrophages and less edema than untreated Twi mice at 36 days, but these abnormalities were observed at 160 days. Neither gene therapy alone nor 2xRx therapy corrected the axonal pathology at any time. Quantification of axon density revealed lower axon density in Twi mice, and incomplete normalization of axon density in Twi mice receiving 3xRx therapy. (Figure 3.8B)

3.2.7 Immunohistochemistry

Compared to WT mice, Twi mice had profound neuroinflammation, characterized by increased $CD68^+$ microgliosis (Figure 3.9) and $GFAP^+$ astrocytosis (Figure 3.10) on immunohistochemistry. Neuroinflammation was much more intense in the hind brain (cerebellum and brain stem) than in the cortex. Combination therapy attenuated microgliosis and astrocytosis in 36 day old Twi mice. As Twi mice aged, both CD68 and GFAP staining increased steadily. However, terminal 3xRx-treated Twi mice had significantly less microgliosis than terminal 2xRx-treated Twi mice, especially in the cortex. Triple therapy significantly increased astrocytosis in WT mice.

3.2.8 Cytokine levels

Whole-brain homogenates showed significant elevations in eotaxin, G-CSF, KC, MCP-1, MIP-1α, MIP-1β, and RANTES in untreated 36 day old Twi brains compared to their WT littermates. (Figure 3.11) Gene therapy alone failed to normalize cytokine overexpression in terminal mice, but both 2xRx and 3xRx therapy normalized cytokine overexpression at earlier and later timepoints in the brain.

3.2.9 Hepatocellular carcinoma

Intravenous administration of AAV gene therapy during the neonatal period has been shown to cause hepatocellular carcinoma (HCC) in mice (Chander et al., 2016). We observed large HCC tumors (Figure 3.12) in 14/16 Twi mice treated with 3xRx therapy, 2/10 Twi mice treated with 2xRx therapy, and 19/19 WT mice treated with 3xRx therapy (Figure 3.13). Because the penetrance of HCC was much lower in 2xRx-treated Twi mice than in 3xRx-treated Twi mice, we hypothesized that L-cycloserine may play an important role in HCC carcinogenesis. L-cycloserine significantly altered the ceramide synthetic pathway by increasing the levels of ceramide 16:0 species, which promote cell proliferation (Senkal et al., 2010; Senkal et al., 2011). (Figure 3.14A) L-cycloserine also decreases the levels of pro-apoptotic ceramide 18:0 species (Koybasi et al., 2004; Karahatay et al., 2007; Senkal et al., 2007) (Figure 3.14B) in liver.

Although AAV is primarily considered to be a non-integrating virus (Naso et al., 2017), integration site analysis revealed frequent AAV integration into the murine genome, with >6,000 unique integration sites in Twi mice and >23,000 unique sites in WT mice. There was an increased number of total unique integration sites in HCC tissue compared to normal liver tissue. (Table 3.1) This finding was present in nearly every chromosome in both WT (Figure 3.15A) and Twi (Figure 3.15B) mice. However, on chromosome 11, the number of unique integration sites found in normal tissue was nearly five times the number found in HCC tissue. Integrations occurred more frequently in introns, genes, and intergenic regions (Figure 3.16).

3.3 Discussion

Globoid cell leukodystrophy is a severe, rapidly progressing pediatric lysosomal disorder for which there is currently no cure. Although GLD is a monogenic disorder and numerous

experimental therapies have been tested since the murine model was first reported in 1980, GLD has remained largely refractory to treatment. This is likely due to the presence of multiple secondary pathogenic mechanisms that must be simultaneously targeted in addition to the primary genetic defect to produce significant therapeutic efficacy. In this study, we treated Twi mice with a triple therapy regimen that simultaneously targets three major mechanisms. Central nervous system-directed, AAV2/9-mediated gene therapy provides long-term GALC expression. Hematopoietic stem cell transplantation ameliorates neuroinflammation (Reddy et al., 2011). L-cycloserine is a small molecule drug that slows psychosine accumulation by targeting serine palmitoyl transferase, an enzyme that catalyzes a step early in the ceramide synthesis pathway (Sundaram and Lev, 1984). This combination therapy resulted in the greatest reported median lifespan of Twi mice to date. This increase in lifespan is a significant improvement over other recently published combination therapy studies (Hawkins-Salsbury et al., 2013; Rafi et al., 2015; Ricca et al., 2015; Karumuthil-Melethil et al., 2016). However, the data presented in those studies are consistent with our observation that combination therapies are much more effective than single therapies in treating Krabbe disease.

These results have important implications for therapy studies that are currently moving to larger mammalian models of Krabbe disease. Preliminary data in dogs have shown that AAV-mediated gene therapy increases the lifespan of Krabbe dogs (Bradbury et al., 2018). Moreover, nonhuman primate studies have shown that gene therapy effectively induces gene transfer in neurons, astrocytes, and oligodendrocytes close to the injection site (Meneghini et al., 2016). It will be very interesting to see whether the synergy observed in murine combination therapy will translate to other larger mammalian models.

Another aspect of GLD that remains largely refractory to treatment is motor dysfunction, which is quantified by the rotarod and wirehang behavioral assays. Rotarod measures coordination, whereas wirehang is a surrogate measure for peripheral neuropathy, limb strength, and coordination. While previous therapy studies have reported some improvements in both rotarod and wirehang performance (Hawkins-Salsbury et al., 2015; Rafi et al., 2015), improvements have been limited, with mice falling off both apparatuses as GLD progressed. In the current study, 3xRx-treated Twi mice were able to stay on the rotarod for their entire lives. The wirehang test is a more challenging exercise since untreated Twi mice cannot perform the task for 60 seconds at any point in their lives, and treated mice fail this test prior to failing on the rotarod. Interestingly, half of the Twi mice receiving 3xRx therapy were able to perform wirehang for the maximal time tested (60 seconds) throughout life. In contrast, Twi mice treated with 2xRx therapy were able to perform the wirehang test for 60 seconds at 10 weeks of age, but experienced a rapid decline in performance after 10 weeks. These data suggest that L-cycloserine plays an important role in correcting peripheral neuropathy in Twi mice. This is supported by the greater pathological improvements observed in the sciatic nerves of 3xRx-treated mice compared to 2xRx-treated mice.

Despite the significant improvement in lifespan and motor function, Twi mice treated with 3xRx therapy retain some signs and symptoms of GLD, including a milder but persistent tremor and hind limb clasping. One potential explanation for continued disease progression is the uneven distribution of AAV2/9-mediated gene expression in the CNS and PNS, which has previously been described in other studies (Cearley and Wolfe, 2006). Although GALC levels were at least physiologic and psychosine accumulation was significantly reduced in whole brain lysates of 3xRx-treated Twi mice, it is possible that uneven distribution of GALC expression, specifically

the lack of GALC expression in certain uncorrected areas of the CNS/PNS, translates to continued, albeit slower disease progression.

Another potential cause of GLD progression is the slow but progressive worsening of neuroinflammation in the treated Twi CNS. Untreated Twi mice have profound microgliosis and astrocytosis (Reddy et al., 2011; Snook et al., 2014), as well as significantly increased expression of pro-inflammatory cytokines as early as postnatal day 2 (Santambrogio et al., 2012). Both 2xRx therapy and 3xRx therapy normalized cytokine levels. However, the increased immunohistochemical staining for CD68 and GFAP as combination treated Twi mice age suggests the existence of localized unattenuated inflammation in the CNS that may be masked in whole brain assays of cytokine expression. It is likely that the uncontrolled microglial and astrocytic activation eventually contribute to Twi disease progression.

It is interesting to note that there is less microglial activation in terminal 3xRx-treated Twi mice than in terminal 2xRx-treated Twi mice. Given this finding, and the observation that 3xRx-treated Twi mice have better motor function than 2xRx-treated Twi mice, it is surprising that there is no significant difference in lifespan between these two groups. In fact, the longest lived Twi mouse was a 2xRx-treated animal that lived to be 673 days. In contrast, the longest lived 3xRx-treated Twi mouse died at 569 days. Since nearly all the 3xRx-treated Twi mice had advanced HCC at necropsy and many of them could still perform the rotarod and wirehang tests just prior to death, it is almost certain that the 3xRx mice did not die of Krabbe disease; rather, they died of HCC. The true efficacy of the triple therapy is likely masked by the presence of HCC.

This is further supported by the fact that Twi mice treated with AAV2/5-GALC, HSCT, and L-cycloserine triple therapy (median lifespan: 454 d) lived much longer than Twi mice treated with AAV2/5-GALC and HSCT double therapy (median lifespan: 120 d). We would expect to see

a similarly dramatic increase in lifespan for the AAV2/9-GALC 3xRx treated Twi mice compared to AAV2/9-GALC 2xRx treated Twi mice, as a result of the addition of L-cycloserine to the 2xRx treatment regimen. This is especially true given that the AAV2/9 2xRx treated Twi mice (269 d) lived more than twice as long as the AAV2/5 2xRx treated Twi mice (120 d) (Hawkins-Salsbury et al., 2015). It is not clear how long the 3xRx Twi mice would have lived if it were not for the HCC.

Systemic AAV administration has now been associated with acute toxicity in primate and porcine models (Hinderer et al., 2018), as well as chronic toxicity (HCC) in mouse models (Donsante et al., 2001; Chandler et al., 2015). The HCC observed in mice is caused by AAV integration into the mouse genome and subsequent dysregulation of genes and non-coding RNAs downstream from the viral-encoded promoter/enhancer. One of the hot spots for integration in the mouse is the *Rian* locus (Donsante et al., 2007; Wang et al., 2012), which disrupts the expression of regulatory microRNA 341 and a host of genes implicated in HCC development (Wang et al., 2012), including *Rtl1* (Chandler et al., 2016). Although it is not known if the link between AAV administration and HCC translates to humans, it is especially concerning that recurrent clonal insertions of AAV2 have been found in human HCC tumors (Nault et al., 2015), and that a subset of these integrations resulted in the dysregulation of genes known to be overexpressed in human HCC tumors (Jiao et al., 2018).

Interestingly, integration site analysis of the mice in this study revealed only a single mouse which had a clear integration site in the *Rian* locus. This suggests that the mechanism by which combination therapies induce AAV-associated HCC may be very different from the mechanism by which AAV therapy alone induces HCC.

Prior studies show that the HCC phenotype has a relatively long latency (12-18mo) and the frequency is greatest (30-75%) when the animals are injected during the neonatal period. Finally, tumorigenesis is independent of serotype but there appears to be a direct correlation between the strength of the promoter/enhancer element and the incidence of HCC (Chandler et al., 2016). Although HCC has been described in mice injected with AAV vectors as young adults (Bell et al., 2006), the incidence is considerably less (10-15%).

In the current study, approximately 90% of the 3xRx-treated Twi and 100% of the 3xRx-treated WT mice had large HCC tumors at death. The fact that these mice developed HCC is noteworthy in itself since these animals received CNS-directed gene therapy. All of the previous studies reporting a high incidence of HCC were performed in newborn animals that received intravenous injections of virus. Another significant difference is that the HCC was observed as early as 8-10 months of age in the current study. Combination therapy decreased the latency of tumorigenesis and increased the incidence of HCC, compared to previously reported latency and incidence of AAV-induced HCC (Chandler et al., 2015).

The shorter latency and higher penetrance of HCC in 3xRx-treated mice may be explained by Knudson's hypothesis, which states that cancer results from the accumulation of multiple 'hits' to the genome (Knudson, 1971). Prior data strongly suggest that AAV integration represents one 'hit' and may even be sufficient to cause HCC in the mouse. Pre-conditioning γ-irradiation could represent an additional 'hit' since ionizing irradiation is known to cause small genomic insertions and deletions (Adewoye et al., 2015). Although there were only a few animals in the 2xRx group that developed HCC, it could be that they simply did not live long enough for the HCC to develop, as most cases of AAV-induced HCC are observed after one year post-exposure.

L-cycloserine might also represent another ‘hit’ that could potentiate carcinogenesis. L-cycloserine, while not a known mutagen, significantly perturbs ceramide metabolism and alters the levels of ceramides that influence cell survival. Twi mice treated with L-cycloserine had higher levels of ceramide 16:0 species, which have been shown to promote cell proliferation and survival (Senkal et al., 2010; Senkal et al., 2011). L-cycloserine also lowers levels of the pro-apoptotic ceramide 18:0 species (Koybasi et al., 2004; Karahatay et al., 2007; Senkal et al., 2007). Disrupting the balance between cell survival and apoptotic factors is likely to facilitate tumorigenesis.

Analysis of AAV integration sites revealed significantly more unique integration events in HCC tissue compared to normal liver tissue. Since normal and HCC tissue samples were collected from each mouse, these results suggest, perhaps unsurprisingly, that increased integration frequency is associated with tumorigenesis.

Breakdown of integration site analysis by chromosome shows that the pattern of increased integration sites in HCC tissue compared to normal tissue holds for nearly every chromosome. The most striking exception is chromosome 11, which appears to have nearly five times as many unique integration sites in normal liver tissue than in HCC tissue. This may indicate the presence of an integration hot spot on this chromosome that is not associated with tumorigenesis.

Functional analysis of AAV integration sites reveals that there are more integration sites localizing to genes in HCC tissue than in noncancerous tissue. While the exact implication of this finding is not yet clear, it is reasonable to speculate that disruption of genes is more likely to result in functional consequences than disruption of noncoding regions. Whether the gene disruptions identified in this study cluster around oncogenes or other genes impacting cell survival remains to be determined.

The 3xRx combination therapy proposed in this study is a very effective therapy for Krabbe disease. Not only does it increase lifespan, it also improves motor function in Twi mice. However, administration of this therapy is not without its risks. Adeno-associated virus-induced HCC in mice is a very real and serious phenomenon that needs further study. There is a clear need to understand the role of AAV in the development of HCC, determine how other therapies interact with AAV to change the penetrance and latency of tumorigenesis, explore alternative methods of bone marrow conditioning, and discover more specific inhibitors of psychosine synthesis. Only when we have successfully eliminated AAV-induced HCC in the mouse can we devise experiments designed to find a cure for this invariably fatal disease.

3.4 Methods

3.4.1 Experimental animals

Animals were housed at Washington University in St. Louis under the supervision of MSS. Heterozygous Twitcher ($GALC^{+/-}$) mice on a C57BL/6J background (Jackson Laboratory, Maine, USA) were bred and maintained. Genotypes of all experimental mice were determined by PCR, as previously described (Sakai et al., 1996; Lin et al., 2005). Mice were housed under standard conditions, on a 12 hr/12 hr light/dark cycle with *ad libitum* access to food and water. Hematopoietic stem cell donors were syngenic $GALC^{+/+}$ mice that expressed GFP under the CAG promoter (Okabe et al., 1997). All animal procedures were approved by the Institutional Animal Studies Committee at Washington University School of Medicine and were in accordance with the guidelines of the National Institutes of Health.

3.4.2 Virus production

The AAV2/9 vector consists of the CMV enhancer, the chicken β-actin promoter, followed by the mouse *GALC* cDNA and the rabbit β-globin polyadenylation signal, as previously described (Lin et al., 2005). The AAV2/9-GALC vector was produced by the Virus Vector Core Facility at the Gene Therapy Center of the University of North Carolina. Virus was diluted in sterile Lactated Ringer's solution to a final concentration of 10^{12} viral particles per mL and stored at -80°C.

3.4.3 Treatment regimen

Intracranial and intrathecal injections of AAV2/9-GALC were administered on postnatal day 0, as previously described (Hawkins-Salsbury et al., 2015). Briefly, mice received one 15 uL intrathecal injection of virus at a concentration of 10^{12} viral particles per mL. In addition, six 2 uL intracranial injections were administered at the same concentration, targeting bilateral hemispheres, thalami, and cerebelli.

Hematopoietic stem cell transplantation was performed on postnatal day 1, as previously described (Hawkins-Salsbury et al., 2015). Briefly, mice were conditioned with 400 rads total body irradiation from a ^{137}Cs source, then injected with 10^6 nucleated donor bone marrow cells from a $GALC^{+/+}GFP^{+/-}$ donor. Quantification of bone marrow chimerism was determined by flow cytometry for donor-derived GFP expression in recipient bone marrow.

L-cycloserine was administered subcutaneously as previously described (Hawkins-Salsbury et al., 2015). Briefly, L-cyloserine was reconstituted fresh in phosphate buffered saline before each injection. Mice received 25 mg/kg L-cycloserine three times a week until postnatal day 28, and 50 mg/kg L-cycloserine three times a week for the rest of their lives.

3.4.4 Galactosylceramidase activity assay

Experimental mice were deeply anesthetized and perfused with phosphate buffered saline. One brain hemisphere was flash frozen and homogenized in ddH2O. Measurement of GALC activity was performed using a radiolabeled ^{3}H-galactosylceramide substrate and reported as the nanomoles of substrate cleaved per hour per milligram of total protein, as previously described (Hawkins-Salsbury et al., 2015).

3.4.5 Mass spectrometry

Galactosylsphingosine (psychosine) and ceramides were measured in brain, liver, and sciatic nerve, essentially as previously described (Sikora et al., 2017). Galactosylsphingosine was separated from glucosylsphingosine and glucosylceramide by hydrophilic interaction liquid chromatography (HILIC) columns. Ceramides were separated on two-dimensional chromatography by HILIC column in the first dimension and by reversed phase column in the second dimension. Multiple reaction monitoring (MRM) was used to detect galactosylsphingosine and ceramides on an AB SCIEX 4000QTRAP tandem mass spectrometer in positive ESI mode. Data processing was conducted with Analyst 1.5.2 (Applied Biosystems). Data are reported as the peak area ratios of lipids to their internal standards.

3.4.6 Behavioral testing

Behavioral testing consisted of the rotarod and wirehang tests, which were conducted as previously reported (Hawkins-Salsbury et al., 2015). Mice were tested once every other week on the rotarod and once every week on the wirehang. Performance was measured as the time it took for the mouse to fall from either apparatus. Three trials were run and the average of the three trials was reported for each time point. For both tests, the maximum tested time was 60 seconds. Each group contained at least n=10 animals.

3.4.7 Immunohistochemistry

Mice were deeply anesthetized and perfused with phosphate-buffered saline. One sagittal half of each brain was harvested immediately following perfusion. Tissues were fixed in 4% paraformaldehyde for 24-48 hours at 4°C and cryoprotected in 30% sucrose. Sixteen micron sections were blocked in normal goat serum then incubated with primary rabbit anti-mouse GFAP (Immunostar) antibody or rat anti-mouse CD68 (BioRad), as previously described (Reddy et al., 2011). The sections were then incubated in the appropriate horse radish peroxidase-conjugated secondary antibody and developed with a commercially available DAB kit (Vector Laboratories).

3.4.8 Histology

Sciatic nerves were isolated and immediately fixed in 4% paraformaldehyde/2% glutaraldehyde. Incubation of nerves in osmium tetroxide was quickly followed by serial dehydration in ethanol and embedding in Araldite 502 (Polysciences). One μm cross sections were prepared using an ultramicrotome. These sections were then stained with 1% toluidine blue and mounted on slides. Image acquisition was completed with a Hitachi CCD KP-MIAN digitizing camera mounted on a Leitz Laborlux S microscope. The Leco IA32 Image Analysis System was used for histomorphometric analysis.

3.4.9 Cytokine measurement

Brains were perfused with phosphate-buffered saline, followed by immediate flash freezing and homogenization in a solution containing protease inhibitor cocktail. Cytokine levels were quantified using the Bio-plex Pro Mouse Cytokine 23-plex Assay (Bio-Rad) with the help of Dr. Camaron Hole and the Doering Lab at Washington University in St. Louis.

3.4.10 Statistical analysis

Statistical significance was calculated using a one-way ANOVA with post-hoc Bonferroni correction for multiple comparisons, unless otherwise specified. P values are denoted as follows: *$p < 0.05$; **$p < 0.01$; ***$p < 0.001$; n.s. denotes not significant, $p \geq 0.05$.

3.5 Tables

Table 3.1 Unique integration sites in normal vs. HCC tissue

Mouse Strain	Treatment	# Unique Integration Sites
Twi	3xRx Normal	2,077
	3xRx HCC	4,334
WT	3xRx Normal	8,260
	3xRx HCC	15,364

Table 3.1. Unique AAV integration sites in HCC tumors vastly outnumber those in normal liver tissue. In tissue isolated from 3xRx-treated Twi mice, there are 2,077 unique integration sites in normal-appearing liver tissue (3xRx Normal) and 4,334 unique integration sites in HCC tissue (3xRx HCC). In 3xRx-treated WT mice, there are 8,260 unique integration sites in normal-appearing liver tissue (3xRx Normal) and 15,364 unique integration sites in HCC tissue (3xRx HCC).

3.6 Figure Legends

Figure 3.1. Triple combination therapy increases lifespan and improves clinicobehavioral performance in Twi mice. Kaplan-Meier curves showing increased lifespan in Twi mice treated with AAV2/9-GALC+HSCT+L-cycloserine triple therapy (3xRx) (n=18), AAV2/9-GALC+HSCT double therapy (2xRx) (n=13); and AAV2/9-GALC single therapy (n=22) compared to untreated Twi mice (n=10). Wild type mice treated with 3xRx therapy (n=19) had a significantly shorter lifespan than untreated WT mice (n=11). Asterisks indicate mice that had large hepatocellular carcinoma tumors at death.

Figure 3.2. Combination therapies improve weight gain in Twi mice but cause weight loss in WT mice. Untreated Twi mice (Twi Untreated) have profoundly impaired weight gain compared to WT mice (WT Untreated). Double (Twi 2xRx) and triple (Twi 3xRx) combination therapy partially improve weight gain in Twi mice, but WT mice receiving 3xRx therapy (WT 3xRx) have mildly impaired weight gain compared to untreated WT mice.

Figure 3.3. Triple combination therapy normalizes rotarod performance in Twi mice. (A) Rotarod testing shows consistently normal rotarod performance in 3xRx-treated Twi mice (Twi 3xRx) throughout life. Double combination therapy (Twi 2xRx) also significantly improves rotarod performance, but Twi mice eventually start falling off the rotarod as disease progresses. In contrast, untreated Twi (Untreated Twi) mice rarely perform the rotarod test for the full 60 seconds and are dead by 5-6 weeks of age. **(B)** Premoribund rotarod performance was assessed one to seven days prior to death. Twitcher mice treated with 3xRx therapy perform just as well as untreated WT (data not shown) and 3xRx-treated WT mice (WT 3xRx) up until death. In contrast, untreated Twi mice and Twi mice treated with 2xRx therapy can no longer perform rotarod when premoribund.

The average age at testing for mice in each experimental group is indicated in its corresponding column.

Figure 3.4. (A) Twitcher mice receiving double therapy (Twi 2xRx) and triple therapy (Twi 3xRx) have near-normalized wirehang performance at 10 weeks of age. Impairment in wirehang performance begins after 10 weeks of age for 2xRx-treated Twi mice. Some 3xRx-treated Twi mice can perform wirehang up to 65 weeks, while others are unable to perform wirehang starting at 20 weeks. In contrast, all untreated Twi mice have died by 10 weeks, and are unable to do the wirehang test at any point in life. Untreated WT mice are able to perform wirehang consistently throughout life (data not shown). **(B)** In 3xRx-treated Twi mice, wirehang performance at 20 weeks is weakly predictive of lifespan ($r^2 = 0.2589$). Twitcher mice living to <300 days perform poorly on wirehang at 20 weeks, whereas Twi mice living >435 days perform well on wirehang at 20 weeks. Between 300 and 435 days, 20-week wirehang behavior is poorly predictive of lifespan.

Figure 3.5. AAV2/9-GALC single therapy and combination therapies significantly increase GALC activity in the brain. GALC activity is deficient in untreated Twi brains (Twi Untr). Compared to untreated WT mice (WT Untr), Twi mice treated with AAV2/9-GALC gene therapy alone (Twi AAV2/9), 2xRx therapy (Twi 2xRx), and 3xRx therapy (Twi 3xRx) have at least physiologic levels of GALC activity in the brain.

Figure 3.6. AAV2/9-GALC single therapy and combination therapies decrease psychosine accumulation in brain and sciatic nerve.* Psychosine levels in **(A)** brain and **(B)** sciatic nerves are much higher in untreated Twi mice (Twi Untr) compared to untreated WT mice (WT Untr) and Twi mice treated with AAV2/9-GALC gene therapy alone (Twi AAV2/9), 2xRx therapy (Twi 2xRx), or 3xRx therapy (Twi 3xRx). All therapies significantly decrease psychosine accumulation in brain and sciatic nerves throughout the lives of Twi mice.

Figure 3.7. Wild type and Twi mice receiving HSCT engraft at the same levels. There is no significant difference in GFP+ bone marrow engraftment in Twi mice receiving 2xRx (Twi 2xRx) or 3xRx (Twi 3xRx) therapies. WT mice receiving 3xRx therapy (WT 3xRx) also have the same level of engraftment as Twi mice receiving 2xRx or 3xRx therapy.

Figure 3.8. Combination therapy significantly delays progression of sciatic nerve pathology. **(A)** Untreated Twi mice (36d Twi) have severe sciatic nerve pathology with decreased myelination, profound axonal degeneration, and macrophage infiltration. Triple combination therapy (36d 3xRx) is more effective than 2xRx therapy (36d 2xRx) at preservation of structural integrity in 36 day old mice. Severe sciatic nerve pathology is observed at terminal age in 3xRx-treated Twi mice (Term 3xRx) compared to WT mice (Term WT). **(B)** Untreated Twi mice (Twi Untr) have significantly decreased axon density in the sciatic nerve. Triple therapy (Twi 3xRx) significantly corrects this abnormality at 36d, but decreased axon density remains uncorrected in 160d and terminal 3xRx-treated Twi mice.

Figure 3.9. Triple therapy attenuates microgliosis early in the GLD disease course. Anti-CD68 immunohistochemistry shows profound microglial activation (brown staining) in untreated Twi (36d Twi) brain stem (BS), cerebellum (CB), and cortex (Cort). Double combination therapy (36d 2xRx Twi) decreases microgliosis at 36d, but is unable to prevent eventual disease progression and development of severe microglial activation by terminal age (Term 2xRx Twi). Microgliosis in terminal 3xRx-treated Twi mice (Term 3xRx Twi) is less severe than that in 2xRx-treated Twi mice (Term 2xRx Twi), especially in the cortex. Aging WT brains (Term WT) develop mild microglial activation throughout the brain.

Figure 3.10. Combination therapies attenuate astroglial activation in the Twi brain. Anti-GFAP immunohistochemistry shows profound astroglial activation (brown staining) in untreated

Twi (36d Twi) brain stem (BS), cerebellum (CB), and cortex (Cort). Astrocyte activation is decreased in 2xRx- (36d 2xRx Twi) and 3xRx-treated (36d 3xRx Twi) 36-day-old Twi mice. Terminal combination therapy-treated (Term 2xRx Twi and Term 3xRx Twi) Twi mice have profound astrogliosis, especially in the cerebellum. Astrocyte activation is slightly decreased in terminal Twi mice treated with 3xRx therapy compared to Twi mice treated with 2xRx therapy. Astrocyte activation increases as WT mice age (Term WT), and 3xRx therapy causes some astroglial activation in WT mice (Term 3xRx WT).

Figure 3.11. Combination therapies normalize cytokine expression in the Twi brain. **(A)** G-CSF, **(B)** KC, **(C)** MCP-1, **(D)** MIP-1α, **(E)** MIP-1β, and **(F)** Eotaxin are significantly elevated in untreated Twi (Twi Untr) CNS. Gene therapy alone (Twi AAV2/9) attenuates expression of these cytokines at 36d. However, by the time these mice are terminal, cytokine expression in Twi mice receiving AAV2/9 alone no longer differs from that of untreated Twi mice. Both 2xRx (Twi 2xRx) and 3xRx (Twi 3xRx) therapies effect long-term normalization of cytokine expression.

Figure 3.12. Large HCC tumors are found during necropsy of 3xRx-treated Twi mice. Representative images of gross normal liver (top panel) and HCC tumor (bottom panel) isolated from a terminal 3xRx-treated mouse.

Figure 3.13. Triple therapy dramatically increases the penetrance of AAV-induced HCC. Penetrance of HCC is significantly increased in 3xRx-treated Twi (Twi 3xRx) and WT (WT 3xRx) mice compared to 2xRx-treated Twi mice (Twi 2xRx).

Figure 3.14. L-Cycloserine administration alters ceramide expression.* Differential expression of **(A)** ceramides 16:0 species (which increase cell proliferation and survival) and **(B)** ceramides 18:0 species (which are pro-apoptotic) in normal-appearing (Twi 3xRx Normal) vs. HCC (Twi 3xRx HCC) liver tissue.

Figure 3.15. Unique integration sites in tumor tissue outnumber those in normal-appearing liver tissue on nearly every chromosome. Chromosomes 4, 11, 17, are relative hotspots for AAV integration in **(A)** WT mice. Chromosomes 4, 8, and 17 are relative hotspots for AAV integration in **(B)** Twi mice. In WT mice, chromosome 11 is an outlier in that there are ~5 times as many unique integration sites in normal-appearing liver tissue compared to HCC tissue. In all other tissues, unique integration sites in HCC tissue outnumber those in normal-appearing liver tissue.

Figure 3.16. Unique integration sites occur in all structurally distinct parts of the genome. Mapping of unique integration sites in **(A)** WT and **(B)** Twi liver tissue shows unique integration sites in all parts of the genome. In WT and Twi mice, genes, introns, and intergenic regions are the most frequent sites of integration.

* Data are reported as the peak area ratios of lipids to their internal standards.

3.7 Figures

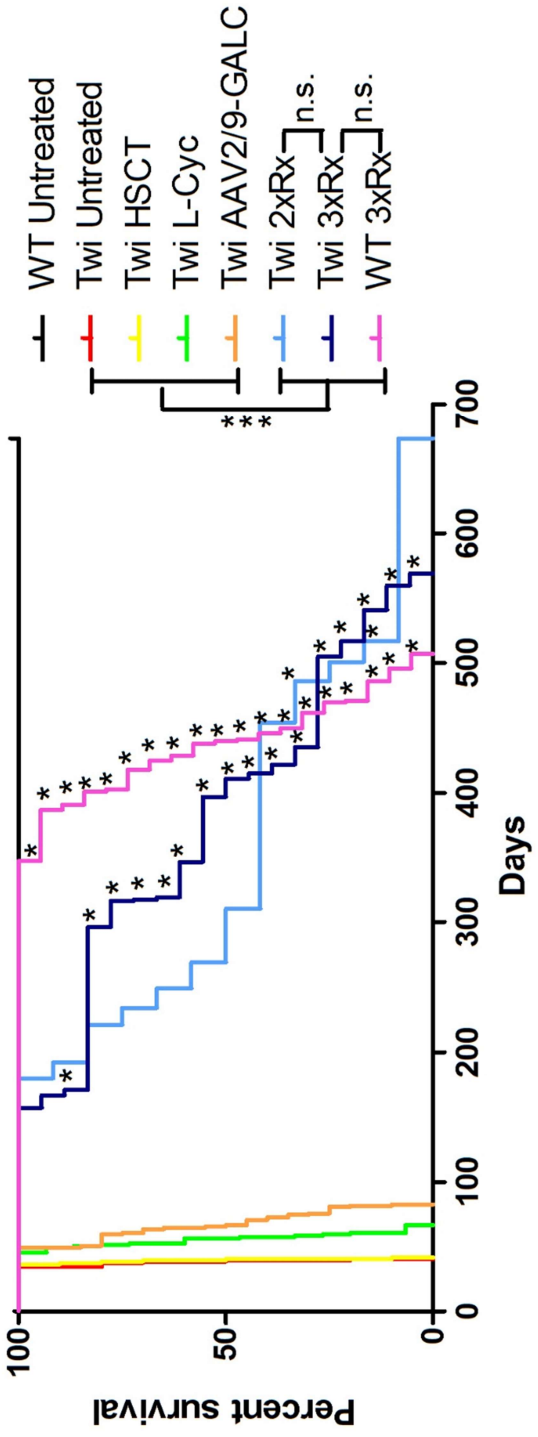

Figure 3.1 Survival

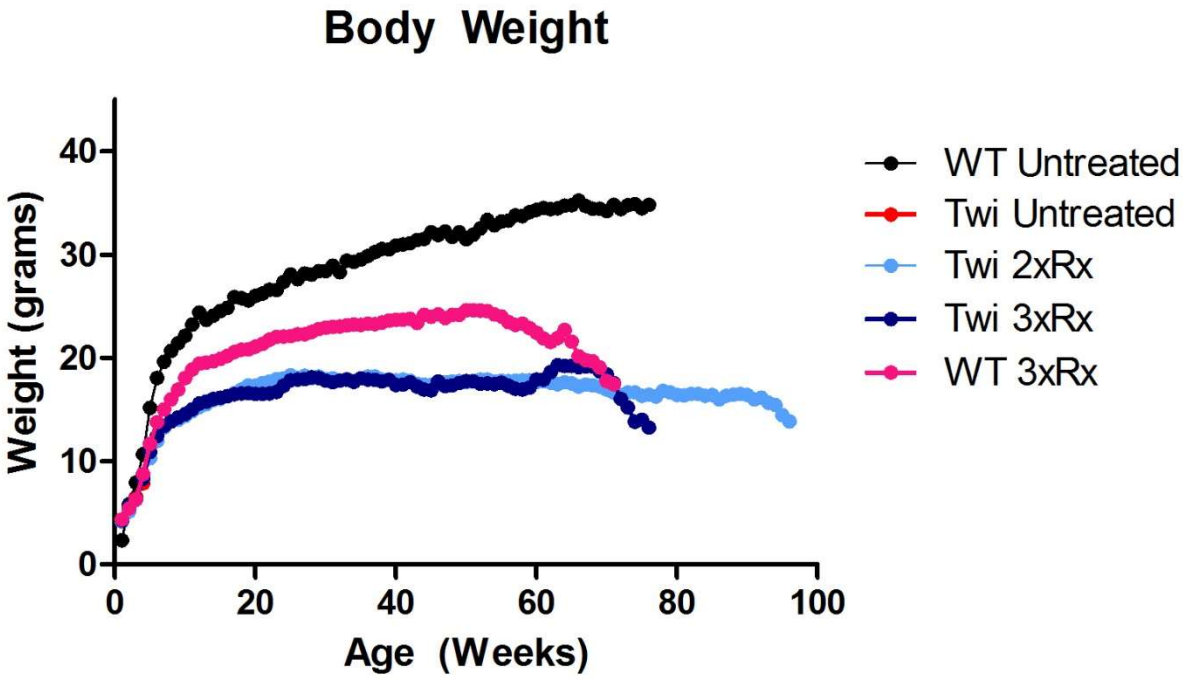

Figure 3.2 Body weight

A

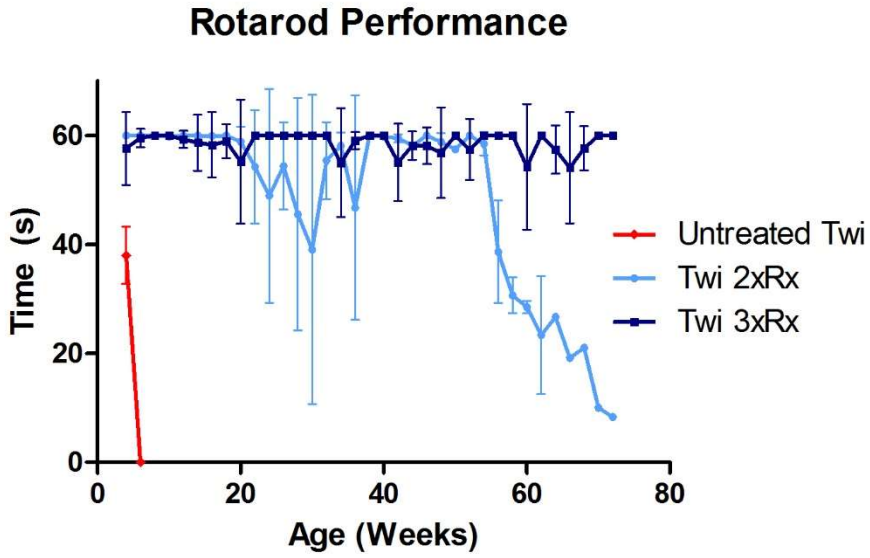

B

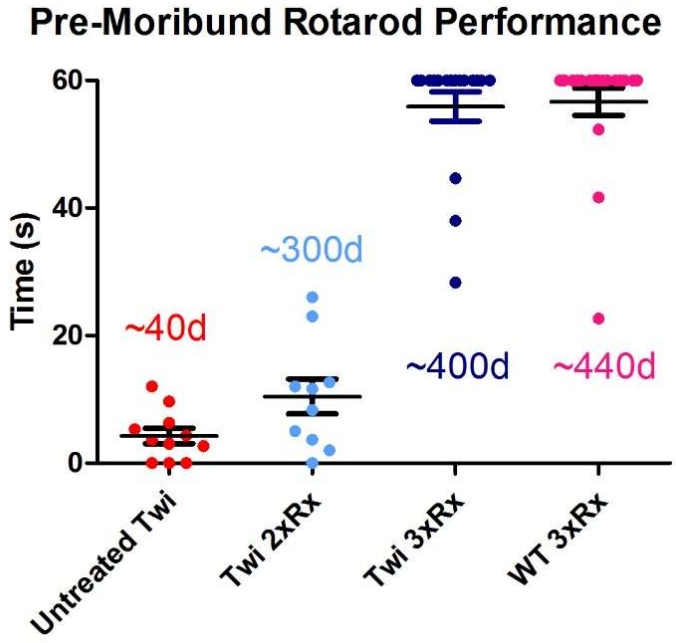

Figure 3.3 Rotarod performance

A

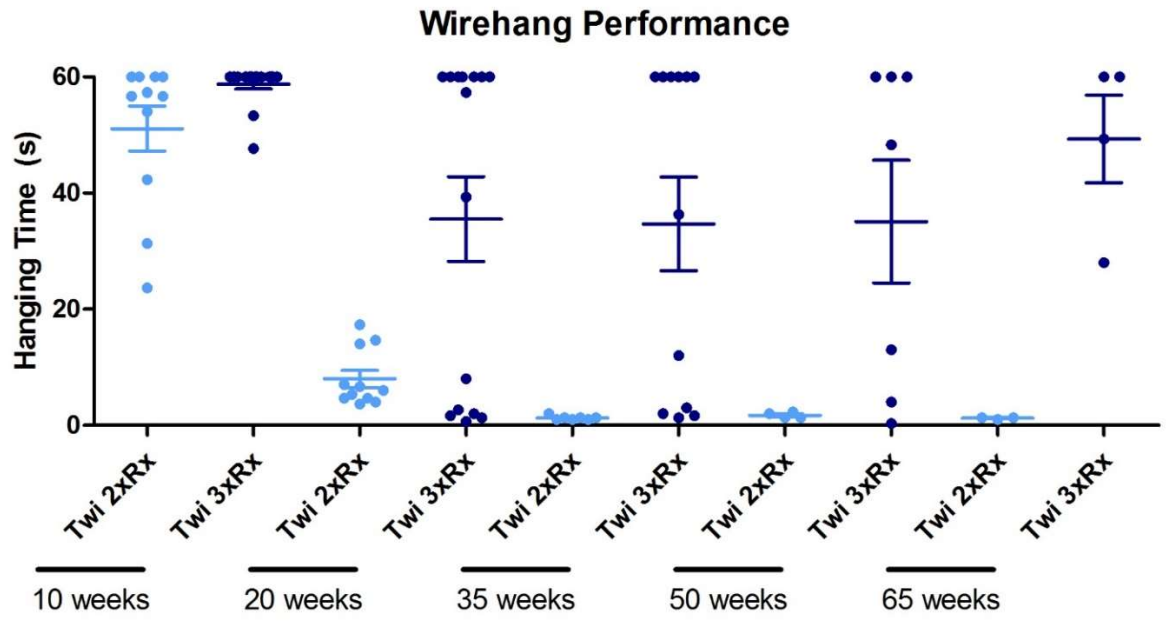

B

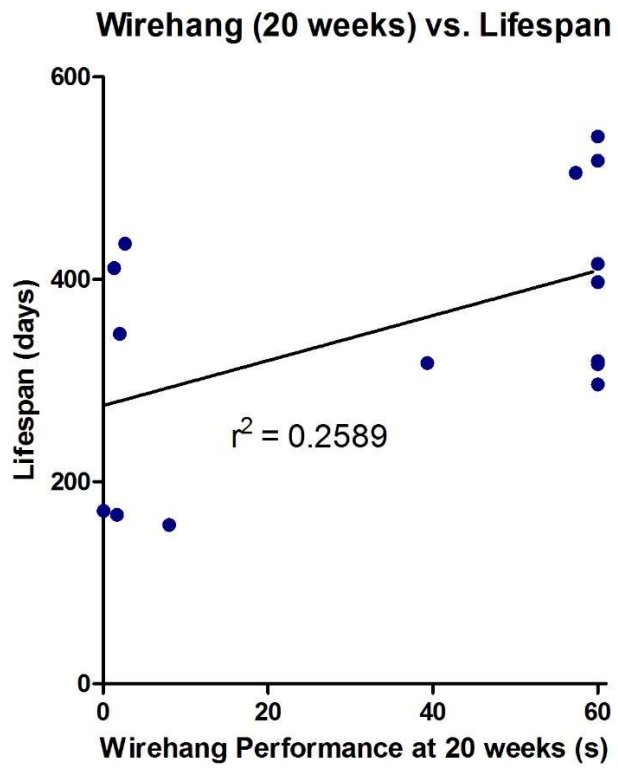

Figure 3.4 Wirehang performance

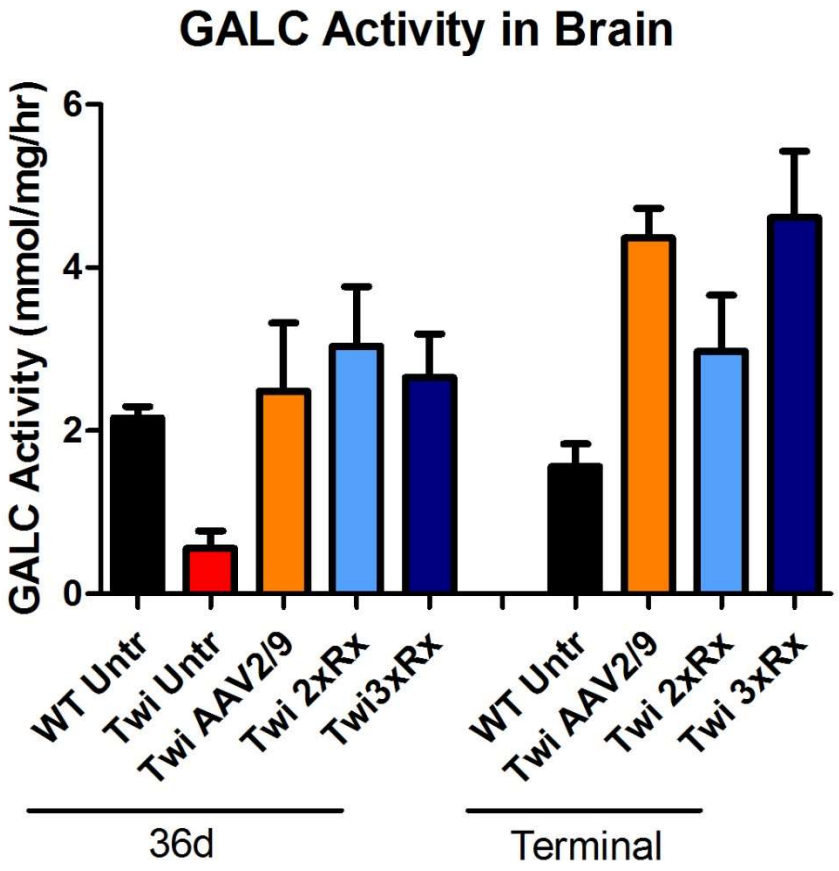

Figure 3.5 Galactosylceramidase activity

A

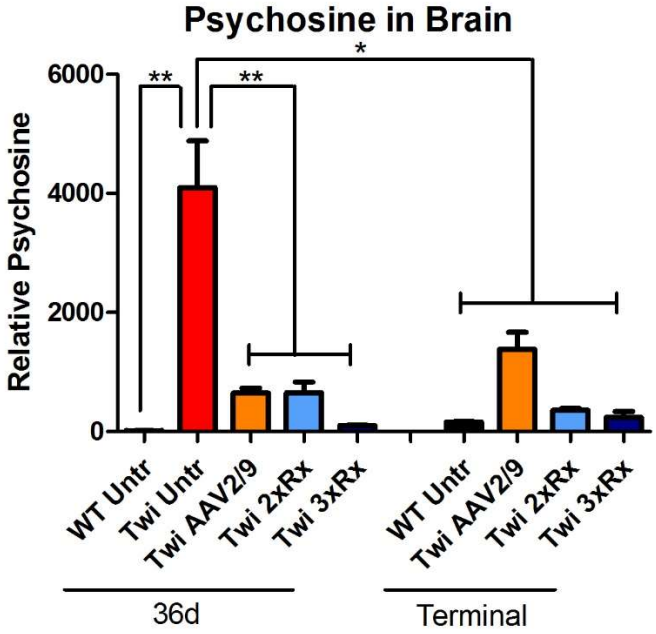

B

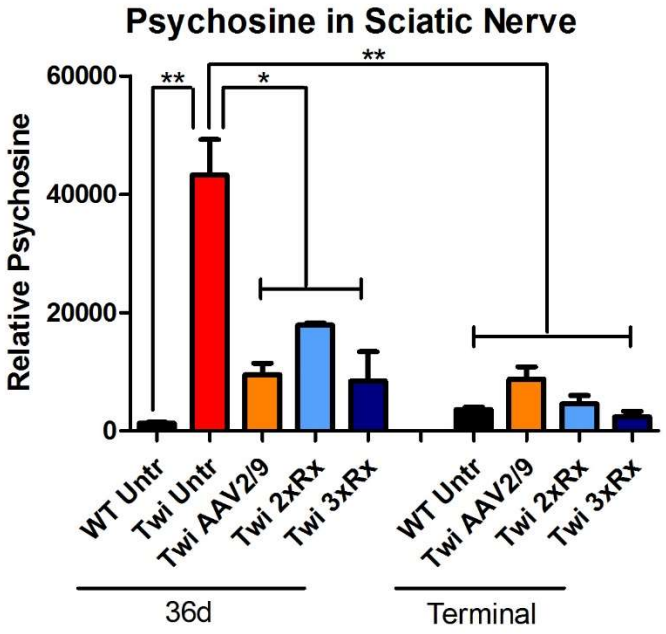

Figure 3.6 Psychosine accumulation*

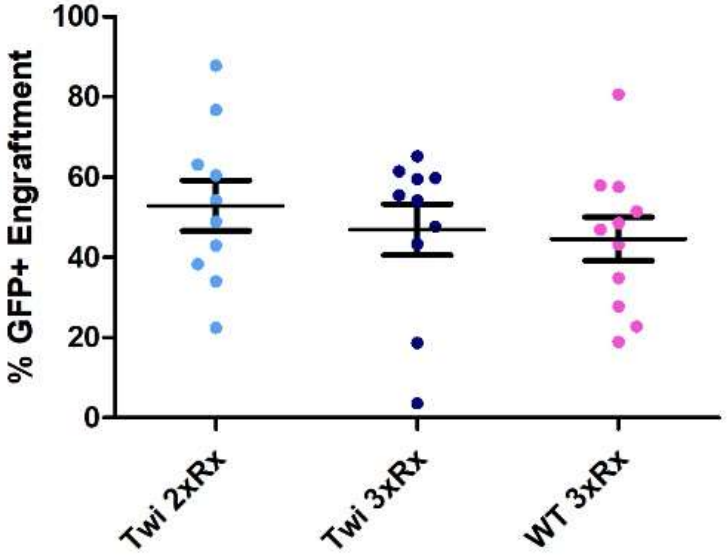

Figure 3.7 GFP$^+$ engraftment

A

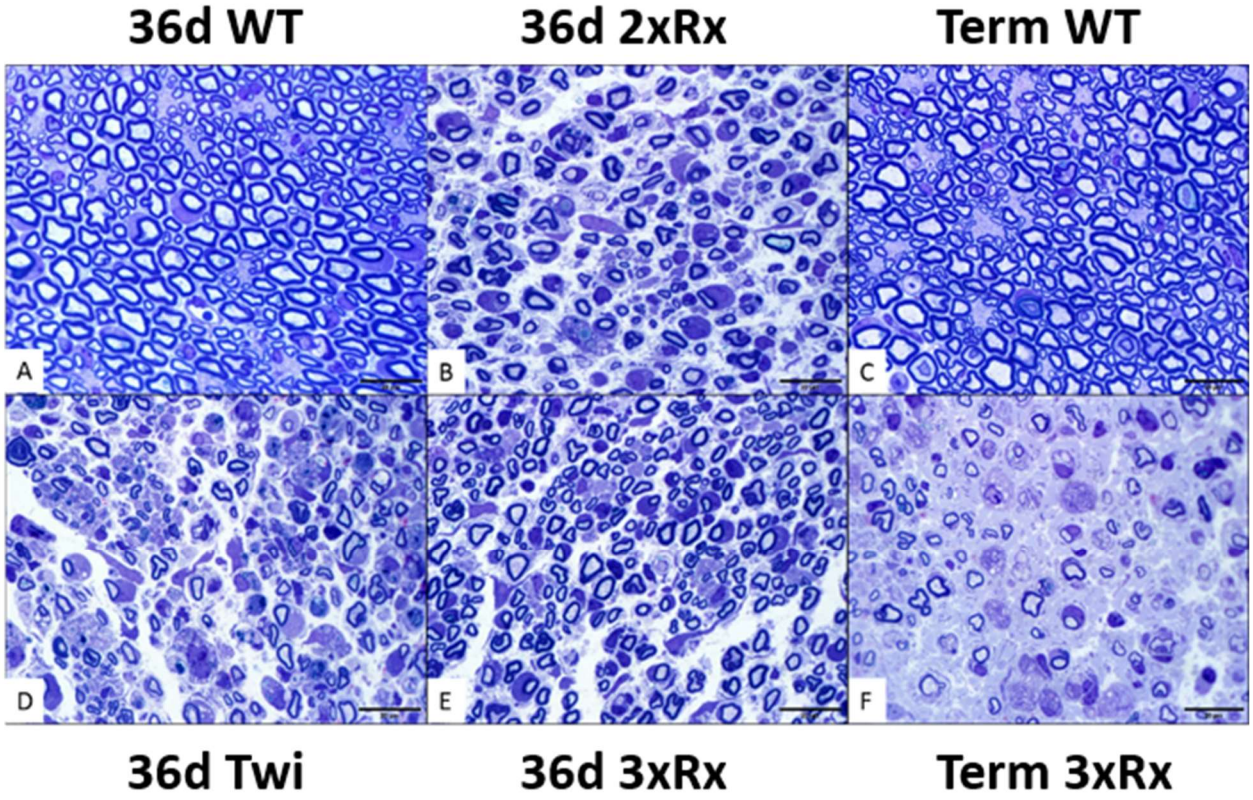

B

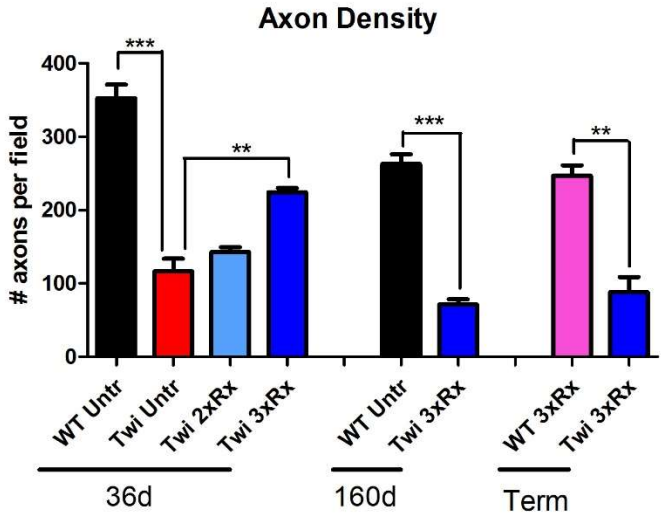

Figure 3.8 Sciatic nerve histology

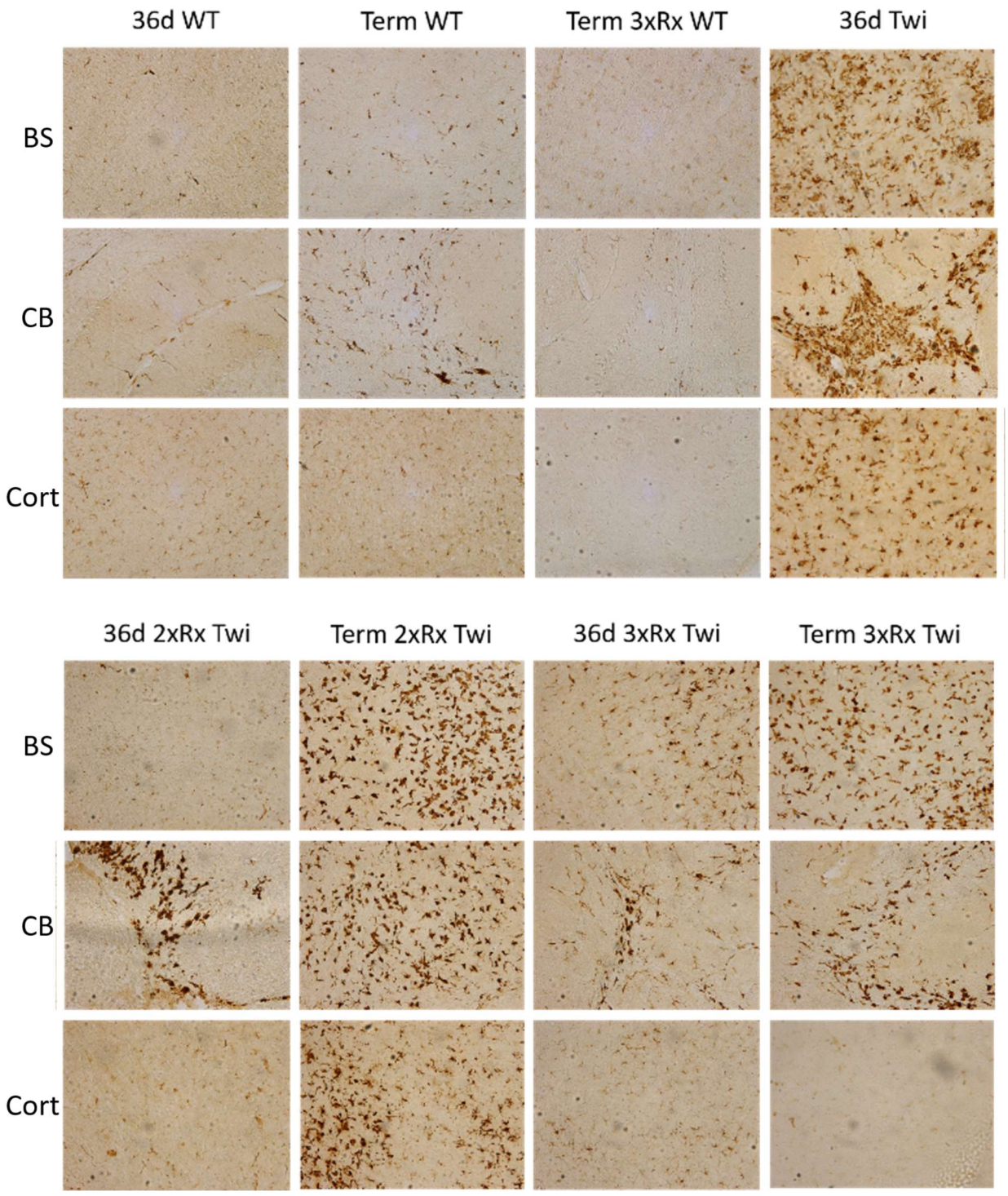

Figure 3.9 CD68^{+} microgliosis

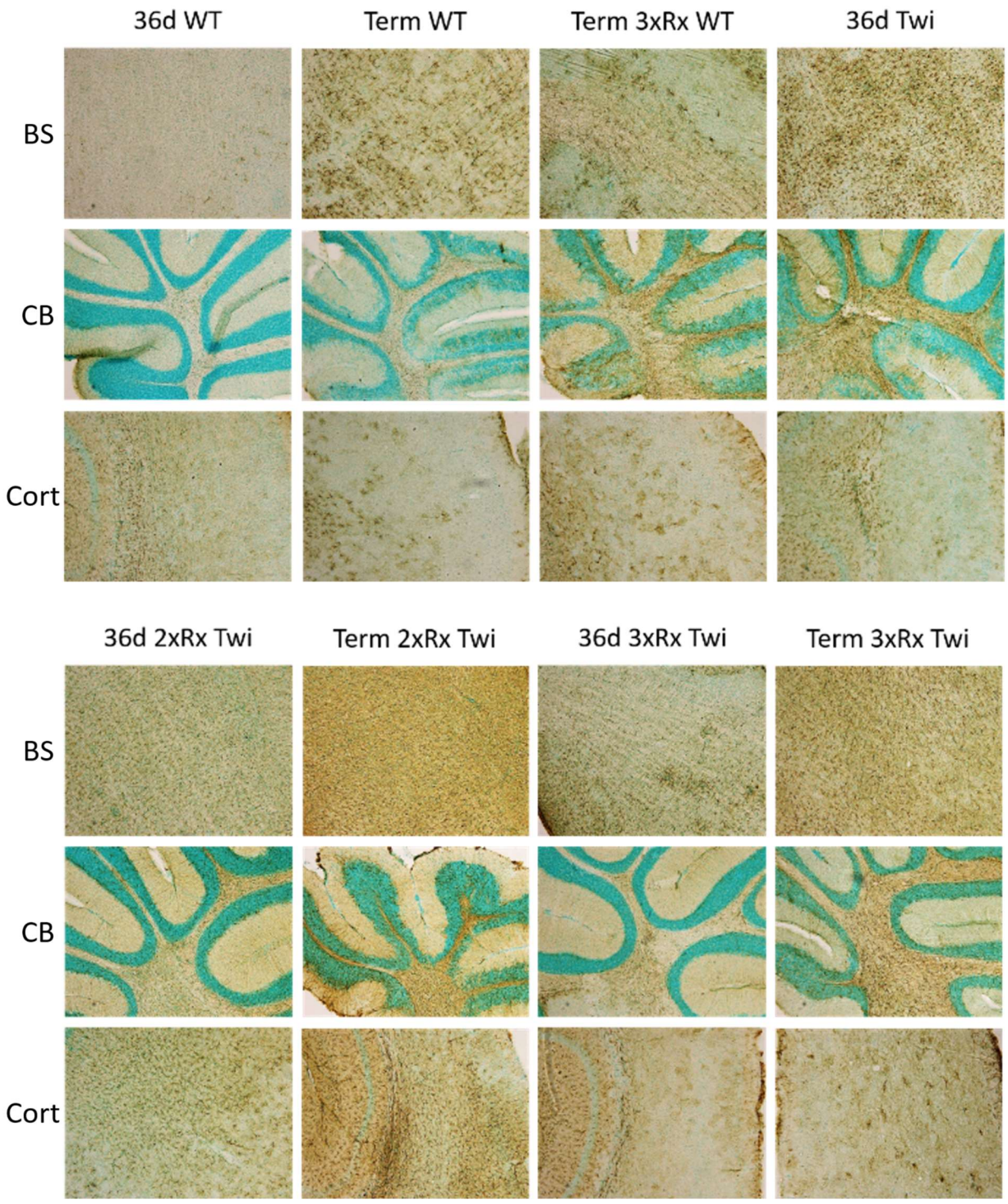

Figure 3.10 GFAP^{+} astrocytosis

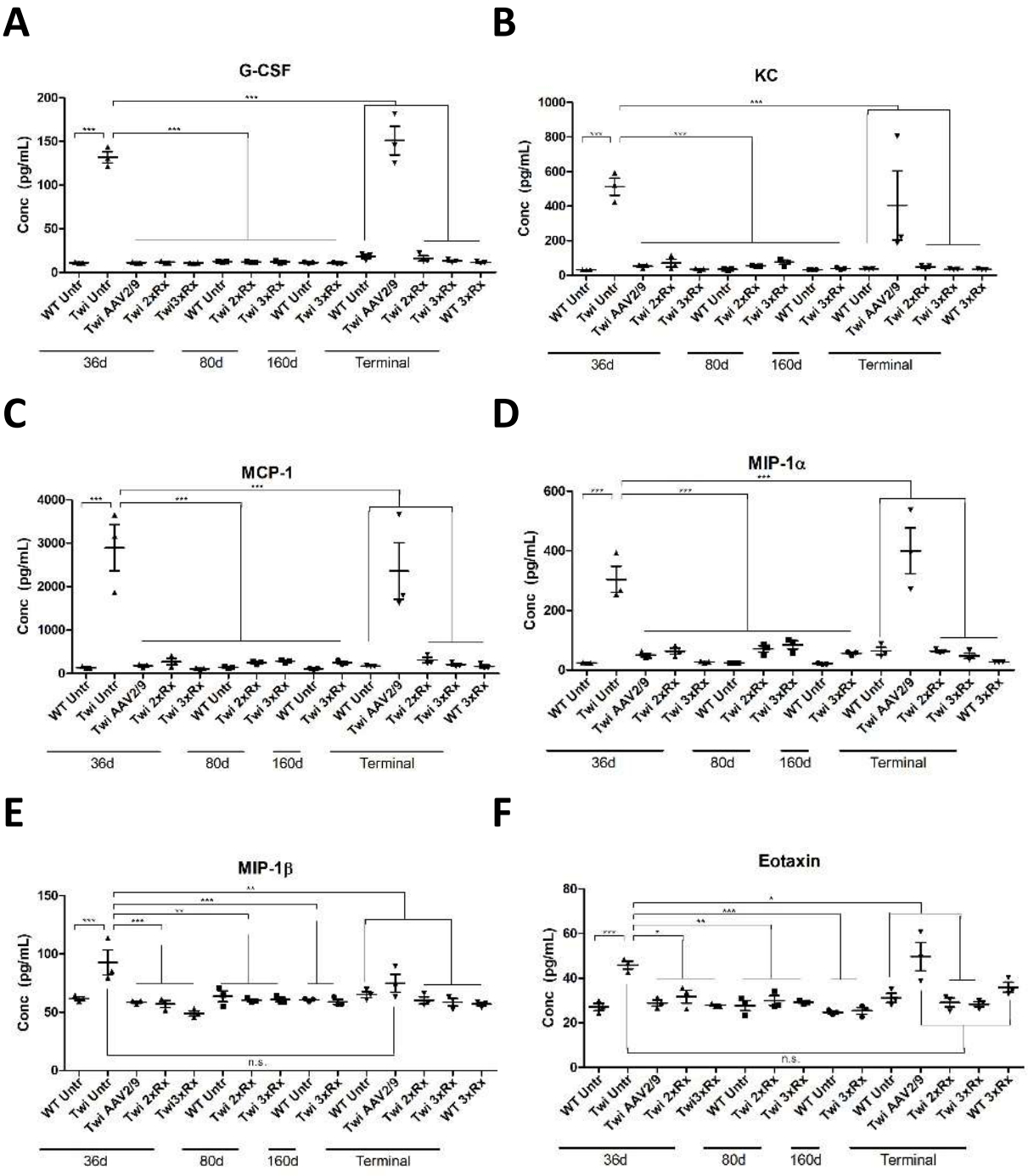

Figure 3.11 Cytokine expression

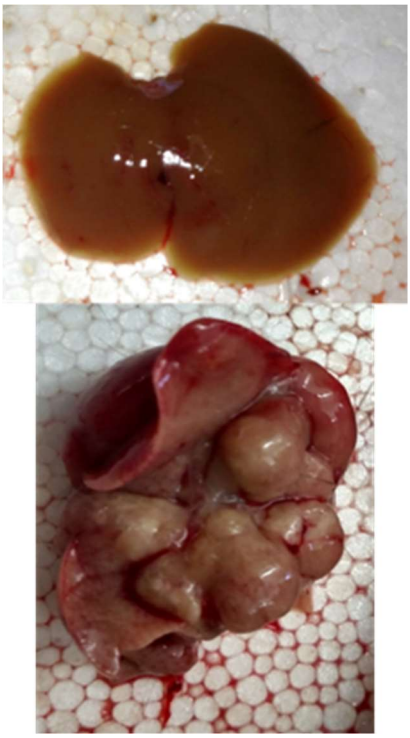

Figure 3.12 Gross pathology of normal-appearing vs. HCC liver

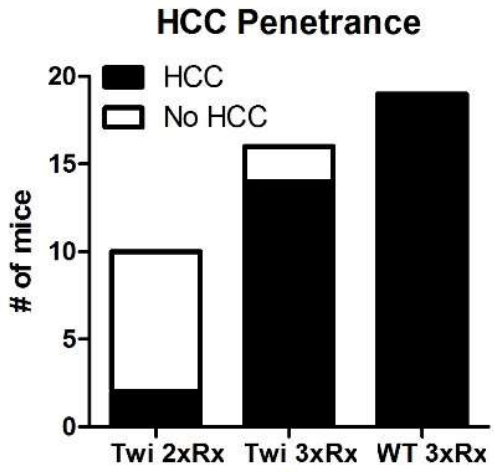

Figure 3.13 Frequency of AAV-induced HCC

A

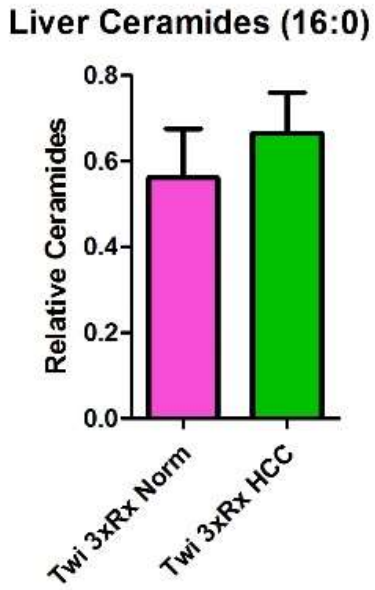

B

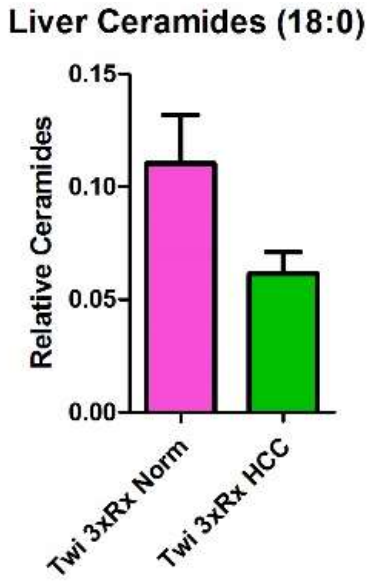

Figure 3.14 Ceramide levels in normal-appearing vs. HCC liver tissue*

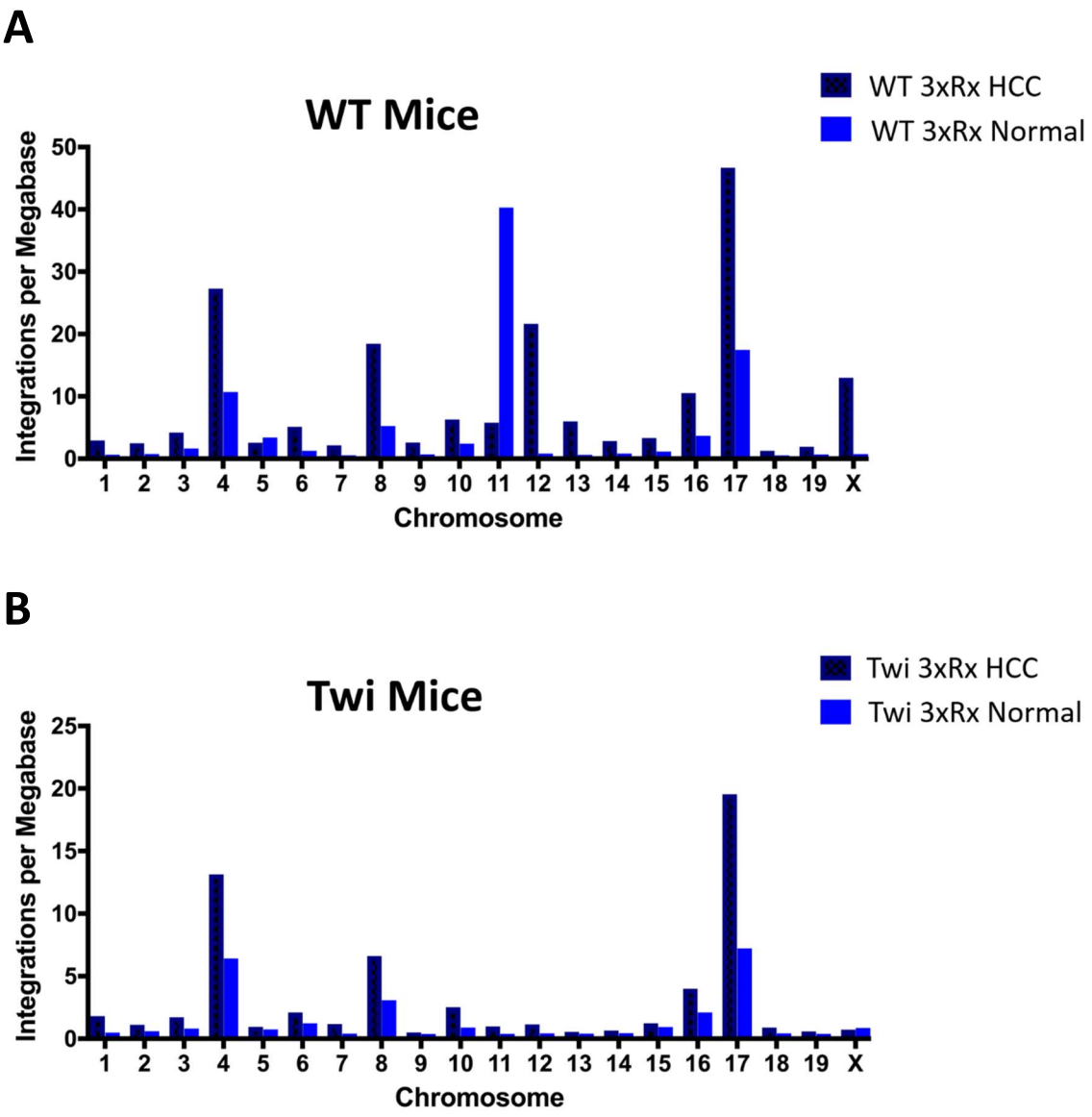

Figure 3.15 Chromosomal breakdown of unique AAV integration sites

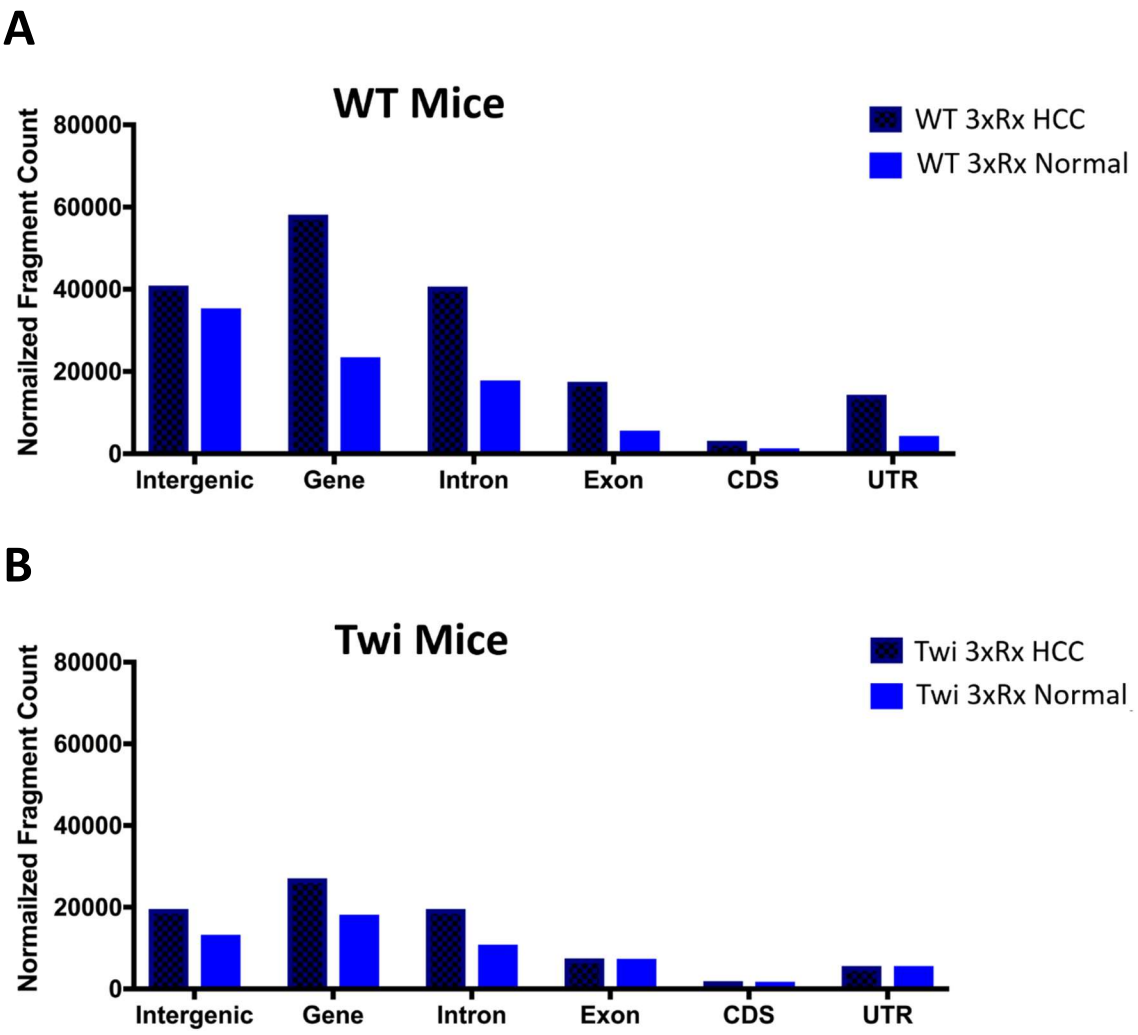

Figure 3.16 Functional breakdown of unique AAV integration sites

CHAPTER FOUR

Conclusions and Future Directions

4.1 Conclusions

Krabbe disease is a pediatric lysosomal storage disorder characterized by deficiency of galactosylceramidase (GALC) activity and psychosine accumulation, which results in severe neurologic impairment and demyelination (Wenger et al., 2016). Psychosine is a toxic metabolite that accumulates most quickly in oligodendrocytes and Schwann cells, but also accumulates in other cells of the body.

Early infantile Krabbe disease is characterized by disease onset before 1 year old, with rapid progression and death usually occurring before 2 years of age. Affected patients present with irritability and gastrointestinal dysmotility, upper and lower motor neuron signs, autonomic dysfunction, immune defects, and sensory loss (Krabbe, 1916; Hagberg, 1963). Patients experience profound demyelination in the central and peripheral nervous systems (CNS and PNS), accompanied by neuronal cell death, axonal damage, and severe neuroinflammation. Globoid cells accumulate in the CNS, as microglia and/or macrophages fuse in an attempt to clean up myelin debris (Collier and Greenfield, 1924; Blackwood and Cumings, 1954; Austin and Lehfeldt, 1965).

Although this disease was described in 1916 (Krabbe), and the first animal model was reported in 1980, there is no cure. Standard of care consists of hematopoietic stem cell transplantation (HSCT), which prolongs life and delays symptom progression if administered before symptoms onset (Wright et al., 2017). Otherwise, patients are managed symptomatically with the goal of keeping them as comfortable as possible (Escolar et al., 2016). There are no clinical trials for Krabbe disease.

The first animal model for Krabbe disease (the Twitcher mouse, Twi) was published in 1980 (Kobayashi et al.; Duchen et al.). This murine model is an excellent model for infantile Krabbe disease because it parallels the genetics, biochemistry, histology, and clinical progression

of the human disease. Because they breed quickly and are relatively cheap to maintain, Twi mice have been the primary animal model in the field of Krabbe research.

4.1.1 Outstanding questions in the field

There are many outstanding questions in the Krabbe field. Of primary importance is the biochemistry of *in vivo* psychosine synthesis. Although psychosine has been hypothesized to be the primary disease-causing agent in Krabbe disease, it is unclear how it is synthesized. A study published in 1960 showed that the anabolic pathway of psychosine synthesis occurs *in vitro*, and another independent study published in 1973 concluded that the catabolic pathway does not occur (Cleland and Kennedy, 1960; Lin and Radin, 1973). Together, these two publications established the dogma that psychosine synthesis occurs through the anabolic dehydration of galactose and sphingosine. However, neither the enzyme nor the cDNA encoding the enzyme has ever been identified, turning this supposed dogma into a mystery that has yet to be solved.

Another puzzling biochemical observation in the field of Krabbe research is the lack of galactosylceramide accumulation in patients and animal models with Krabbe disease (Eto et al., 1970; Svennerholm et al., 1980). Galactosylceramidase, the enzyme defective in this disease, is so named because galactosylceramide is its substrate. However, galactosylceramide does not accumulate in the absence of the enzyme responsible for degrading it. It has been assumed that another pathway of galactosylceramide degradation that is independent of GALC must exist. However, such a pathway has never been identified, and the enzyme catalyzing this putative reaction remains elusive.

A better understanding of psychosine synthesis may provide a way to test the 40-year-old 'Psychosine Hypothesis,' which states that psychosine accumulation, rather than GALC deficiency, is the primary cause of symptomatology and disease progression in Krabbe disease (Miyatake and

Suzuki, 1972). Although this hypothesis is generally accepted in the field, there has so far been no way to test it because of the inability to experimentally dissociate GALC deficiency from psychosine accumulation. Once the enzyme that catalyzes psychosine synthesis is identified, inhibition of this enzyme in a GALC-deficient background may finally provide the experimental setup to test this >45-year-old hypothesis.

A better understanding of the biochemistry of Krabbe disease is also critical for development of substrate reduction therapy (SRT). Substrate reduction therapy uses small molecule drugs that cross the blood brain barrier to inhibit psychosine synthesis and slow the buildup of this toxic compound. Currently, there are no SRTs in use in the clinic, and L-cycloserine is the experimental SRT therapy of choice (LeVine et al., 2000). Unfortunately, L-cycloserine is very unlikely to be approved for patient use, because it inhibits serine palmitoyl transferase, an enzyme that is many steps upstream of psychosine synthesis (Sundaram and Lev, 1984; Sundaram and Lev, 1985). As such, it perturbs many lipid metabolism pathways, and is known to cause unintended effects, including decreased synthesis of myelin (Sundaram and Lev, 1984) and changes in neuronal firing (Haas et al., 1980).

Discovery of a more specific inhibitor of psychosine synthesis is impeded by the lack of understanding of how psychosine is produced. Identification of the enzyme directly responsible for catalyzing psychosine formation would likely facilitate the development of a drug that specifically targets this enzyme. Until this enzyme is identified, progress in SRT development for Krabbe disease will be restricted.

Krabbe disease has been remarkably refractory to treatment. The current standard of care is not curative, and derives from a murine experimental therapy study that was published in 1984 (Yeager et al.). No single therapy since then has been able to effect a greater increase in lifespan.

In more recent years, we have shown that combination therapies have much greater efficacy than single therapies, likely because they simultaneously target more than one major pathogenic mechanism of Krabbe disease. In addition, some experimental therapies synergize to dramatically increase Twi lifespan (Reddy et al., 2013; Hawkins-Salsbury et al., 2015; Rafi et al., 2017). Despite significant progress made in lifespan extension, the motor deficits associated with Krabbe disease have been largely refractory to treatment for all experimental therapies published so far. Peripheral neuropathy and neuromuscular dysfunction significantly impair quality of life for patients with Krabbe disease. Future therapies that successfully treat this facet of the disease would significantly improve the quality of life for Krabbe patients.

Although much progress has been made in gene therapy for this monogenic disease, data have come to light that show a causative relationship between adeno-associated virus (AAV) administration and hepatocellular carcinoma (HCC) in mice (Wang et al., 2012; Chandler et al., 2015). This is a very concerning finding, as HCC is an incurable cancer that results inevitably in patient death. While it is unclear whether the AAV-HCC relationship observed in mice will translate to humans, research in this area is urgently needed. In addition to determining the mechanism by which AAV causes hepatocarcinogenesis, research is also needed to determine how other therapies could change the penetrance of AAV-induced HCC. This is especially true, because clinical trials for Krabbe will likely consist of an experimental therapy that is added to the current standard of care. If gene therapy is to be studied in a clinical trial, we need to understand how HSCT could affect the penetrance of AAV-induced HCC.

4.1.2 Questions answered in chapter two

In chapter two, we showed that acid ceramidase (ACDase) catalyzes the *in vitro* and *in vivo* catabolic deacylation of galactosylceramide to psychosine. We cultured fibroblasts that were

deficient in GALC and ACDase activity, and showed that these fibroblasts did not accumulate any psychosine compared to Twi fibroblasts. We then restored ACDase activity through lentiviral transduction, and showed that restoring ACDase activity resulted in significant psychosine accumulation. These data completely overturn the 60-year-old dogma of anabolic psychosine synthesis and identify ACDase as the direct catalyzer of catabolic psychosine synthesis.

We next bred and characterized the *GALC*$^{-/-}$*Asah1*$^{-/-}$ (Twitcher/Farber, Twi/FD) double mutant mouse. We showed that Twi/FD mice do not accumulate psychosine. As such, it is an experimental system that completely dissociates GALC deficiency from psychosine accumulation. We showed that the absence of psychosine accumulation in the context of the *GALC*$^{-/-}$ mutation completely abolishes all signs and symptoms of Krabbe disease. These results confirm the >45-year-old hypothesis, at least within the lifespan of the Twi/FD mouse, and show that psychosine accumulation, not GALC deficiency, causes the Krabbe phenotype.

The lack of the Krabbe phenotype in the double mutant is accompanied by a dramatic elevation of galactosylceramide that is unique to the Twi/FD mouse. Because Twi/FD mice don't live as long as FD mice but resemble FD mice phenotypically in all other aspects, we hypothesized that galactosylceramide accumulation is the likely cause of the slightly shortened lifespan. These data show that ACDase provides an alternate pathway for galactosylceramide metabolism in the absence of GALC activity. This explains why galactosylceramide elevation is not observed in Twi mice. Only when GALC activity and ACDase activity are both deficient does galactosylceramide accumulate.

Finally, we identified ACDase as a novel SRT target for Krabbe disease, and showed that pharmacologic inhibition of ACDase activity extends Twi lifespan. These data will catalyze the search for more potent and specific inhibitors of ACDase. Unlike L-cycloserine, which is a

nonspecific inhibitor of psychosine synthesis, small molecule drugs targeting ACDase will be much more specific for psychosine synthesis, and would thus be more likely to have safety profiles acceptable for clinical use.

4.1.3 Questions answered in chapter three

In chapter three, we characterized the efficacy of a combination therapy consisting of AAV2/9-mediated gene therapy, HSCT, and L-cycloserine. We previously tested the same triple therapy, but with a second-generation AAV2/5 vector, and showed that the combination therapy produced a dramatic increase in lifespan (Hawkins-Salsbury et al., 2015). In this study, we show that using a newer third generation AAV2/9 vector not only produces a greater improvement in lifespan, but also successfully treats the motor deficits associated with Krabbe disease. Every Twi mouse treated with the triple therapy (3xRx) combination was able to perform the rotarod function test from weaning until death. Although the wirehang test is significantly harder than the rotarod, half the 3xRx-treated Twi mice were able to consistently perform the wirehang test from weaning until death. Such normalization of motor function has never before been reported for the Twi mouse.

These results suggest that AAV2/9, which has been shown to have increased axonal transport (Foust et al., 2009; Aschauer et al., 2013), increased CNS penetrance (Cearley and Wolfe, 2006), and increased transduction (Cearley and Wolfe, 2006), effectively targets the peripheral neuropathy and neuromuscular deficits in Krabbe disease. Because Twi mice treated with AAV2/9-mediated gene therapy and HSCT double therapy do not experience correction of motor deficits, L-cycloserine must interact with gene therapy and/or HSCT to restore motor function and prevent peripheral neuropathy.

Although AAV2/9 is a more effective vector than AAV2/5 in many respects, AAV2/9 is also associated with an increased penetrance of AAV-induced HCC. We showed that the administration of other therapies in conjunction with AAV2/9-mediated gene therapy could significantly decrease the latency and increase the penetrance of AAV-induced HCC. In particular, L-cycloserine seems to dramatically increase the frequency of AAV-induced HCC in Twi and WT mice to nearly 100%. Whether this is a function of L-cycloserine alone, or whether L-cyloserine must interact with the other administered therapies to produce this effect is unknown. Metabolomic comparison of HCC vs. normal-appearing liver tissue indicates that L-cycloserine alters the levels of different ceramide species, which may alter cell survival. If this is indeed how L-cycloserine effects its carcinogenic properties, it is possible that the use of a more specific inhibitor of psychosine synthesis that doesn't perturb other pathways of lipid metabolism may prevent the unintended, increased penetrance of AAV-induced HCC.

We performed integration site analysis to determine if AAV integration sites differed between HCC liver tissue and normal liver tissue from the same animal. Integration analysis shows that the number of unique AAV integration sites is much higher in HCC liver tissue than in normal liver tissue. Integrations occur most frequently in genes, especially in HCC tissue. This is not surprising, as we would expect disruptions to genes to produce a negative functional effect. It is unclear if the proteins expressed by genes that are most perturbed by AAV integration cluster in any gene ontology group. If, for example, oncogenes are commonly affected, that could explain the mechanism for AAV-induced HCC.

4.2 Future Directions

4.2.1 Small molecule inhibitors of acid ceramidase

Current SRT for Krabbe disease relies on inhibiting psychosine synthesis by inhibition of serine palmitoyl transferase, an upstream enzyme in lipid metabolism (Sundaram and Lev, 1984). Identification of ACDase as the enzyme directly responsible for psychosine synthesis provides the impetus to perform large-scale drug screens to discover potent inhibitors of ACDase to more specifically inhibit psychosine synthesis.

Carmofur is a chemotherapeutic that has also been identified as an inhibitor of ACDase activity (Realini et al., 2013). In chapter 2, we showed that Carmofur extended the lifespan of Twi mice heterozygous at the ACDase-encoding locus, but not of Twi mice WT at that locus. The natural follow-up study is to increase the dose of Carmofur. However, increasing the dose of Carmofur may produce unintended results, as over-inhibition of ACDase may produce a Farber phenotype, similar to the phenotype of Twi/FD mice. Therefore, we hypothesize that combining Carmofur with another small molecule inhibitor that acts at a different point in the psychosine synthesis pathway may result in significant lifespan extension in Twi mice. Since psychosine is produced from galactosylceramide and ceramide galactosyltransferase (CGT) catalyzes the formation of galactosylceramide, simultaneous SRT inhibition of ACDase and CGT may produce a significant therapeutic effect without causing unwanted adverse effects. Combination of such an SRT with other therapies, such as gene therapy and HSCT, would likely further increase Twi lifespan beyond that reported in chapter 3 of this dissertation.

4.2.2 Liver-detargeted gene therapy

The triple combination therapy consisting of AAV2/9-GALC gene therapy, HSCT, and L-cycloserine significantly extended Twi lifespan beyond any reported in previously published

studies. We made the argument in chapter 3 that the Twi mice treated with this triple combination therapy died from HCC instead of Krabbe disease. Thus, HCC represents a brick wall that is impeding further therapeutic progress.

One way to scale this brick wall is to use a liver de-targeted AAV vector to minimize AAV transduction in the liver. Liver-detargeted AAV9 vectors have been published (Pulicheria et al., 2011), and a liver-detargeted AAV 2/8 vector has been successfully used *in vivo* to enhance gene delivery to muscle in a hamster model of muscular dystrophy (Rotundo et al., 2013). Systemic delivery of AAV-GALC has been shown to significantly increase Twi survival (Rafi et al., 2017). Thus, intravenous administration of a liver de-targeted AAV vector that penetrates the blood brain barrier may not only decrease the penetrance of AAV-induced HCC, but also enhance survival in Krabbe disease by increasing gene delivery to both the CNS, PNS, and systemic tissues.

4.2.3 Systematic study of AAV-induced hepatocellular carcinoma

We observed a decreased latency and a dramatically increased incidence of AAV-induced HCC in mice treated with AAV2/9-GALC, HSCT, and L-cycloserine triple combination therapy. Penetrance was 100%, an especially startling percentage, because C57BL6 mice are known to be relatively cancer resistant (Nakamura et al., 1992). In contrast, we did not observe an increase in AAV-induced HCC penetrance in AAV2/9-GALC and HSCT double therapy (2xRx) treated Twi mice. This may be because most of the 2xRx-treated mice died before the end of the latency period of approximately one year. In order to determine the effect of HSCT on AAV-induced HCC, WT mice need to be treated with the double therapy regimen and assessed for development of liver tumors.

Although AAV integration into the mouse genome causes HCC, the mechanism by which carcinogenesis occurs is unclear. One hypothesis is that integration disrupts the expression of cell

survival genes, which in turn renders the cell resistant to apoptosis. We isolated tumor and normal liver tissue from each mouse that developed HCC in the combination therapy study to identify integration sites that contribute to HCC carcinogenesis. Although the data obtained from this analysis are important, the combination therapy study was not originally designed to compare HCC and normal tissue, and thus has many limitations. To test the hypothesis proposed above, a larger study designed specifically for this purpose must be set up to facilitate genomic analysis of AAV integration sites in conjunction with gene expression profiling.

4.2.4 In utero hematopoietic stem cell transplantation

Although HSCT for Krabbe disease is generally performed in infancy or early childhood, abnormal levels of psychosine elevation are detectable in the affected fetus as early as the second trimester of pregnancy (Ida et al., 1994). The existence of *in utero* HSCT (IUHCT) raises the possibility of prenatal therapeutic intervention (Vrecenak and Flake, 2013). Although IUHCT has not yet achieved clinical potential, the technique is well-documented in mice (Nijaga et al., 2011). Proof-of-concept experiments should be performed to determine if IUHCT could improve clinical outcome in Twi mice. If IUHCT is indeed effective, combining IUHCT with other therapies could produce greater therapeutic benefits than current postnatal transplantation techniques.

4.3 Concluding Remarks

Krabbe disease is a monogenic disease with a complex pathophysiology. Finding an effective therapy to target its many facets has been exceedingly difficult. The data presented in this dissertation significantly advance the field in numerous ways. We answered one of the most basic questions of Krabbe pathophysiology by determining the pathway of psychosine synthesis as the catabolic deacylation of galactosylceramide. By identifying the enzyme catalyzing this

reaction as acid ceramidase, we also identified a novel and specific therapeutic target that will catalyze the development of more potent SRTs. Finally, we set up an experimental system that dissociates GALC deficiency from psychosine accumulation, which allowed us to test and confirm the long-standing 'Psychosine Hypothesis.'

In terms of therapy, we developed a new combination therapy that significantly prolonged Twi lifespan. Equally importantly, this therapy corrected the motor deficits associated with Krabbe disease. Finally, we showed that HSCT and L-cycloserine administration decreased the latency of AAV-induced HCC from 1 year to 8 months. Combination therapy also increased the penetrance of AAV-induced HCC to nearly 100%. Although additional research is needed to determine the mechanism responsible for these changes, these data emphasize that AAV-induced HCC is a serious complication of AAV-mediated gene therapy that needs to be addressed. We hypothesize that the use of a liver-detargeted AAV vector will significantly decrease the penetrance of AAV-induced HCC.

We have systematically tested combination therapies by changing only one treatment at a time. However, all three therapies in the current combination therapy regimen could be improved. Gene therapy could be improved by using a liver-detargeted gene delivery system; hematopoietic stem cell transplantation may be more efficacious if administered *in utero*; a combination SRT targeting ACDase and CGT would likely be more potent and benign than the currently-used L-cycloserine. (Figure 4.1) We hypothesize that a combination therapy with all three of those modifications would be a synergistic, effective therapy for Krabbe that may bring us very close to a cure.

4.4 Figure Legends

Figure 4.1. Potential improvements to the current triple combination therapy. Gene delivery using a liver-detargeted AAV9 vector may significantly reduce the frequency of AAV-induced HCC. *In utero* hematopoietic stem cell transplantation may provide prenatal correction of psychosine elevation and other abnormalities in Krabbe disease. Combination substrate reduction therapy that targets ACDase and CGT may result in significant retardation of psychosine accumulation while minimizing adverse effects.

4.5 Figures

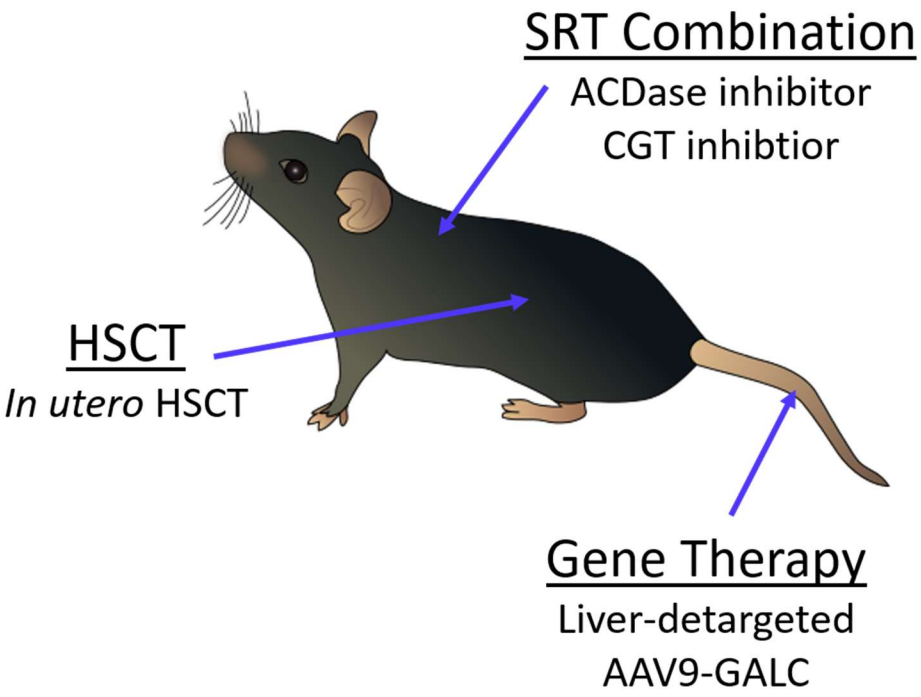

Figure 4.1. Potential improvements to the current triple combination therapy

REFERENCES

Adewoye AB, Lindsay SJ, Dubrova YE, Hurles ME. 2015. The genome-wide effects of ionizing radiation on mutation induction in the mammalian germline. Nat Commun 6:6684.

Aschauer DE, Kreuz S, Rumpel S. 2013. Analysis of transduction efficiency, tropism, and axonal transport of AAV serotypes 1, 2, 5, 6, 8, and 9 in the mouse brain. PLoS One 8(9):e76310.

Alayoubi AM, Wang JC, Au BC, Carpentier S, Garcia V, Dworski S, El-Ghamrasni S, Kirouac KN, Exertier MJ, Xiong ZJ, Privé GG, Simonaro CM, Casas J, Fabrias G, Schuchman EH, Turner PV, Hakem R, Levade T, Medin JA. 2013. Systemic ceramide accumulation leads to severe and varied pathological consequences. EMBO Mol Med 5(6):827-42.

Anderson HM, Wilkes J, Korgenski EK, Pulsipher MA, Blaschke AJ, Hersh AL, Sriastava R, Bonkowsky JL. 2014. Preventable infections in children with leukodystrohy. Ann Clin Transl Neurol 1:370-374.

Austin JH, Lehfeldt D. 1965. Studies in globoid (Krabbe) leukodystrophy. 3. Significance of experimentally-produced globoid-like elements in rat white matter and spleen. J Neuropathol Exp Neurol 24:265-289.

Bainbridge JW, Smith AJ, Barker SS, Robbie S, Henderson R, Balaggan K, Viswanathan A, Holder GE, Stockman A, Tyler N, Peterson-Jones S, Battacharya SS, Thrasher AJ, Fitzke FW, Carter BJ, Rubin S, Moore AT, Ali RR. 2008. Effect of gene therapy on visual function in Leber's congenital amaurosis. N Engl J Med 358(21):2231–9.

Baskin GB, Ratterree M, Davison BB, Falkenstein KP, Clarke MR, England JD, Vanier MT, Luzi P, Rafi MA, Wenger DA. 1998. Genetic galactocerebrosidase deficiency (globoid cell leukodystrophy, Krabbe disease) in rhesus monkeys (Macaca mulatta). Lab Anim Sci 48(5):476-82.

Bell P, Moscioni AD, McCarter RJ, Wu D, Gao G, Hoang A, Sanmiguel JC, Sun X, Wivel NA, Raper SE, Furth EE, Batshaw ML, Wilson JM. 2006. Analysis of tumors arising in male B6C3F1 mice with and without AAV vector delivery to liver. Mol Ther 14(1):34-44.

Biswas S, LeVine SM. 2002. Substrate-reduction therapy enhances the benefits of bone marrow transplantation in young mice with globoid cell leukodystrophy. Pediatr Res 51(1):40-47.

Blackwood W, Cumings JN. 1954. A histochemical and chemical study of three cases of diffuse cerebral sclerosis. J Neurol Neurosurg Psychiatry 17:33-49.

Borda JT, Alvarez X, Mohan M, Ratterree MS, Phillippi-Falkenstein K, Lackner AA, Bunnell BA. 2008. Clinical and immunopathological alterations in rhesus macaques affected with globoid cell leukodystrophy. Am J Pathol 172(1):98-111.

Bradbury AM, Rafi MA, Bagel JH, Brisson BK, Marshall MS, Pesayco Salvador J, Jiang X, Swain GP, Prociuk ML, O'Donnell PA, Fitzgerald C, Ory DS, Bongarzone ER, Shelton GD, Wenger DA, Vite CH. 2018. AAVrh10 gene therapy ameliorates central and peripheral nervous system disease in canine globoid cell leukodystrophy (Krabbe Disease). Human Gene Ther 29(7):785-801.

Cantuti-Castelvetri L, Zhu H, Givogri MI, Chidavaenzi RL, Lopez-Rosas A, Bongarzone ER. 2012. Psychosine induces the dephosphorylation of neurofilaments by deregulation of PP1 and PP2A phosphatases. Neurobiol Dis 46:325–335.

Cantuti-Castelvetri L, Givogri MI, Hebert A, Smith B, Song Y, Kaminska A, Lopez-Rosas A, Morfini G, Pigino G, Sands M, Brady ST, Bongarzone ER. 2013. The sphingolipid psychosine inhibits fast axonal transport in Krabbe disease by activation of GSK3beta and deregulation of molecular motors. J Neurosci 33:10048-56.

Castelvetri LC, Givogri MI, Zhu H, Smith B, Lopez-Rosas A, Qiu X, van Breemen R, Bongarzone ER. 2011. Axonopathy is a compounding factor in the pathogenesis of Krabbe disease. Acta Neuropathol 122:35–48.

Cearley CN, Wolfe JH. 2006. Transduction characteristics of adeno-associated virus vectors expressing cap serotypes 7, 8, 9, and Rh10 in the mouse brain. Mol Ther 13(3):528–37.

Chandler RJ, LeFave MC, Varshney GK, Trivedi NS, Carrillo-Carrasco N, Senac JS, Wu W, Hoffmann V, Elkahloun AG, Burgess SM, Venditti CP. 2015. Vector design influences hepatic genotoxicity after adeno-associated virus gene therapy. J Clin Invest 125(2):870-80.

Chandler RJ, LaFave MC, Varshney GK, Burgess SM, Venditti CP. 2016. Genotoxicity in mice following AAV gene delivery: a safety concern for human gene therapy? Mol Ther 24(2):198-201.

Chen YQ, Rafi MA, De Gala G, Wenger DA. 1993. Cloning and expression of cDNA encoding human galactocerebrosidase, the enzyme deficient in globoid cell leukodystrophy. Hum Mol Genet 2:1841-1845.

Cho KH, Kim MW, Kim SU. 1997. Tissue culture model of Krabbe's disease: psychosine cytotoxicity in rat oligodendrocyte cultures. Dev Neurosci 19:321–327.

Chung SH, Johnson MS, Gronenborn AM. 1984. L-cycloserine: a potent anticonvulsant. Epilepsia 25:353-362.

Cleland WW, Kennedy EP. 1960. The enzymatic synthesis of psychosine. J Biol Chem 235:45-51.

Collier J, Greenfield JG. 1924. The encephalitis periaxialis of Schilder: a clinical and pathological study with an account of two cases, one of which was diagnosed during life. Brain 47:489–519.

Contreras MA, Haq E, Uto T, Singh I, Singh AK. 2008. Psychosine-induced alterations in peroxisomes of twitcher mouse liver. Arch Biochem Biophys 477:211–218.

Cornell NW, Zuurendonk PF, Kerich MJ, Straight CB. 1984. Selective inhibition of alanine aminotransferase and aspartate aminotransferase in rat hepatocytes. Biochem J 220:707-716.

Cunningham J, Pivirotto P, Bringas J, Suzuki B, Vijay S, Sanftner L, Kitamura M, Chan C, Bankiewicz KS. 2008. Biodistribution of adeno-associated virus type-2 in nonhuman primates after convection-enhanced delivery to brain. Mol Ther 16(7):1267–75.

Debs R, Froissart R, Aubourg P, Papeix C, Douillard C, Degos B, Fontaine B, Audoin B, Lacour A, Said G, Vanier MT, Sedel F. 2013. Krabbe disease in adults: phenotypic and genotypic update from a series of 11 cases and a review. J Inherit Metab Dis 36:859-868.

Donsante A, Vogler C, Muzyczka N, Crawford JM, Barker J, Flotte T, Campbell-Thompson M, Daly T, Sands MS. 2001. Observed incidence of tumorigenesis in long-term rodent studies of rAAV vectors. Ther 8(17):1343-6.

Donsante A, Miller DG, Li Y, Vogler C, Brunt EM, Russell DW Sands MS. 2007. AAV vector integration sites in mouse hepatocellular carcinoma. Science 317(5837):477.

Duchen LW, Eicher EM, Jacobs JM,Scaravilli F, Teixeira F. 1980. Hereditary leucodystrophy in the mouse: the new mutant twitcher. Brain 103:695–710.

Duffner PK, Caviness VS Jr, Erbe RW, Patterson MC, Schultz KR, Wenger DA, Whitley C. 2009. The long-term outcomes of presymptomatic infants transplanted for Krabbe disease: report of the workshop held on July 11 and 12, 2008. Holiday Valley, New York. Genet Med 11:450-454.

Escolar ML, Poe MD, Martin HR, Kurtzberg J. 2006. A staging system for infantile Krabbe disease to predict outcome after unrelated umbilical cord blood transplantation. Pediatrics 118:e879-889.

Escolar ML, West T, Dallavecchia A, Poe MD, LaPoint K. 2016. Clinical management of Krabbe disease. J Neurosci Res 94(11):118-25.

Escolar ML, Kiely BT, Shawgo E, Hong X, Gelb MH, Orsini JJ, Matern D, Poe MD. 2017. Psychosine, a marker of Krabbe phenotype and treatment effect. Mol Genet Metab 121(3):271-278.

Eto Y, Suzuki K, Suzuki K. 1970. Globoid cell leukodystrophy (Krabbe's disease): Isolation of myelin with normal glycolipid composition. J Lipid Res 11:473-479.

Ferraz MJ, Marques AR, Appelman MD, Verhoek M, Strijland A, Mirzaian M, Scheji S, Ouairy CM, Lahav D, Wisse P, Overkleeft HS, Boot RG, Aerts JM. 2016. Lysosomal glycosphingolipid catabolism by acid ceramidase: formation of glycosphingolipid bases during deficiency of glycosidases. FEBS Lett 590(6):716-25.

Fletcher JL, Williamson P, Horan D, Taylor RM. 2010. Clinical signs and neuropathologic abnormalities in working Australian Kelpies with globoid cell leukodystrophy (Krabbe disease). J Am Vet Med Assoc 237(6):682-8.

Formichi P, Radi E, Battisti C, Pasqui A, Pompella G, Lazzerini PE, Laghi-Pasini F, Leonini A, Di Stefano A, Federico A. 2007. Psychosine-induced apoptosis and cytokine activation in immune peripheral cells of Krabbe patients. J Cell Physiol 212(3):737-43.

Foust KD, Nurre E, Montgomery CL, Hernandez A, Chan CM, Kaspar BK. 2009. Intravascular AAV9 preferentially targets neonatal neurons and adult astrocytes. Nat Biotechnol 27(1):59-65.

Fowler SC, Birkestrand BR, Chen R, Moss SJ, Vorontsova E, Wang G, Zarcone TJ. 2001. A force-plate actometer for quantitating rodent behaviors: illustrative data on locomotion, rotation, spatial patterning, stereotypes, and tremor. J Neurosci Methods 107(1-2):107-24.

Galbiati F, Basso V, Cantuti L, Givogri MI, Lopez-Rosas A, Perez N, Vasu C, Cao H, van Breemen R, Mondino A, Bongarzone ER. 2007. Autonomic denervation of lymphoid organs leads to epigenetic immune atrophy in a mouse model of Krabbe disease. J Neurosci 27:13730 –13738.

Giri S, Khan M, Nath N, Singh I, Singh AK. 2008. The role of AMPK in psychosine mediated effects on oligodendrocytes and astrocytes: implication for Krabbe disease. J Neurochem 105:1820–1833.

Haas HL, Wieser HG. 1980. Effect of L-cycloserine on cortical neurons in the rat. Eur J Pharmacol 61:79-83.

Hagberg B, Sourander P, Svennerholm L. 1963. Diagnosis of Krabbe's infantile leukodystrophy. J Neurol Neurosurg Psychiatry 26:195-198.

Hammond SL, Leek AN, Richman EH, Tjalkens RB. 2017. Cellular selectivity of AAV serotypes for gene delivery in neurons and astrocytes by neonatal intracerebroventricular injection. PLoS One 12(12):e0188830.

Haq E, Giri S, Singh I, Singh AK. 2003. Molecular mechanism of psychosine-induced cell death in human oligodendrocyte cell line. J Neurochem 86: 1428–1440.

Haraoka G, Muraoka M, Yoshioka N, Wakami S, Hayashi I. 1997. First case of surgical treatment of Farber’s disease. Ann Plast Surg 39:405-410.

Hawkins-Salsbury JA, Parameswar AR, Jiang X, Schlesinger PH, Bongarzone E, Ory DS, Demchenko AV, Sands MS. 2013. Psychosine, the cytotoxic sphingolipid that accumulates in globoid cell leukodystrophy, alters membrane architecture. J Lipid Res 54(12):3303-11.

Hawkins-Salsbury JA, Shea L, Jiang X, Hunter D, Reddy A, Qin EY, Li Y, Gray SJ, Ory DS, Sands MS. 2015. Mechanism-based combination therapy dramatically increases therapeutic efficacy in murine globoid cell leukodystrophy. J Neurosci 35(16):6495-505.

Higashi Y, Komiyama A, Suzuki K. 1992. The twitcher mouse: immunocytochemical study of Ia expression in macrophages. J Neuropathol Exp Neurol 51(1):47-57.

Hinderer C, Katz N, Buza EL, Dyer C, Goode T, Bell P, Richman LK, Wilson JM. 2018. Severe toxicity in nonhuman primates and piglets following high-dose intravenous administration of an adeno-associated virus vector expressing human SMN. Hum Gene Ther 29(3):285-298.

Hoogerbrugge PM, Poorthuis BJ, Romme AE, van de Kamp JJ, Wagemaker G, van Bekkum DW. 1988. Effect of bone marrow transplantation on enzyme levels and clinical course in the neurologically affected twitcher mouse. J Clin Invest 81(6):1790-4.

Hu P, Li Y, Nikolaishvili-Feinberg N, Scesa G, Bi Y, Pan D, Moore D, Bongarzone ER, Sands MS, Miller R, Kafri T. 2016. Hematopoietic stem cell transplantation and lentiviral vector-based gene therapy for Krabbe's disease: present convictions and future prospects. J Neurosci Res 94(11):1152-68.

Ida H, Rennert OM, Watabe K, Eto Y, Maekawa K. 1994. Pathological and biochemical studies of fetal Krabbe disease. Brain Dev 16(6):480-4.

Ijichi K, Brown G, Moore CS, Lee JP, Winokur PN, Pagarigan R, Snyder EY, Bongarzone ER, Crocker SJ. 2013. MMP-3 mediates psychosine-induced globoid cell formation: implications for leukodystrophy pathology. Glia 61(5):765-77.

Im DS, Heise CE, Nguyen T, O'Dowd BF, Lynch KR. 2001. Identification of a molecular target of psychosine and its role in globoid cell formation. J Cell Biol 153:429-434.

Isakova IA, Baker KC, Dufour J, Phinney DG. 2017. Mesenchymal stem cells yield transient improvements in motor function in an infant rhesus macaque with severe early-onset Krabbe disease. Stem Cells Transl Med 6(1):99-109.

Jatana M, Giri S, Singh AK. 2002. Apoptotic positive cells in Krabbe brain and induction of apoptosis in rat C6 glial cells by psychosine. Neurosci Lett 330:183–187.

Jiao J, Watt GP, Stevenson HL, Calderone TL, Fisher-Hoch SP, Ye Y, Wu X, Vierling JM, Beretta L. 2018. Telomerase reverse transcriptase mutations in plasma DNA in patients with hepatocellular carcinoma or cirrhosis: Prevalence and risk factors. Hepatol Commun 2(6):718-731.

Karahatay S, Thomas K, Koybasi S, Senkal CE, Elojeimy S, Liu X, Bielawski J, Day TA, Gillespie MB, Sinha D, Norris JS, Hannun YA, Ogretmen B. 2007. Clinical relevance of ceramide metabolism in the pathogenesis of human head and neck squamous cell carcinoma (HNSCC): Attenuation of C(18)-ceramide in HNSCC tumors correlates with lymphovascular invasion and nodal metastasis. Cancer Lett 256:101–111.

Karumuthil-Melethil S, Marshall MS, Heindel C, Jakubauskas B, Bongarzone ER, Gray SJ. 2016. Intrathecal administration of AAV/GALC vectors in 10-11-day-old Twitcher mice improves survival and is enhanced by bone marrow transplant. J Neurosci Res 94(11):1138-51.

Khan M, Haq E, Giri S, Singh I, Singh AK. 2005. Peroxisomal participation in psychosine-mediated toxicity: implications for Krabbe's disease. J Neurosci Res 80:845–854.

Knudson A. Mutation and cancer: statistical study of retinoblastoma. 1971. Proc Natl Acad Sci USA 68(4):820-823.

Kobayashi T, Yamanaka T, Jacobs JM, Teixeira F, Suzuki K. 1980. The Twitcher mouse: an enzymatically authentic model of human globoid cell leukodystrophy (Krabbe's disease). Brain Res 202:479–483.

Kondo Y, Adams JM, Vanier MT, Duncan ID. 2011. Macrophages counteract demyelination in a mouse model of globoid cell leukodystrophy. J Neurosci 31(10):3610-24.

Kornfeld S. 1992. Structure and function of the mannose 6-phosphate/insulinlike growth factor II receptors. Annu Rev Biochem 61:307-330.

Krabbe K. 1916. A new familial, infantile form of diffuse brain-sclerosis. Brain 39:74-114.

Koybasi S, Senkal CE, Sundararaj K, Spassieva S, Bielawski J, Osta W, Day TA, Jiang JC, Jazwinski SM, Hannun YA, Obeid LM, Ogretmen B. 2004. Defects in cell growth regulation by C18:0-ceramide and longevity assurance gene 1 in human head and neck squamous cell carcinomas. J Biol Chem 279(43):44311–9.

Kubota T, Fujita S, Kodaira S, Yamamoto T, Josui K, Arisawa Y, Suto A, Ishibiki K, Abe O, Mabuchi K, Fuse M. 1991. Antitumor activity of fluoropyrimidines and thymidylate synthetase inhibition. Jpn J Cancer Res 82(4):476–482.

Lee WC, Tsoi YK, Dickey CA, Delucia MW, Dickson DW, Eckman CB. 2006. Suppression of galactosylceramidase (GALC) expression in the twitcher mouse model of globoid cell leukodystrophy (GLD) is caused by nonsense-mediated mRNA decay (NMD). Neurbiol Dis 23(2):273-80.

Lee JH, Cho MH, Hersh CP, McDonald ML, Wells JM, Dransfield MT, Bowler RP, Lynch DA, Lomas DA, Crapo JD, Silverman EK, COPDGene and ECLIPSE Investigators. 2015. IREB2 and GALC are associated with pulmonary artery enlargement in chronic obstructive pulmonary disease. Am J Respir Cell Mol Biol 52:365–376.

Levade T, Moser HW, Fensom AH, Harzer K, Moser AB, Salvayre R. 1995. Neurodegenerative course in ceramidase deficiency (Farber disease) correlates with the residual lysosomal ceramide turnover in cultured living patient cells. J Neurol Sci 134:108-114.

LeVine SM, Brown DC. 1997. IL-6 and TNF alpha expression in brains of twitcher, quaking, and normal mice. J Neuroimmunol 73(1-2):47-56.

LeVine SM, Pedchenko TV, Bronshteyn IG, Pinson DM. 2000. L-cycloserine slows the clinical and pathological course in mice with globoid cell leukodystrophy (twitcher mice). J Neurosci Res 60:231-236.

Lin D, Fantz CR, Levy B, Rafi MA, Vogler C, Wenger DA, Sands MS. 2005. AAV2/5 vector expressing galactocerebrosidase ameliorates CNS disease in the murine model of globoid-cell leukodystrophy more efficiently than AAV2. Mol Ther 12(3):422-30.

Lin YN, Radin NS. Alternate pathways of cerebroside catabolism. 1973. Lipids 8(12):732-6.

Liu Y, Gibson J, Wheeler J, Kwee LC, Santiago-Turla CM, Akafo SK, Lichter PR, Gaasterland DE, Moroi SE, Challa P, Herndon LW, Girkin CA, Budenz DL, Richards JE, Allingham RR, Hauser MA. 2011. GALC deletions increase the risk of primary open-angle glaucoma: the role of Mendelian variants in complex disease. PLoS One 6:e27134.

Lowther J, Yard BA, Johnson KA, Carter LG, Bhat VT, Raman MC, Clarke DJ, Ramakers B, McMahon SA, Naismith JH, Campopiano DJ. 2010. Inhibition of the PLP-dependent enzyme serine palmitoyltransferase by cycloserine: evidence for a novel decarboxylative mechanism of inactivation. Mol Biosyst 6:1682-1693.

Luzi, P, Rafi, MA, Wenger DA. 1995. Characterization of the large deletion in the GALC gene found in patients with Krabbe disease. Hum Molec Genet 4:2335-2338.

Luzi P, Rafi MA, Victoria T, Baskin GB, Wenger DA. 1997. Characterization of the rhesus monkey galactocerebrosidase (GALC) cDNA and gene and identification of the mutation causing globoid cell leukodystrophy (Krabbe disease) in this primate. Genomics 42(2):319-24.

Luzi P, Abraham RM, Rafi MA, Curtis M, Hooper DC, Wenger DA. 2009. Effects of treatment on inflammatory and apoptotic markers in the CNS of mice with globoid cell leukodystrophy. Brain Res 1300:146-58.

Lyon G, Hagberg B, Evrard P, Allaire C, Pavone L, Vanier M. 1991. Symptomatology of late onset Krabbe's leukodystrophy: the European experience. Dev Neurosci 13:240-244.

Malone M. 1970. Deficiency in degradative enzyme system in globoid leucodystrophy. Tran Am Soc Neurochem 1:56.

Mattar CNZ, Gil-Farina I, Rosales C, Johana N, Tan YYW, McIntosh J, Kaeppel C, Waddington SN, Biswas A, Choolani M, Schmidt M, Nathwani AC, Chan JKY. 2017. In utero transfer of adeno-associated viral vectors produces long-term factor IX levels in a cynomolgus macaque model. Mol Ther 25(8):1843-1853.

Mendell JR, Al-Zaidy S, Shell R, Arnold WD, Rodino-Klapac LR, Prior TW, Lowes L, Alfano L, Berry K, Church K, Kissel JT, Nagendran S, L'Italien J, Sproule DM, Wells C, Cardenas JA, Heitzer MD, Kaspar A, Corcoran S, Braun L, Likhite S, Miranda C, Meyer K, Foust KD, Burghes AHM, Kaspar BK. 2017. Single-dose gene-replacement therapy for spinal muscular atrophy. N Engl J Med 377(18):1713-1722.

Meneghini V, Lattanzi A, Tirdani L, Bravo G, Morena F, Sanvito F, Calabria A, Bringas J, Fisher-Perkins JM, Dufour JP, Baker KC, Doglioni C, Montini E, Bunnell BA, Bankiewicz K, Martino S, Naldini L, Gritti A. 2016. Pervasive supply of therapeutic lysosomal enzymes in the CNS of normal and Krabbe-affected non-human primates by intracerebral lentiviral gene therapy. EMBO Mol Med 8(5):489-510.

Miller N. 2012. Glybera and the future of gene therapy in the European Union. Nat Rev Drug Discov 11(5):419.

Mikulka CR, Sands MS. 2016. Treatment for Krabbe's disease: Finding the combination. J Neurosci Res. 94(11):1126-37.

Miyatake T, Suzuki K. 1972. Globoid cell leukodystrophy: additional deficiency of psychosine galactosidase. Biochem Biophys Res Commun 48:538-43.

Nakamura K, Kuramoto K, Shibasaki K, Shumiya S, Ohtsubo K. 1992. [Age-related incidence of spontaneous tumors in SPF C57BL/6 and BDF1 mice]. Jikken Dobutsu 41(3):279-285.

Naso MF, Tomkowicz B, Perry WL, Strohl WR. 2017. Adeno-associated virus (AAV) as a vector for gene therapy. BioDrugs 31:317-334.

Nathwani AC, Tuddenham EG, Rangarajan S, Rosales C, McIntosh J, Linch DC, Chowdary P, Riddell A, Pie AJ, Harrington C, O'Beirne J, Smith K, Pasi J, Glader B, Rustagi P, Ng CY, Kay MA, Zhou J, Spence Y, Morton CL, Allay J, Coleman J, Sleep S, Cunningham JM, Srivastava D, Basner-Tschakarjan E, Mingozzi F, High KA, Gray JT, Reiss UM, Nienhuis AW, Davidoff AM. 2011. Adenovirus-associated virus vector-mediated gene transfer in hemophilia B. N Engl J Med 365(25):2357-65.

Nault JC, Datta S, Imbeaud S, Franconi A, Mallet M, Couchy G, Letouze E, Pilati C, Verret B, Blanc JF, Balabaud C, Calderaro J, Laurent A, Letexier M, Bioulac-Sage P, Calvo F, Zucman-Rossi J. 2015. Recurrent AAV2-related insertional mutagenesis in human hepatocellular carcinomas. Nat Genet 47(10):1187-93.

Neufeld EF, Fratantoni JC. 1970. Inborn errors in mucopolysaccharide metabolism. Science 169:141-146.

Nijagal A, Le T, Wegorzewska M, Mackenzie TC. 2011. A mouse model of in utero transplantation. J Vis Exp (47):2303.

Ohno M, Komiyama A, Martin PM, Suzuki K. 1993. MHC Class II antigen expression and T-cell infiltration in the demyelinating CNS and PNS of the twitcher mouse. Brain Res 625(2):186-96.

Ojala DS, Amara DP, Schaffer DV. 2015. Adeno-associated virus vectors and neurological gene therapy. Neuroscientist 21(1):84-98.

Okabe M, Ikawa M, Kominami K, Nakanishi T, Nishimune Y. 1997. 'Green mice' as a source of ubiquitous green cells. FEBS Lett 407(3):313-9.

Orsini JJ, Saavedra-Matiz CA, Gelb MH, Caggana M. 2016. Newborn screening for Krabbe disease. J Neurosci Res 94(11):1063-75.

Pasqui AL, Di Renzo M, Auteri A, Federico G, Pucetti L. 2007. Increased TNF-alpha production by peripheral blood mononuclear cells in patients with Krabbe's disease: effect of psychosine. Eur J Clin Invest 37(9):742-5.

Passini MA, Macauley SL, Huff MR, Taksir RV, Bu J, Wu IH, Piepenhagen PA, Dodge JC, Shihabuddin LS, O'Riordan CR, Schuchman EH, Stewart GR. 2005. AAV vector-mediated correction of brain pathology in a mouse model of Niemann-Pick A disease. Mol Ther 11:754-762.

Passini MA, Dodge JC, Bu J, Yang W, Zhao Q, Sondhi D, Hackett NR, Kaminsky SM, Mao Q, Shihabuddin LS, Cheng SH, Sleat DE, Stewart GR, Davidson BL, Lobel P, Crystal RG. 2006. Intracranial delivery of CLN2 reduces brain pathology in a mouse model of classical late infantile neuronal ceroid lipofuscinosis. J Neurosci 26:1334-1342.

Pedchenko TV, LeVine SM. 1999. IL-6 deficiency causes enhanced pathology in Twitcher (globoid cell leukodystrophy) mice. Exp Neurol 158(2):459-68.

Pedchenko TV, Bronshteyn IG, LeVine SM. 2000. TNF-receptor 1 deficiency fails to alter the clinical and pathological course in mice with globoid cell leukodystrophy (twitcher mice) but affords protection following LPS challenge. J Neuroimmunol 110(1-2):186-94.

Potter GB, Santos M, Davisson MT, Rowitch DH, Marks DL, Bongarzone ER, Petryniak MA. 2013. Missense mutation in mouse GALC mimics human gene defect and offers new insights into Krabbe disease. Hum Mol Genet 22:3397-414.

Potter GB, Petryniak MA. 2016. Neuroimmune mechanisms in Krabbe's Disease. J Neurosci Res 94(11):1341-48.

Pritchard DH, Napthine DV, Sinclair AJ. 1980. Globoid cell leukodystrophy in polled Dorset sheep. Vet Pathol 17(4):399-405.

Pulicheria N, Shen S, Yadav S, Debbink K, Govindasamy L, Agbandje-McKenna M, Asokan A. 2011. Engineering liver-detargeted AAV9 vectors for cardiac and musculoskeletal gene transfer. Mol Ther 19(6):1070-8.

Rafi MA, Rao HZ, Passini MA, Curtis M, Vanier MT, Zaka M, Luzi P, Wolfe JW, Wenger DA. 2005. AAV-mediated expression of galactocerebrosidase in brain results in attenuated symptoms and extended life span in murine models of globoid cell leukodystrophy. Mol Ther 11:734-744.

Rafi MA, Rao HZ, Luzi P, Curtis MT, Wenger DA. 2012. Extended normal life after AAVrh10-mediated gene therapy in the mouse model of Krabbe disease. Mol Ther 20(11):2031-42.

Rafi MA, Rao HZ, Luzi P, Wenger DA. 2015. Long-term improvements in lifespan and pathology in CNS and PNS after BMT plus one intravenous injection of AAVrh10-GALC in Twitcher mice. Mol Ther 23(11):1681-1690.

Realini N, Solorzano C, Pagliuca C, Pizzirani D, Amirotti A, Luciani R, Costi MP, Bandiera T, Piomelli D. 2013. Discovery of highly potent acid ceramidase inhibitors with in vitro tumor chemosensitizing activity. Sci Rep 3:1035.

Reddy AS, Kim JH, Hawkins-Salsbury JA, Macauley SL, Tracy ET, Vogler CA, Han X, Song SK, Wozniak DF, Fowler SC, Klein RS, Sands MS. 2011. Bone marrow transplantation augments the effect of brain- and spinal-cord-directed AAV 2/5 gene therapy by altering inflammation in the murine model of GLD. J Neurosci 31(27):9945-57.

Ricca A, Rufo N, Ungari S, Morena F, Martino S, Kulik W, Alberizzi V, Bolino A, Bianchi F, Del Carro U, Biffi A, Gritti A. 2015. Combined gene/cell therapies provide long-term and pervasive rescue of multiple pathological symptoms in a murine model of globoid cell leukodystrophy. Hum Mol Genet 24(12):3372-89.

Ripoll CB, Flaat M, Klopf-Eiermann J, Fisher-Perkins JM, Trygg CB, Scruggs BA, McCants ML, Leonard HP, Lin AF, Zhang S, Eagle ME, Alvarez X, Li YT, Li SC, Gimble JM, Bunnell BA. 2011. Mesenchymal-lineage stem cells have pronounced anti-inflammatory effects in the twitcher mouse model of Krabbe disease. Stem Cells 29(1):67-77.

Rotundo IL, Lancioni A, Savarese M, D'Orsi L, Iacomino M, Nigro G, Piluso G, Auricchio A, Nigro V. 2013. Use of a lower dosage liver-detargeted AAV vector to prevent hamster muscular dystrophy. Hum Gene Ther 24(4):424-30.

Sakai N, Inui K, Tatsumi N, Fukushima H, Nishigaki T, Taniike M, Nishimoto J, Tsukamoto H, Yanagihara I, Ozono K, Okada S. 1996. Molecular cloning and expression of cDNA for murine galactocerebrosidase and mutation analysis of the twitcher mouse, a model of Krabbe's disease. J Neurochem 66(3):118-24.

Sands MS, Davidson BL. 2006. Gene therapy for lysosomal storage diseases. Mol Ther 13(5):839-49.

Santambrogio S, Ricca A, Maderna C, Ieraci A, Aureli M, Sonnino S, Kulik W, Aimar P, Bonfanti L, Martino S, Gritti A. 2012. The galactocerebrosidase enzyme contributes to maintain a functional neurogenic niche during early postnatal CNS development. Hum Mol Genet 21:4732-4750.

Senkal CE, Ponnusamy S, Rossi MJ, Bialewski J, Sinha D, Jiang JC, Jazwinski SM, Hannun YA, Ogretmen B. 2007. Role of human longevity assurance gene 1 and C18-ceramide in chemotherapy-induced cell death in human head and neck squamous cell carcinomas. Mol Cancer Ther 6(2):712-722.

Senkal CE, Ponnusamy S, Bielawski J, Hannun YA, Ogretmen, B. 2010. Antiapoptotic roles of ceramide-synthase-6-generated C16-ceramide via selective regulation of the ATF6/CHOP arm of ER-stress-response pathways. FASEB J 24: 296-308.

Senkal CE, Ponnusamy S, Manevich Y, Meyers-Needham M, Saddoughi SA, Mukhopadyay A, Dent P, Bielawski J, Ogretmen B. 2011. Alteration of ceramide synthase 6/C16-ceramide induces activating transcription factor 6-mediated endoplasmic reticulum (ER) stress and apoptosis via perturbation of cellular Ca2+ and ER/Golgi membrane network. J Biol Chem 286:42446-58.

Shyng C, Nelvagal HR, Dearborn JT, Tyynela J, Schmidt RE, Sands MS, Cooper JD. 2017. Synergistic effects of treating the spinal cord and brain in CLNL1 disease. Proc Natl Acad Sci USA 114(29):E5920-E5929.

Sigurdson CJ, Basaraba RJ, Mazzaferro EM, Gould DH. 2002. Globoid cell-like leukodystrophy in a domestic longhaired cat. Vet Pathol 39(4):494-6.

Sikora J, Dworski S, Jones EE, Kamani MA, Micsenyi MC, Sawada T, Le Faouer P, Bertrand-Michel J, Dupuy A, Dunn CK, Xuan ICY, Casas J, Fabrias G, Hampson DR, Levade T, Drake RR, Medin JA, Walkley SU. 2017. Acid ceramidase deficiency in mice results in a broad range of central nervous system abnormalities. Am J Pathol 187(4):864-883.

Skorupa AF, Fisher KJ, Wilson JM, Parente MK, Wolfe JH. 1999. Sustained production of β-glucuronidase from localized sites after AAV vector gene transfer results in widespread

distribution of enzyme and reversal of lysosomal storage lesions in a large volume of brain in mucopolysaccharidosis VII mice. Exp Neurol 160:17-27.

Smith B, Galbiati F, Castelvetri LC, Givogri MI, Lopez-Rosas A, Bongarzone ER. 2011. Peripheral neuropathy in the Twitcher mouse involves the activation of axonal caspase 3. ASN Neuro 3:213-222.

Snook ER, Fisher-Perkins JM, Sansing HA, Lee KM, Alvarez X, MacLean AG, Peterson KE, Lackner AA, Bunnell BA. 2014. Innate immune activation in the pathogensis of a murine model of globoid cell leukodystrophy. Am J Pathol 184:382-396.

Sundaram KS, Lev M. 1984. Inhibtion of sphingolipid synthesis by cycloserine in vitro and in vivo. J Neurochem 42:577-581.

Sundaram KS, Lev M. 1985. Inhibition of cerebroside synthesis in the brains of mice treated with L-cycloserine. J Lipid Res 26(4):473-7.

Suzuki K, Suzuki Y. 1970. Globoid cell leucodystrophy (Krabbe's disease): deficiency of galactocerebroside β-galactosidase. Proc Natl Acad Sci USA 66:302-309.

Suzuki K, Suzuki K. 1983. The twitcher mouse. A model of human globoid cell leukodystrophy (Krabbe's disease). Am J Pathol 111(3):394-397.

Svennerholm L, Vanier M-T, Mansson J-E. 1980. Krabbe disease: a galactosylsphingosine (psychosine) lipidosis. J Lipid Res 21:53-64.

Tanaka K, Webster HD. 1993. Effects of psychosine (galactosylsphingosine) on the survival and the fine structure of cultured Schwann cells. J Neuropathol Exp Neurol 52: 490-498.

Taniike M, Suzuki K. 1994. Spacio-temporal progression of demyelination in Twitcher mouse: With clinic–pathological correlation. Acta Neuropathol 88: 228-236.

Turgeon CT, Orsini JJ, Sanders KA, Magera MJ, Langan TJ, Escolar ML, Duffner P, Oglesbee D, Gavrilov D, Tortorelli S, Rinaldo P, Raymond K, Matern D. 2015. Measurement of psychosine in dried blood spots – a possible improvement to newborn screeningprograms for Krabbe disease. J Inherit Metab Dis 38(5):923-9.

Victoria T, Rafi MA, Wenger DA. 1996. Cloning of the canine GALC cDNA and identification of the mutation causing globoid cell leukodystrophy in West Highland White and Cairn terriers. Genomics 33(3):457-62.

Vrecenak JD, Flake AW. 2013. In utero hematopoietic cell transplantation – recent progress and the potential for clinical application. Cytotherapy 15(5):525-35.

Wang PR, Xu M, Toffanin S, Li Y, Llovet JM, Russell DW. 2012. Induction of hepatocellular carcinoma by in vivo gene targeting. Proc Natl Acad Sci USA 109(28):11264-9.

Watakabe A, Ohtsuka M, Kinoshita M, Takaji, M, Isa K, Mizukami H, Ozawa K, Isa T, Yamamori T. 2015. Comparative analyses of adeno-associated viral vector serotypes 1, 2, 5, 8 and 9 in marmoset, mouse and macaque cerebral cortex. Neurosci Res 93:144-157.

Watanabe M, Kodaira S, Takahashi T, Tominaga T, Hojo K, Kato T, Kunitomo K, Isomoto H, Ohashi Y, Yasutomi M. 2006. Randomized trial of the efficacy of adjuvant chemotherapy for colon cancer with combination therapy incorporating the oral pyrimidine 1-hexylcarbamoyl-5-fluorouracil. Langenbecks Arch Surg 391(4):330-7.

Wenger DA, Victoria T, Rafi MA, Luzi P, Vanier MT, Vite C, Patterson DF, Haskins MH. 1999. Globoid cell leukodystrophy in cairn and West Highland white terriers. J Hered 90(1):138-42.

Wenger DA. 2000. Murine, canine and non-human primate models of Krabbe disease. Mol Med Today 6(11):449-51.

Wenger DA, Rafi MA, Luzi P. 2016. Krabbe disease: one hundred years from the bedside to the bench to the bedside. J Neurosci Res 94(11):982-9.

White AB, Givogri MI, Lopez-Rosas A, Cao H, van Breemen R, Thinakaran G, Bongarzone ER. 2009. Psychosine accumulates in membrane microdomains in the brain of Krabbe patients, disrupting the raft architecture. J Neurosci 29:6068–6077.

Wiktor-Jedrzejczak W, Bartocci A, Ferrante AW Jr, Ahmed-Ansari A, Sell KW, Pollard JW, Stanley ER. 1990. Total absence of colony-stimulating factor 1 in the macrophage-deficient osteopetrotic (op/op) mouse. Proc Natl Acad Sci USA 87(12):4828-32.

Wright MD, Poe MD, DeRenzo A, Haldal S, Escolar ML. 2017. Developmental outcomes of cord blood transplantation for Krabbe disease: a 15-year study. Neurology 89(13):1365-1372.

Wu YP, McMahon EJ, Matsuda J, Suzuki K, Matsushima GK, Suzuki K. 2001. Expression of immune-related molecules is downregulated in twitcher mice following bone marrow transplantation. J Neuropathol Exp Neurol 60(11):1062-74.

Yamada H, Suzuki K. 1999. Responses to cyclic AMP is impaired in the twitcher Schwann cells in vitro. Brain Res 816:390–395.

Yamaguchi Y, Sasagasako N, Goto I, Kobayashi T. 1994. The synthetic pathway for glucosylsphingosine in cultured fibroblasts. J Biochem 116(3):704-10.

Yeager AM, Brenner S, Tiffany C, Moser HW, Santos GW. 1984. Prolonged survival and remyelination after hematopoietic cell transplantation in the twitcher mouse. Science 225(4666):1052-1054.

Zoglotora J, Chakraborty S, Knowlton R, Wenger DA. 1990. Krabbe disease locus mapped to chromosome 14 by genetic linkage. Am J Hum Genet 47: 37-44.

CURRICULUM VITAE

YEDDA LI
yedda.li@wustl.edu

Department of Internal Medicine
Dr. Mark Sands Lab
Southwest Tower 644
Campus Box 8007
660 S. Euclid Avenue
St. Louis, MO 63110
314-362-5496

EDUCATION

Washington University in St. Louis School of Medicine — **St. Louis, MO**
Medical Scientist Training Program (MD/PhD) — 2011 – Present
Anticipated degree date: May 2020

Washington University in St. Louis — **St. Louis, MO**
BA, *summa cum laude*, Biology. — 2010

AWARDS

2017 ASCI/AAP/APSA Joint Conference Poster Presentation Award — **April 2017**
Chicago, IL

2017 Association of American Physicians Travel Award — **April 2017**
Chicago, IL

2017 HOPE Center Retreat Oral Presentation Award — **May 2017**
St. Louis, MO

RESEARCH EXPERIENCE

Washington University in St. Louis — **St. Louis, MO**
Graduate student; Advisor: Dr. Mark S. Sands — 2013 – Present
Pathophysiology and treatment of murine globoid cell leukodystrophy (GLD)

- Developed a method to test and prove the 45-year-old Psychosine Hypothesis
- Conclusively demonstrated that the *in vivo* pathway of psychosine synthesis is primarily catabolic, overturning the 60-year-old dogma stating that *in vivo* psychosine synthesis is anabolic
- Identified a novel therapeutic target for GLD, and showed that this target can be successfully inhibited to slow the clinical progression of GLD

- Developed and tested a combination therapy regimen that synergistically improves lifespan and behavioral performance in mice with GLD
- Systematically studied the frequency of adeno-associated virus (AAV)-induced hepatocellular carcinoma in mice and determined how other therapies given in combination with AAV can change the penetrance of this phenotype
- Characterized the neuroinflammatory process in the natural progression of murine GLD
- Used novel bone marrow transplantation techniques to determine the neuroimmunomodulatory roles of different donor cell populations in the treatment of GLD
- Determined how different donor engraftment levels change the therapeutic efficacy of bone marrow transplantation

Undergraduate student; Advisor: Dr. Timothy A. Graubert 2008-2011
Impact of copy number variation on local gene expression in hematopoietic stem and progenitor cells (HSCs)

- Validated the computational aCGH-based method used to detect copy number variant regions (CNVRs) in the murine genome
- Identified numerous small insertions/deletions associated with CNVRs
- Identified two novel isoforms of Caspase-9, a gene whose expression levels in HSCs are strongly associated with the presence or absence of a copy number variant localized to the same area of the genome

TEACHING EXPERIENCE

Washington University in St. Louis School of Medicine **St. Louis, MO**
Teaching Assistant, Medical School Neurosciences Course Spring 2014

PROFESSIONAL ASSOCIATIONS

American Medical Student Association
American Physician Scientist Association
Child Neurology Society

CONFERENCE PRESENTATIONS

1. **Li Y**, Shea LK, Jiang X, Gray SJ, Ory DS, Sands MS. 2017. Combination therapy increases lifespan and improves clinicobehavioral performance in the murine model of globoid cell leukodystrophy. 2017 ASCI/AAP/ASCI Joint Conference. Chicago, IL. [poster]
2. **Li Y**, Shea LK, Jiang X, Gray SJ, Ory DS, Sands MS. 2017. Combination therapy increases lifespan and improves clinicobehavioral performance in the murine model of globoid cell leukodystrophy. 2017 HOPE Center Retreat. St. Louis, MO. [oral]
3. **Li Y**, Shea LK, Jiang X, Gray SJ, Ory DS, Sands MS. 2016. Combination therapy increases lifespan and improves clinicobehavioral performance in the murine model of globoid cell leukodystrophy. WORLD Conference. San Diego, CA. [oral]

4. **Li Y**, Shea LK, Jiang X, Gray SJ, Ory DS, Sands MS. 2016. Combination therapy increases lifespan and improves clinicobehavioral performance in the murine model of globoid cell leukodystrophy. 2016 MSTP Retreat. Potosi, MO. [oral]
5. **Li Y**, Shea LK, Jiang X, Gray SJ, Ory DS, Sands MS. 2015. Combination therapy increases lifespan and improves clinicobehavioral performance in the murine model of globoid cell leukodystrophy. 2015 HOPE Center Retreat. St. Louis, MO. [poster]
6. **Li Y**, Shea LK, Jiang X, Gray SJ, Ory DS, Sands MS. 2015. Combination therapy increases lifespan and improves clinicobehavioral performance in the murine model of globoid cell leukodystrophy. Regional APSA Conference. St. Louis, MO. [poster]

PEER-REVIEWED PUBLICATIONS

1. **Li Y**, Smith SN, Shea LK, Jiang X, Guzman MA, Chang D, Vogler CA, Gray SJ, Ory DS, Venditti C, Sands MS. Increased efficacy and toxicity associated with combination therapy for murine globoid cell leukodystrophy (Krabbe disease). [Manuscript in preparation]
2. **Li Y**, Xu Y, Benitez BA, Nagree MS, Dearborn JT, Jiang X, Guzman MA, Woloszynek JC, Giaramita A, Yip BK, Elsbernd J, Babcock MC, Lo M, Fowler SC, Wozniak DF, Vogler CA, Medin JA, Crawford BE, Sands MS. Genetic ablation of acid ceramidase in Krabbe disease confirms the psychosine hypothesis and identifies a new therapeutic target. *Proc Natl Acad Sci*. 2019; 116(40):20097-20103. PMID: 31527255
3. Hu P, **Li Y**, Nikolaishvili-Feinberg N, Scesa G, Bi Y, Pan D, Moore D, Bongarzone ER, Sands MS, Miller R, Kafri T. Hematopoietic stem cell transplantation and lentiviral vector-based gene therapy for Krabbe's disease: Present convictions and future prospects. *J. Neurosci Res*. 2016; 94(11):1152-68. PMID: 27638600.
4. Hu P, **Li Y**, Sands MS, McCown T, Kafri T. Generation of a stable packaging cell line producing high-titer PPT-deleted integration-deficient lentiviral vectors. *Mol Ther Methods Clin Dev.* 2015; 2:15025. PMID: 26229972.
5. Hawkins-Salsbury J, Shea L, Jiang X, Hunter DA, Guzman AM, Reddy AS, Qin EY, **Li Y**, Gray SJ, Ory DS, Sands MS. Mechanism-Based Combination Therapy Dramatically Increases Therapeutic Efficacy in Murine GLD. *J. Neurosci*. 2015; 35(16):6495-505. PMID: 25904800.
6. **Li Y** and Sands MS. Experimental Therapies in the Murine Model of Globoid Cell Leukodystrophy. *Pediatric Neurology.* 2014; 51(5):600-6. PMID: 25240259.
7. Leung W, Shaffer CD, Reed LK, … **Li Y**…, Elgin SC. Drosophila Muller F elements maintain a distinct set of genomic properties over 40 million years of evolution. *G3* (Bethesda). 2015; 5(5):719-40. PMID: 25740935.
8. Cahan P, **Li Y**, Izumi M, Graubert TA. The impact of copy number variation on local gene expression in mouse hematopoietic stem and progenitor cells. Nat Genet. 2009; 41(4):430-7. PMID: 19270704.